

AD/A-002 143

TIME DOMAIN APERTURE ANTENNA STUDY. VOLUME I

Morris Handelsman

Vermont University

Prepared for:

Rome Air Development Center

October 1974

DISTRIBUTED BY:

**NTIS**

National Technical Information Service  
U. S. DEPARTMENT OF COMMERCE

357016

RADC-TR-74-254, Volume I  
Final Report  
October 1974



AD A002143

TIME DOMAIN APERTURE ANTENNA STUDY  
University of Vermont

Approved for public release;  
distribution unlimited.

Reproduced by  
NATIONAL TECHNICAL  
INFORMATION SERVICE  
US Department of Commerce  
Springfield, VA. 22151

Rome Air Development Center  
Air Force Systems Command  
Griffiss Air Force Base, New York

UNCLASSIFIED

SECURITY CLASSIFICATION OF THIS PAGE (When Data Entered)

AD/A0021431

REPORT DOCUMENTATION PAGE		READ INSTRUCTIONS BEFORE COMPLETING FORM
1. REPORT NUMBER RADC-TR-74-254, Volume I (of 2)	2. GOVT ACCESSION NO.	3. RECIPIENT'S CATALOG NUMBER
4. TITLE (and Subtitle) TIME DOMAIN APERTURE ANTENNA STUDY	5. TYPE OF REPORT & PERIOD COVERED Final Report 21 Dec 72 - 21 May 74	
7. AUTHOR(s) Dr. Morris Handelsman	6. PERFORMING ORG. REPORT NUMBER None	
9. PERFORMING ORGANIZATION NAME AND ADDRESS Electrical Engineering Department University of Vermont Burlington, Vermont 05401	8. CONTRACT OR GRANT NUMBER(s) F30602-73-C-0104	
11. CONTROLLING OFFICE NAME AND ADDRESS Rome Air Development Center (OCTS) Griffiss Air Force Base, New York 13441	10. PROGRAM ELEMENT, PROJECT, TASK AREA & WORK UNIT NUMBERS Job Order No. 45060468	
14. MONITORING AGENCY NAME & ADDRESS (if different from Controlling Office) Same	12. REPORT DATE October 1974	
	13. NUMBER OF PAGES 126	
	15. SECURITY CLASS. (of this report) UNCLASSIFIED	
	15a. DECLASSIFICATION/DOWNGRADING SCHEDULE N/A	
16. DISTRIBUTION STATEMENT (of this Report)  Approved for public release; distribution unlimited.		
17. DISTRIBUTION STATEMENT (of the abstract entered in Block 20, if different from Report)  Same		
18. SUPPLEMENTARY NOTES RADC Project Engineer: John A. Potenza (OCTS) AC 315 330-4437		
19. KEY WORDS (Continue on reverse side if necessary and identify by block number) Antennas Transient Aperture Radiation Pulsed Paraboloid/Horn Radiation Time Domain Antenna Response  Reproduced by NATIONAL TECHNICAL INFORMATION SERVICE US Department of Commerce Springfield, VA 22151		
20. ABSTRACT (Continue on reverse side if necessary and identify by block number)  This final report contains the results of a study to develop a time-domain analysis for impulse-excited aperture antennas such as the paraboloid/TEH horn system. The principal approach used is the Chernousov aperture-fields formulation, based upon the Huygens-Kirchoff principle, to obtain time domain equations for antenna radiation.  The aperture fields over the front and two side apertures of a constant-impedance TEH horn are obtained by modeling it as a transmission-line,		

DD FORM 1 JAN 74 14/3 EDITION OF 1 NOV 68 IS OBSOLETE

UNCLASSIFIED

SECURITY CLASSIFICATION OF THIS PAGE (When Data Entered)

UNCLASSIFIED

SECURITY CLASSIFICATION OF THIS PAGE(When Data Entered)

## 20. Abstract (Cont'd)

TEM-mode, traveling-wave system with TDR-measured reflection coefficients. The equations derived from this approach were programmed for digital-computer numerical calculation. A second approach developed for the horn is the vector potential formulation using a current distribution on the conductors consistent with the fields in the TEM traveling-wave model. A third approach used for small-aperture horns is to model them as V-dipoles. Equations are given for calculating transient radiation from linear dipoles in any direction, including near endfire, from the currents on the dipole. Approximate closed-form expressions are derived for small-aperture horns for the radiation waveform in the boresight or backfire directions, using all three above approaches, which agree with each other. Comparison on a relative basis between computed and available experimental radiation vs. time curves for four TEM horns in various directions shows reasonably good agreement.

The paraboloid aperture fields are obtained by a point-to-point transformation from the fields at the paraboloid surface. The latter fields are calculated from a non-isotropic point source with arbitrary time excitation at the focus. Any given horn is replaced by an equivalent point source through an approximate closed-form equation characterizing the horn's fields in its principal planes. For gaussian pulse excitation, computed radiation vs. time curves are presented for an isotropic feed and for a particular 8" TEM horn both feeding a 48" paraboloid, in the boresight direction and other directions to display the sidelobe structure. Comparison, on a relative basis, with experimental curves for the boresight direction, shows reasonably good agreement.

The report consists of two volumes, each of which is self-contained. In addition, Volume I references, discusses, and incorporates the results of Volume II in such a manner that the reader, if desired, can obtain an overview of the entire project from Volume I.

UNCLASSIFIED

SECURITY CLASSIFICATION OF THIS PAGE(When Data Entered)

TIME DOMAIN APERTURE ANTENNA STUDY

Dr. Morris Handelsman

University of Vermont

Approved for public release;  
distribution unlimited.

## FOREWORD

This two-volume, final technical report was prepared by the Electrical Engineering Department, University of Vermont, Burlington, Vermont under Contract F30602-73-C-0104, Job Order Number 45060468 for Rome Air Development Center, Griffiss Air Force Base, New York. The work was performed during the period from 21 December 1972 through 21 May 1974.

John A. Potenza (OCTS) was RADC Project Engineer.

This report has been reviewed by the Office of Information (OI), RADC, and approved for release to the National Technical Information Service (NTIS).

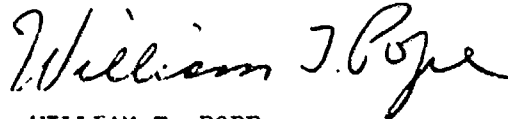
This report has been reviewed and is approved.

APPROVED:



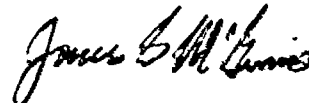
JOHN POTENZA  
Project Engineer

APPROVED:



WILLIAM T. POPE  
Assistant Chief  
Surveillance and Control Division

FOR THE COMMANDER:



JAMES G. MCGINNIS, Lt Col, USAF  
Deputy Chief, Plans Office

## ABSTRACT

This final report contains the results of a study to develop a time-domain analysis for impulse-excited aperture antennas such as the paraboloid/TEM horn system. The principal approach used is the Chernousov aperture-fields formulation, based upon the Huygens-Kirchoff principle, to obtain time domain equations for antenna radiation.

The aperture fields over the front and two side apertures of a constant-impedance TEM horn are obtained by modeling it as a transmission-line, TEM-mode, traveling-wave system with TDR-measured reflection coefficients. The equations derived from this approach were programmed for digital-computer numerical calculation. A second approach developed for the horn is the vector potential formulation using a current distribution on the conductors consistent with the fields in the TEM traveling-wave model. A third approach used for small-aperture horns is to model them as V-dipoles. Equations are given for calculating transient radiation from linear dipoles in any direction, including near endfire, from the currents on the dipole. Approximate closed-form expressions are derived for small-aperture horns for the radiation waveform in the boresight or backfire directions, using all three above approaches, which agree with each other. Comparison on a relative basis between computed and available experimental radiation vs. time curves for four TEM horns in various directions shows reasonably good agreement.

The paraboloid aperture fields are obtained by a point-to-point transformation from the fields at the paraboloid surface. The latter fields are calculated from a non-isotropic point source with arbitrary time excitation at the focus. Any given horn is replaced by an equivalent point source through an approximate closed-form equation characterizing the horn's fields in its principal planes. For gaussian pulse excitation, computed radiation vs. time curves are presented for an isotropic feed and for a particular 8" TEM horn both feeding a 48" paraboloid, in the boresight direction and other directions to display the sidelobe structure. Comparison, on a relative basis, with experimental curves for the boresight direction, show reasonably good agreement.

The report consists of two volumes, each of which are self-contained. In addition, Vol. 1 references, discusses, and incorporates the results of Vol. 2 in such a manner that the reader, if desired, can obtain an overview of the entire project from Vol. 1.

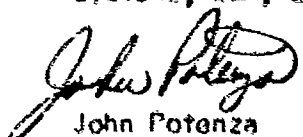
## EVALUATION

Over the past decade, the RADC Antenna Community has continued its interest and involvement in the behavior of antennas when excited by short time duration impulsive like signals and fields. While substantial advancements have been made for simple antenna structures (monopole, dipole and TEM horns) the more complex antenna systems have not been sufficiently considered. Although considerable experimentation using time domain techniques has been performed on reflector/feed systems, a concerted engineering approach for time domain analysis and synthesis is lacking. The purpose of the work reported on herein was to develop direct time domain models suitable for analyzing and predicting the time domain behavior of reflector/TEM horn antenna systems.

These reports contain the results of an 18 month study performed by the Electrical Engineering Department, University of Vermont. Three approaches were developed directly in the time domain suitable for predicting the impulsive radiation for reflector/feed antenna systems. Complete and detailed expressions and formulations are provided and all assumptions and approximations are completely described. Comparisons of the utility of the analytical solutions are provided by comparison with available experimental data for a number of TEM horns and reflector/horn configurations.

The results of this research provide a unified and concerted approach for analyzing the radiation v.s. time behavior of anerture type antennas. It has been shown that the approaches developed are theoretically sound and self-consistent within themselves as well as with C.W. antenna theory. A number of problem areas are identified and recommendations for further study made.

This effort supports TPO-5 "Electromagnetic Generation and Control" referenced under paragraph 3.5.2.2 in RADC Technology Plan Part III dated Sept. 73. Specifically these results are applicable to wide bandwidth antenna systems, ECM, ECCM and SEW efforts.

  
John Potenza  
Project Engineer



## TABLE OF CONTENTS

<u>Chapter</u>		<u>Page</u>
1	INTRODUCTION	1
	1.1 Introduction	1
	1.2 Purpose of Program	1
	1.3 Contents of This Report	2
	1.3.1 Introduction	2
	1.3.2 Volume 1	2
	1.3.3 Volume 2	3
	1.4 Program Organization	4
2	TRANSIENT RADIATION FROM TEM HORNS	5
	2.1 Introduction	5
	2.2 Radiation From a TEM Horn; Assumptions	6
	2.2.1 TEM Mode	6
	2.2.2 Use of the Field Equivalence Theorem	9
	2.3 Radiation From Front Aperture of TEM Horn, Sinusoidal Time Variation	15
	2.3.1 Introduction	15
	2.3.2 Radiation From a Small Differential Area	16
	2.3.3 Radiation From a Finite Area	21
	2.3.4 Comparison With Silver (1949)	25
	2.3.5 Comparison With Martins (1973)	27
	2.4 Radiation in the Boresight Direction; Comparison With Martins (1973)	31
	2.5 Derivation of the Boresight Radiated Fields in the Time Domain, Using Three Different Approaches, Small TEM Horns	33
	2.5.1 Introduction	33
	2.5.2 Aperture Approach	34
	2.5.3 Current-Sheet Approach	42
	2.5.4 V-Dipole Approach	44
	2.6 Comparison of Theory With Experiment	54
	2.6.1 Comparisons Using Normalized Curves	54
	2.6.2 Discussion of Predicted Vs. Measured Results Obtained by Martins (1973)	56
3	TRANSIENT RADIATION FROM A PARABOLOID	58
	3.1 Introduction	58
	3.2 Assumptions	59
	3.3 Exit-Aperture Excitation Produced by an Isotropic Primary Feed	60
	3.4 Principal-Plane Radiation From a Rectangular Aperture With TEM-Wave Excitation	66
	3.5 Boresight Radiation From Any Planar Aperture With TEM-Wave Excitation	68

# TABLE OF CONTENTS (continued)

<u>Chapter</u>		<u>Page</u>
3.6	Ratio of Paraboloid to Primary Feed Boresight Fields	69
3.6.1	Isotropic Feed Approximation to TEM Horn	69
3.6.2	Actual 8-Inch TEM Horn Feed	73
3.7	Comparison of Theory With Experiment	74
4	CONCLUSIONS AND RECOMMENDATIONS	75
4.1	Conclusions	75
4.1.1	Aperture-Field and Current-Sheet Approaches to the TEM Horn	75
4.1.2	V-Dipole Model of Small-Aperture Horn	76
4.1.3	Assumptions Underlying TEM Horn Model	76
4.1.4	TEM Horn Radiation Formula by BDM	77
4.1.5	Paraboloid Antenna Radiation	77
4.1.6	Radiation From Transients on Linear Dipole Antennas	79
4.2	Recommendations	80
	REFERENCES	81

## Appendixes

A	RADIATION FROM TRANSIENTS ON LINEAR DIPOLE ANTENNAS	84
1.	Introduction	84
2.	Derivation of Radiation Equation	84
3.	Simple Illustrative Example - A Dipole With Matched Ends	89
4.	Radiation in End-Fire Directions $\Theta = 0^\circ, 180^\circ$	91
4.1	Theory	91
4.2	Comparison With Published Results	94
5.	Summation Formula for Equation (A-6)	96
6.	Additional Cases of Interest	96
6.1	Introduction	96
6.2	Special Case, Impulse Excitation, $R_1 = -1, R_2 = 1$	97
6.3	Special Case, Impulse Excitation, $R_1 = 0, R_2 = 1$	99
6.4	General Excitation, Broadside Direction ( $\Theta = 90^\circ$ ), $R_1 = 0$ (Matched Input), $R_2 = 1$	99
6.4.1	Introduction	99
6.4.2	General Result	101
6.4.3	Short Dipole	101
6.5	Ramp Excitation, $R_1 = 0$ (Matched Input), $R_2 = 1$	102
6.6	Pulse Excitation, $R_1 = 0$ (Matched Input), $R_2 = 1$	104
6.6.1	Pulse Duration $\tau_{44}$ Antenna Trip Time $h/c$	104

# TABLE OF CONTENTS (continued)

<u>Appendixes</u>	<u>Page</u>
6.6.2 Pulse Duration >> Antenna Trip Time h/c	105
7. Broadside Radiation Field in Terms of Incident Impulse Voltage	105
B ADDITIONAL DISCUSSION ON TERMINAL REFLECTION COEFFICIENTS FOR LINEAR DIPOLE ANTENNA	110
1. Introduction	110
1.1 Purpose	110
1.2 General "Physical" Discussion	110
2. Input Reflection Coefficient	112
3. End (or Tip) Reflection Coefficient	116
4. Approximate Model of Dipole Antenna With TDR-Measured Reflection Coefficients	117
5. Summary and Conclusions	123

# LIST OF ILLUSTRATIONS

<u>Figure</u>		<u>Page</u>
1	Radiating differential area.	20
2	Component cardioid patterns.	20
	(a) Cardioid ( $1 + \cos \theta$ )	20
	(b) Cardioid $k_v$ ( $1 - \cos \theta$ )	20
3	Various front apertures and coordinates.	22
	(a) TEM horn front aperture, standard spherical coordinates	22
	(b) Rectangular waveguide aperture, $TE_{10}$ mode Silver (1949)	22
	(c) TEM horn front aperture and coordinates, Martins (1973)	22
4	TEM horn.	35
	(a) 3-D view	35
	(b) Side view	35
	(c) Top view	35
	(d) Front aperture approximated by planar rectangle	35
5	Dipoles.	46
	(a) Straight symmetrical dipole	46
	(b) V-dipole side view	46
6	Boresight radiation, V-dipole upper arm.	46
7	Paraboloidal reflector/feed geometry.	61
8	Dipole geometry.	86
9	Dipole with matched ends.	90
10	Dipole radiation, pulse excitation, $k_e = 0$ .	90
11	Trapezoidal pulse shape $I(t)$ .	90
12	Radiation of impulse excitation, $R_1 = - R_1 $ , $R_2 = 1$ .	100

# LIST OF ILLUSTRATIONS (continued)

<u>Figure</u>		<u>Page</u>
13	Radiation of impulse excitation, $R_1=0$ , $R_2=1$ .	100
14	Ramp excitation waveform.	103
15	Radiation of ramp waveform, $R_1=0$ , $R_2=1$ .	103
	(a) Component waveforms	103
	(b) Sum = $E_{\theta}$	103
16	Rectangular pulse excitation waveform.	106
17	Radiation for $\tau \ll \frac{h}{c}$ , broadside direction, $R_1=0$ , $R_2=1$ .	106
18	Radiation for $\tau \gg \frac{h}{c}$ , broadside direction, $R_1=0$ , $R_2=1$ .	109
19	Transmission line circuit.	109

## CHAPTER 1

### INTRODUCTION

#### 1.1 INTRODUCTION

This final report, consisting of two volumes, reports on work performed from 21 Dec. 1972 to June 30, 1974, under RADC Contract No. F30602-73-C-0104, entitled Time Domain Aperture Antenna Study, for the Air Force Systems Command, Rome Air Development Center, Griffiss Air Force Base, N. Y. Volume 1 is written by Prof. M. Handelsman, Electrical Engineering Department, University of Vermont, Project Director. Volume 2 is identical to a Ph.D. thesis, with the title The Transient Electromagnetic Far Fields of a Paraboloid Reflector/TEM Horn Antenna Using Time Domain Techniques, submitted to the Department of Electrical Engineering, University of Vermont, by Mr. Hugh C. Maddocks, referred to as Maddocks (1974) in Vol. 1.

#### 1.2 PURPOSE OF PROGRAM

The purpose of this program is to develop a time-domain approach to the analysis and synthesis of impulse-excited high gain aperture antennas such as the paraboloid/TEM horn feed type. The principal approach is to be Chernousov's formulation (Chernousov 1965) based on the Huygens-Kirchoff principle to obtain time domain expressions for antenna radiation. The existing formulation as presented by Chernousov is to be extended in detail and scope, and systematically applied to obtain solutions to time domain radiation performance, using the analysis technique. The utility and validity of this approach is to be tested by comparison with published results and available experimental data.

### 1.3 CONTENTS OF THIS REPORT

#### 1.3.1 INTRODUCTION

Volumes 1 and 2 of this report are each self-contained volumes. In addition, Vol. 1 references, discusses, and incorporates the results of Vol. 2 in such a manner that the reader, if desired, can obtain an overview of the entire project from Vol. 1.

#### 1.3.2 VOLUME 1

Chapter 2 in Vol. 1 discusses the calculation and characteristics of transient radiation from TEM horns, use of the field equivalence theorem, assumptions underlying the TEM-mode model of the horn, derivation of a closed-form expression for the boresight radiation in the time domain using three different approaches (Chernousov aperture formulation, current-sheet plus vector potential approach, and a V-dipole approach), and comparison of theory with experiment. Chapter 3 discusses transient radiation from a paraboloid, the characteristics of radiation from planar apertures with TEM-wave excitation, paraboloid aperture excitation produced by an isotropic primary feed and by an 8" TEM horn feed, and comparison of theory with experiment. Chapter 4 contains conclusions and recommendations. References are listed after Chap. 4. Appendix A discusses radiation from transients on linear dipole antennas, clears up a problem concerning radiation in the end-fire directions reported previously (Harrelman 1972), and examines the radiation for various special cases. Appendix B contains a discussion on terminal reflection coefficients, and the state of the art on time domain, transmission-line models for dipole antennas.

### 1.3.2 VOLUME 2

Chapter 1 in Vol. 2 contains a statement and background of the problem, which is the study of the transient far fields of a paraboloid/TEM horn antenna system in the time domain. Chapter 2 contains an analysis of the transient far fields of TEM horn antennas using the Chernousov aperture-field method. This includes analysis of the three radiating apertures, approximate closed-form expressions for the radiation in the boresight and backfire directions and also for azimuth-plane directions well removed from boresight and backfire, and comparisons between theory and experimental results for three Sperry Rand horns, and the 8" BDM horn. Chapter 3 contains an analysis of the radiation from an approximation to a TEM horn with small E-plane flare consisting of a sectioned biconical antenna. The radiation is calculated from the vector potential resulting from the assumed current-sheet flow on the conducting surfaces. Approximate closed-form equations for the radiation in the boresight and backfire directions are derived which agree with those derived in Chapter 2 using the aperture fields. Chapter 4 analyzes the transient far fields of a paraboloid excited by a point source feed, with a non-isotropic (in angle) primary pattern, develops various required coordinate transformations from the horn to the paraboloid exit aperture to the far field points, and develops an equation for the paraboloid boresight field with an isotropic feed. Chapter 5 analyzes the fields when the paraboloid is excited by a TEM horn feed, and compares theoretical to available experimental results for the BDM 48" paraboloid/6" TEM horn for the boresight direction. Chapter 6 contains conclusions and summary. A list of references starts on p. 106. There are 5 appendixes containing the



details of various mathematical derivations and the listing of 2 Fortran programs. Appendixes A, B, and C, respectively, contain derivations of the Chernousov equations, the paraboloid/isotropic point source feed radiation fields, and the paraboloid/TEM horn feed radiation fields. Appendixes D and E, respectively, describe and list Fortran programs to compute the radiation fields of a paraboloid excited by an isotropic point source feed and by a TEM horn feed which produces a tapered illumination over the paraboloid exit aperture computed from an approximate closed-form expression matched to the radiation characteristics of the horn.

#### 1.4 PROGRAM ORGANIZATION

The persons who performed this work are Dr. Morris Handelsman, project director and author of Vol. 1, and Mr. Hugh C. Maddocks, Graduate Assistant, author of Vol. 2, both of the Electrical Engineering Department, College of Engineering, Mathematics and Business Administration, University of Vermont.

## CHAPTER 2

### TRANSIENT RADIATION FROM TEM HORNS

#### 2.1 INTRODUCTION

The characteristics of radiation from TEM horns excited at the input (apex) by arbitrary time waveforms are discussed in this chapter. There are two principal approaches to radiation models of the TEM horn discussed (i.e., the use of the aperture fields, and the use of the vector potential based upon the current distribution on the wedge conductors), both in the time domain. A complete and detailed time-domain analysis of the TEM horn radiation at all angles, using the above two approaches, is given by Maddocks (1974). Maddocks (1974) also presents digital computer calculations and graphs for a number of special cases for which experimental data is available for comparison of theory with experiment. Maddocks (1974) also develops approximate closed-form expressions for the radiation from small horns in the azimuth plane, by suitable reduction of his complete equations. These will be discussed further in this chapter.

It is also shown that the small TEM horn may be modeled as a V-dipole. Using the results of Appendix A, it is shown that to within the accuracy of the small-horn approximation described herein, this third model produces identical results with those obtained by Maddocks (1974) using the two models

described in the preceding paragraph.

In summary, the purpose of this chapter is first to discuss, from an engineering viewpoint, some of the more important results obtained by Maddocks (1974). Second, additional discussion is given concerning the basic assumptions and necessary simplifications underlying the radiation models employed in the analysis. Third, comparison is made with a TEM horn analysis published by Martins (1973).

## 2.2 RADIATION FROM A TEM HORN; ASSUMPTIONS

### 2.2.1 TEM MODE

The first and perhaps most important assumption made in calculating the radiation from a "TEM" horn is that the horn propagates only one mode, the TEM mode. It is true that practical closed waveguides usually allow propagation of only one mode, the dominant mode, although higher-order modes may be excited by discontinuities.

The TEM horns built to date may allow propagation of various TE and TM modes (i.e., non-TEM fields) assuming there are sufficiently high frequency components in the excitation which exceed the cut-off frequencies of these modes, and conditions exist to excite such modes. It is pointed out that while the general problem area of transmission-line or guide discontinuities from the multi-mode viewpoint has received vast attention for steady-state  $e^{j\omega t}$  excitation, there is practically nothing published concerning discontinuities from the time-domain viewpoint,

as far as this writer knows.

The exact structure of the fields, especially at the TEM horn apertures, is a separate and difficult boundary value problem which is beyond the intent of this investigation. From a practical and engineering viewpoint, it is therefore necessary to content oneself with assuming propagation of only the TEM mode, the usefulness of this simplifying assumption being verified by comparison of the resulting theoretical predictions with experiment. This then assumes that while non-TEM modes may be excited, they do not propagate within the TEM horn.

There is a discussion on waveguide and horn feeds in Silver (1949:chap. 10) which makes a number of points pertinent to this discussion, if it is assumed as above that only the TEM mode propagates in the TEM horn, which completes the analogy to a waveguide with its single dominant mode. Then over a cross-section inside the horn sufficiently far from the front aperture, the field is the sum of the incident and reflected waves of the TEM mode only, the higher-order modes generated by this aperture being assumed to decay in distance with sufficient rapidity. This assumes that the open sides of the TEM horn present a relatively small and negligible continuous discontinuity to the TEM mode, as compared to the abrupt discontinuity presented by the front aperture, an assumption which seems to be borne out by reflectometry measurements (Martins, 1973:147). However, in the front aperture, non-TEM higher-order modes can be generated and exist

locally, excited by the sudden discontinuity in the TEM guiding structure. Unless the detailed distribution of these higher modes is known, their contribution to the radiation must be neglected. This is one source of inaccuracy in calculating the radiation from the aperture fields (Silver 1949:334).

However, as pointed out in Silver (1949:334) the effects of the aperture-reflected dominant mode (TEM in this case) can be taken into account in terms of a reflection coefficient  $R$  which is the ratio of the reflected and incident electric fields. In the waveguide  $e^{j\omega t}$  case  $R$  is determined experimentally by standing-wave measurements in the guide (which involves only the dominant mode). In the corresponding TEM horn time-domain case,  $R$  is determined experimentally by time-domain reflectometry (TDR) measurements, involving the TEM mode in the transmission line input to the horn (Martins 1973:122,143). Assuming that the reflection coefficient  $R$  of the front aperture is determined by measurements, then the total TEM E field in the aperture is given by (Silver 1949:335 Eq. (2))

$$E_a = (1+R)E_i \quad (1)$$

where:

$E_a$  = TEM transverse field in front aperture

$E_i$  = incident TEM transverse field

The corresponding total TEM H field in the aperture is then

$$H_a = (1-R) H_i \quad (2)$$

Since for the TEM mode

$$\frac{E_i}{H_i} = \eta_0 = \sqrt{\frac{\mu_0}{\epsilon_0}} = 120 \pi \quad (3)$$

then  $H_a$  can also be written as follows:

$$H_a = \frac{1-R}{1+R} \frac{E_a}{\eta_0} \quad (4)$$

This equation is the same as Silver (1949:335 Eq. (4)), where

$$\Gamma = R, \text{ and } t = H_i/E_i = 1/\eta_0.$$

The fields in the open sides of the TEM horn, following the discussion given previously, are assumed to be the fields of the traveling TEM waves in the horn; no discontinuity, reflection or fringing is assumed. This is probably another source of inaccuracy in the aperture-field radiation model; however it does not appear to be particularly significant, based upon experimental results.

#### 2.2.2 USE OF THE FIELD EQUIVALENCE THEOREM

The field equivalence theorem or the equivalence principle as set forth by Schelkunoff and Friis (1952:516-520) underlies the necessity for a closed surface  $S$ , required by the Chernousov (1965) formulation, over which the fields must be known or estimated. The Chernousov formulation in terms of aperture fields is one of the two TEM horn radiation models used by Maddocks (1974:chap. 2). Hence a brief discussion of the equivalence theorem in the context of its application to the TEM horn is now presented.

Schelkunoff and Friis (1952:520) sum up the application of the equivalence theorem to a waveguide horn problem. The following statements are taken (almost verbatim) from this reference. A closed surface  $S$  is considered which covers the aperture and encloses the horn itself. If the tangential  $E$  and  $H$  fields on surface  $S$  are known exactly, then by the equivalence theorem the fields outside  $S$  may be calculated exactly from the virtual sources which replace the fields. Schelkunoff and Friis make the specific point that in this case the horn may then be removed (for reasons explained previously in Schelkunoff and Friis (1952:519)), and the fields of the virtual sources (equivalent electric and magnetic currents) calculated as if these sources were in free space. This is an important point, as it allows calculation of the radiation fields as if the horn were not present.

In practice, as Schelkunoff and Friis point out, usually we do not know the true fields over surface  $S$ , and must resort to approximations. These approximations (in reality educated estimates of the true fields) in the case of the TEM horn, are discussed by Maddocks (1974:chap. 2).

The fields over the front and side apertures are assumed to be due to incident and front-aperture-reflected traveling TEM waves. No other traveling waves are necessary, as the TEM horns are assumed to be matched at their inputs.

Over the part of surface  $S$  occupied by the exterior surfaces of the two metal wedges, the tangential  $E$  field is very closely equal to zero (the wedges are good conductors), but the tangential  $H$  field is not known. This tangential  $H$  field is related to the "leakage" currents  $\bar{J}_e$  on the exterior surfaces by  $\bar{J}_e = \hat{M} \times \bar{H}$ . Since  $\bar{J}_e$  is also not known, this equation cannot be used to find tangential  $H$ . However, it is known, based upon much practice and experience, that at least for open-ended waveguides and the like, neglect of the effects of the currents on the exterior walls results in radiation calculations which are a first approximation to the measured data (Jordan and Balmain 1968:495). Neglect of these exterior currents, which is equivalent to assuming zero tangential  $H$  field over the exterior surfaces of the wedges is therefore a third source of inaccuracy, but is common practice. This same approximation is also invoked for waveguide horns by Silver (1949:336), with the precautionary note that the approximation improves with increase in the size of the aperture dimensions. Thus for small or large TEM horns the statements by Jordan and Balmain (1968:495) or Silver (1949:336), respectively, may be used to justify the approximation of zero  $H$  fields over the exterior wedge surfaces.

The remaining portion of  $S$  is the small open-ended back aperture of the TEM horn. It was decided to ignore the contribution to the radiation from the fields over this small aperture surface of the horn for several reasons. The first and



principal justification for this is that this aperture is relatively small, and therefore its contribution to the radiation, especially in the important forward-fire direction (forward-fire of the entire TEM horn) is small in any event. A second reason is that due to the relatively close proximity between this aperture and the exposed inner conductor of the coaxial line (which extends across the apex of the horn and excites the TEM mode in the horn), there is a large degree of uncertainty concerning the detailed structure of the fields in this region of the horn. In other words, the fields in this region are undoubtedly quite geometry-sensitive. In view of this uncertainty, and especially in view of the relatively small contribution to the total radiation from this part of the horn, the fields over this portion of surface S were ignored (i.e., taken to be zero).

There is a discussion of the radiation from the open end of an infinitely-wide, semi-infinitely-long parallel-plate guide in Collin and Zucker (1969:621-630) for sinusoidal time variation. An incident dominant TEM mode is assumed. An exact solution (first obtained in 1948) for the radiation is presented, using the Wiener-Hopf technique. The fields within the guide consist of the incident TEM mode, a reflected TEM mode, characterized by a reflection coefficient  $\Gamma = R$ , plus higher-order TM modes. The plate separation  $2a$  and the operating wavelength  $\lambda_0$  are selected ( $\lambda_0 > 2a$ ) so that only the TEM mode propagates

(note: this condition might not hold in time-domain applications, depending upon the upper frequency content of the exciting transient waveform). It is shown that  $|R| = \exp. (-k_0 a)$ , where  $k_0 = 2\pi/\lambda_0$ . The phase of R is given by an infinite series. Again, in time-domain or transient analysis, an "average" R might be defined, averaged over the frequency content of the exciting waveform. This has been done for a linear dipole antenna by King and Schmitt (1962).

The analysis in Collin and Zucker (1969) also shows that there are currents flowing on the outside of the plates which implies an H field over the exterior surfaces. However, it is also shown that the normalized exact radiation pattern is approximated remarkably well by the normalized radiation pattern, especially over the forward-fire direction, when calculated using a simple rough estimate of the fields over the aperture only (= constant over the aperture). This excellent agreement between exact and approximate normalized radiation patterns is also shown to hold for an incident  $TE_{10}$  mode, using very simple estimated fields over the aperture only. The point of this is that it is possible to calculate approximate normalized radiation patterns which are surprisingly close to the exact patterns which arise from a complex current and field distribution over the entire guide, by using very rough estimates of the fields over only the aperture, as has been done in the case of the TEM horn.

Thus, the common practice of using estimated fields over the apertures only continues to be justified, at least insofar as normalized patterns are concerned.

Since, as described above, the parallel-plate guide radiation problem has been solved exactly for  $e^{j\omega t}$  excitation, it would be possible, in theory, to solve for the radiation with transient excitation. This has not been done, to this writer's knowledge. It is probably a formidable but achievable task. Additional and possibly more serious difficulties arise in the application to the actual TEM horn because it is flared, and definitely non-infinite in width. In this report, an approximate but much simpler time-domain approach using traveling waves and estimated aperture fields (an estimated current distribution consistent with the estimated fields is also used) is employed. As discussed previously, approximations based upon simple estimated aperture fields only, lead to reasonably good radiation pattern results, especially for radiation near the forward-fire direction. This is important, because this is the direction of most significance in considering the radiation from a TEM horn plus parabolic dish system. The question of the scale of absolute value of the radiation fields is not resolved by comparison of normalized patterns. It is possible that the available exact parallel-plate solution above might yield absolute value results for the more complicated TEM horn structure, but this has not been attempted.

## 2.3 RADIATION FROM FRONT APERTURE OF TEM HORN, SINUSOIDAL TIME VARIATION

### 2.3.1 INTRODUCTION

There are several objectives of the following discussion on the radiation from the front apertures of TEM horns, excited by conventional steady-state sinusoidal time-varying excitation (hereinafter designated as  $e^{j\omega t}$  excitation). The first objective is to show that the equations for the radiation fields, in the presence of reflection of the incident wave from the front aperture, are identical in their functional dependence on the reflection coefficient  $R$  and polar angle  $\theta$  with those for open circular and rectangular waveguides with dominant mode reflections from their open ends, as given in Silver (1949:334-344, especially Eqs. 11,13,20,22,23a,23b) and also in Ramo & Whinnery (1953:537-538).

The second objective is to compare these results with those obtained by Martins (1973), who uses  $e^{j\omega t}$  excitation solutions to develop time-domain solutions. It is shown that the two sets of  $e^{j\omega t}$  solutions do not agree because as believed to be demonstrated herein, the effects of the aperture reflection coefficient are incorrectly accounted for in setting up the aperture fields in Martins (1973), which in turn makes the amplitude and the angular variations of the radiation patterns also incorrect.

### 2.3.2 RADIATION FROM A SMALL DIFFERENTIAL AREA

Figure 1 shows a differential area  $dA = dx dy$  in the XY plane upon which is normally incident a TEM wave traveling in the +Z direction, polarized parallel to the X direction. Let the aperture electric field (or voltage) reflection coefficient be  $K_v$  (same as  $R_2$  in Martins (1973) and  $\Gamma$  in Silver (1974)). Since the incident fields  $E_{xi}$  and  $H_{yi}$  belong to a TEM mode in free space, they are related by the "Huygens' source" equation (Jordan and Balmain 1968:522)

$$E_{xi} = \mu_0 H_{yi} \quad (5)$$

where  $\mu_0$  is given by Eq. (3). Then the aperture fields  $E_{xa}$  and  $H_{ya}$  are given by the standard reflection-transmission equations (Jordan and Balmain 1968:Eqs. 5-78 thru 5-82) as follows:

$$E_{xa} = E_{xi} + k_v E_{xi} = (1 + k_v) E_{xi} \quad (6A)$$

$$H_{ya} = H_{yi} - k_v H_{yi} = (1 - k_v) H_{yi} \quad (6B)$$

The aperture fields given by Eq. (6) do not comprise a Huygens' source satisfying Eq. (5) unless  $k_v = 0$ , which is the reflectionless case in which the aperture fields are the same as the incident fields. Thus the aperture field  $E_{xa}$  given by Eq. (6A) cannot be substituted for  $E_{xi}$  in radiation equations which are designed for Huygens'-type fields. Instead it is necessary to calculate the separate radiation fields due to both types of equivalent current sources, as given by Eq. (7) below, and add the results.

The equivalent current sources over surface  $dA$  are given by the equations (Ramo, Whinnery and Van Duzer 1965:663)

$$\bar{J} = \hat{a}_z \times H_{ya} \hat{a}_y = -H_{yi} (1 - \kappa_v) \hat{a}_x \quad (7A)$$

$$\bar{M} = -\hat{a}_z \times E_{xa} \hat{a}_x = -E_{xi} (1 + \kappa_v) \hat{a}_y \quad (7B)$$

The radiation fields due to these sources acting over area  $dA$  are calculated below using a systematic formulation described in Ramo and Whinnery (1953:530); this is the reference cited in Martins (1973:40) for calculation of the radiated fields from the TEM horn front aperture. The fields are given by

$$dE_\theta = -j \frac{e^{-jkr}}{2\lambda r} (\eta_0 dN_\theta + dL_\phi) \quad (8A)$$

$$dE_\phi = j \frac{e^{-jkr}}{2\lambda r} (-\eta_0 dN_\phi + dL_\theta) \quad (8B)$$

where for the differential area source (Ramo and Whinnery 1953: 506, 530)

$$d\bar{N} = \int_{V'} \bar{J}_a e^{-jkr' \cos \psi} dV = \bar{J} dA = -H_{ya} dA \hat{a}_x \quad (9A)$$

$$d\bar{L} = \int_{V'} \bar{M}_a e^{-jkr' \cos \psi} dV = \bar{M} dA = -E_{xa} dA \hat{a}_y \quad (9B)$$

Thus

$$\begin{aligned} d\bar{N} &= -H_{yi} (1-k_v) dA \hat{a}_x \\ dN_x &= -H_{yi} (1-k_v) dA \end{aligned} \quad (10A)$$

$$\begin{aligned} d\bar{L} &= -E_{xi} (1+k_v) dA \hat{a}_y \\ dL_y &= -E_{xi} (1+k_v) dA \end{aligned} \quad (10B)$$

Hence there follows, using standard cartesian to spherical co-ordinate transformations,

$$dN_\theta = dN_x \cos\theta \cos\phi = -H_{yi} (1-k_v) dA \cos\theta \cos\phi \quad (11A)$$

$$dN_\phi = -dN_x \sin\phi = H_{yi} (1-k_v) dA \sin\phi \quad (11B)$$

$$dL_\theta = dL_y \cos\theta \sin\phi = -E_{xi} (1+k_v) dA \cos\theta \sin\phi \quad (11C)$$

$$dL_\phi = dL_y \cos\phi = -E_{xi} (1+k_v) dA \cos\phi \quad (11D)$$

Substituting Eq. (11) into (8), and using Eq. (5) gives

$$dE_\theta = j \frac{e^{-jkr}}{2\lambda r} E_{xi} dA \cos\phi \left[ (1-k_v) \cos\theta + (1+k_v) \right] \quad (12A)$$

$$dE_\phi = -j \frac{e^{-jkr}}{2\lambda r} E_{xi} dA \sin\phi \left[ (1-k_v) + (1+k_v) \cos\theta \right] \quad (12B)$$

The bracketed terms in Eq. (12) may be interpreted as the sum of "forward-fire" and "backward-fire" cardioid patterns, if Eq. (12) is rewritten as follows:

$$dE_{\theta} = \frac{jE_{xi} dA e^{-jkr} \cos \phi}{2\lambda r} \left[ (1 + \cos \theta) + k_v (1 - \cos \theta) \right] \quad (13A)$$

$$dE_{\phi} = \frac{-jE_{xi} dA e^{-jkr} \sin \phi}{2\lambda r} \left[ (1 + \cos \theta) - k_v (1 - \cos \theta) \right] \quad (13B)$$

The  $(1 + \cos \theta)$  term represents a forward-fire cardioid, with maximum in the forward direction  $\theta = 0^\circ$ , while the  $(1 - \cos \theta)$  term represents a backward-fire cardioid, with maximum in the backward direction  $\theta = 180^\circ$ . These two cardioids are shown in Fig. 2. In any principal plane, such as the XZ plane ( $\phi = 0$ )

$$dE_{\theta} = \frac{jE_{xi} dA e^{-jkr}}{2\lambda r} \left[ (1 + \cos \theta) + k_v (1 - \cos \theta) \right] \quad (14A)$$

In the boresight direction ( $\theta = 0$ ), Eq. (14A) yields

$$dE_{\theta} = \frac{jE_{xi} dA e^{-jkr}}{\lambda r} \quad (14B)$$



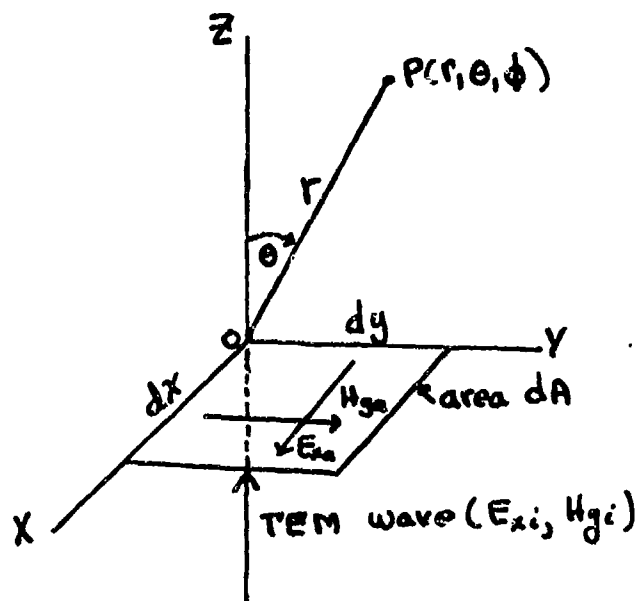
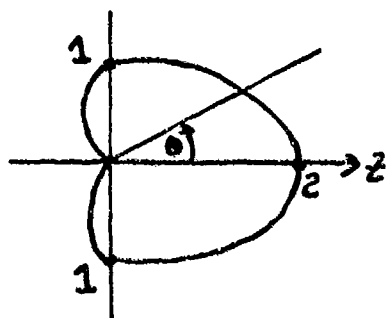
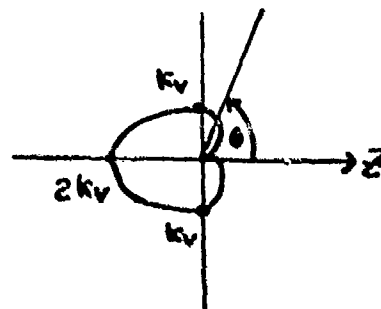


FIG. 1 Radiating differential area.



(a) Cardioid ( $1 + \cos \theta$ )



(b) Cardioid  $k_v (1 - \cos \theta)$

FIG. 2 Component cardioid patterns.

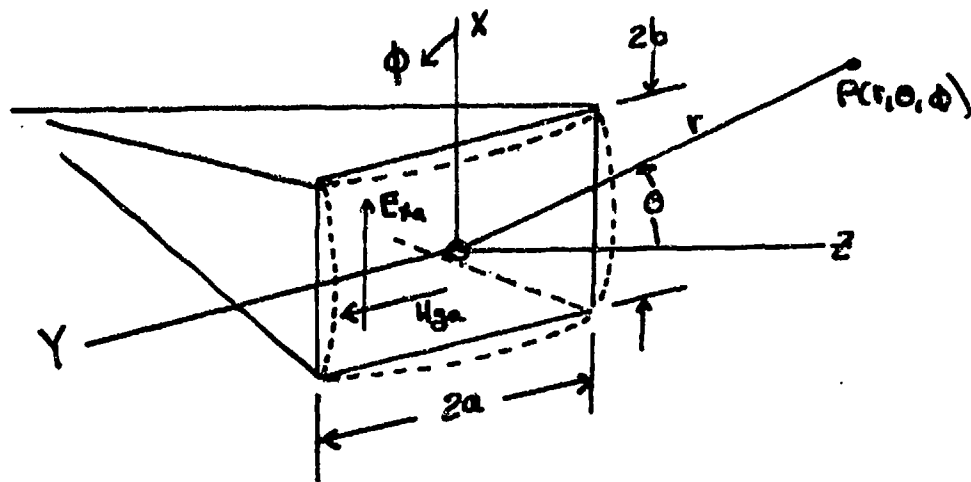
In the backfire direction ( $\theta = \pi$ ), Eq. (14A) yields

$$dE_{\theta} = \frac{j k_v E_{xi} dA e^{-jkr}}{\lambda r} \quad (14C)$$

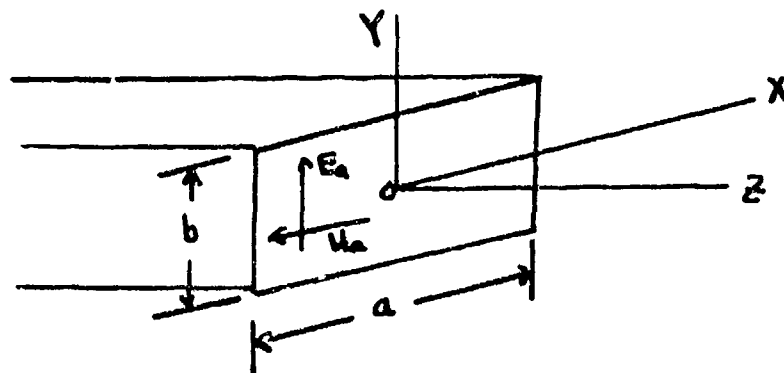
It is to be noted that the radiation in the boresight direction (forward-fire,  $\theta = 0^\circ$ ) is independent of the reflection coefficient  $k_v$ , while that in the backfire direction ( $\theta = \pi$ ) depends entirely upon  $k_v$ . However, the radiation in other directions depends upon both  $k_v$  and the angular direction ( $\theta, \phi$ ), and is the superposition of the two basic cardioids given in Eq. (13), consisting of a "reflectionless" forward-fire cardioid, and a backward-fire cardioid whose magnitude is determined by the reflection coefficient  $k_v$ .

### 2.3.3 RADIATION FROM A FINITE AREA

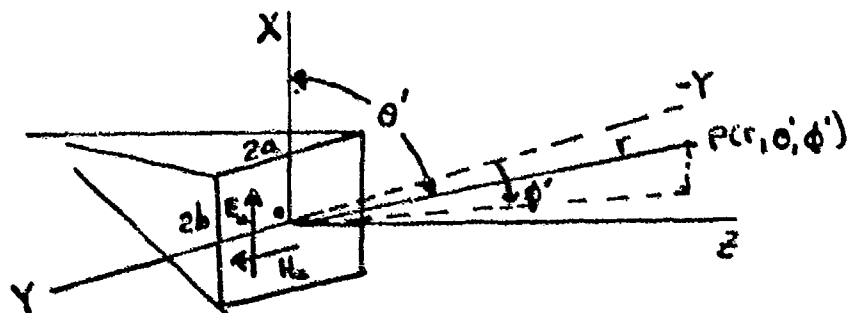
The TEM horn in Maddocks (1974:Fig. 2.1) consists of two circular conducting sectors; the front aperture is a spherical sector at  $r = r_a$ . This is the same as the Sperry Rand horn (Susman and Lamensdorf 1970, 1971). The BD and M 8-inch horn (Martins 1973) Fig. 3(c)) consists of two triangular wedges; the front aperture is a planar rectangle. The two types of horns are assumed to be approximately equivalent, especially for smaller horns with small E-plane flare (Maddocks 1974:chap. 2). Consider a TEM horn front aperture with finite area  $A = 2a \times 2b$ , as shown in Fig. 3(a), excited by an incident TEM wave traveling in the +Z direction, with aperture reflection coefficient  $k_v$ .



(a) TEM horn front aperture, standard spherical coordinates.



(b) Rectangular waveguide aperture,  $TE_{10}$  mode Silver (1949).



(c) TEM horn front aperture and coordinates, Martins (1973).

FIG. 3 Various front apertures and coordinates.

The aperture, which is approximated by a planar rectangle, may be divided up into a large number of differential area sources, similar to the source discussed in 2.3.2 above, where it is assumed that all these sources are excited simultaneously by the incident TEM wave. The aperture may then be treated as a planar rectangular array of these differential sources, and its radiation field will be given by the product of the aperture array space factor (or group factor)  $S_{xy}$  by the radiation from the basic differential area source  $S_{dA}$  (Jordan and Balmain 1968:494) as follows:

$$S_{xy} = \frac{A}{dA} \cdot \frac{\sin(ka \sin \theta \sin \phi)}{ka \sin \theta \sin \phi} \cdot \frac{\sin(kb \sin \theta \cos \phi)}{kb \sin \theta \cos \phi} \quad (15A)$$

$$S_{dA} = \text{given by Eq. (13)} \quad (15B)$$

Eq. (15A) follows from Jordan and Balmain (1968:Eq. (13-60)), with  $a$  replaced by  $2b$  and  $b$  replaced by  $2a$ . The incident  $\vec{E}$  field is polarized parallel to the  $+X$  axis, and  $\vec{H}$  is parallel to the  $+Y$  axis in Fig. 3a, which is the same as in Jordan and Balmain (1968:Figs. 13-14 and 13-16). However, the  $a$  and  $b$  dimensions are interchanged, and doubled in this report. The results are as follows:

$$E_{\theta} = \frac{j E_{xi} e^{-jkr} A \cos \phi}{2 \lambda r} \left[ (1 + \cos \theta) + k_v (1 - \cos \theta) \right] \times \frac{\sin(\kappa a \sin \theta \sin \phi)}{\kappa a \sin \theta \sin \phi} \cdot \frac{\sin(\kappa b \sin \theta \cos \phi)}{\kappa b \sin \theta \cos \phi} \quad (16A)$$

$$E_{\phi} = \frac{-j E_{xi} e^{-jkr} A \sin \phi}{2 \lambda r} \left[ (1 + \cos \theta) - k_v (1 - \cos \theta) \right] \times \frac{\sin(\kappa a \sin \theta \sin \phi)}{\kappa a \sin \theta \sin \phi} \cdot \frac{\sin(\kappa b \sin \theta \cos \phi)}{\kappa b \sin \theta \cos \phi} \quad (16B)$$

Equations (16) are identical with those in Jordan and Balmain (1968, Eqs. (13-61, 62)), with  $a$  replaced by  $2b$  and  $b$  replaced by  $2a$ , and with  $k_v = 0$ , since this reference considers only the reflectionless case. There is a typographical error in Jordan and Balmain (1968, Eq. (13-62)), in that  $\cos \phi$  should be  $\sin \phi$ , as can be seen from Eq. (13-52) in that reference. The radiation patterns in the two principal planes and in the boresight and backfire directions are as follows:

XZ-plane ( $\phi = 0, \pi$ ) or the E-plane:

$$E_{\theta} = \frac{j E_{xi} A e^{-jkr}}{2 \lambda r} \left[ (1 + \cos \theta) + k_v (1 - \cos \theta) \right] \frac{\sin(\kappa b \sin \theta)}{\kappa b \sin \theta} \quad (17A)$$

YZ-plane ( $\phi = \pi/2, 3\pi/2$ ) or the H-plane:

$$E_{\phi} = -\frac{j E_{xi} A e^{-jkr}}{2 \lambda r} \left[ (1 + \cos \theta) - k_v (1 - \cos \theta) \right] \frac{\sin(\kappa a \sin \theta)}{\kappa a \sin \theta} \quad (17B)$$

Boresight (  $\theta = 0^\circ$  ) direction:

$$E_\theta = \frac{j E_{xi} A e^{-jkr}}{\lambda r} \quad (17C)$$

Backfire (  $\theta = 180^\circ$  ) direction:

$$E_\theta = \frac{j k_v E_{xi} A e^{-jkr}}{\lambda r} \quad (17D)$$

#### 2.3.4 COMPARISON WITH SILVER (1949)

Equations (17A,17B) are now compared with similar equations in Silver (1949). These equations are for open-ended circular and rectangular waveguides. Attention is especially directed to the bracketed terms in Eqs. (17A,17B), which specifically show dependence on  $k_v$  and the basic cardioid patterns.

For a circular waveguide, Silver (1949:Eqs. (10-11, 10-13)) gives the radiation equations for  $TE_{mn}$  and  $TM_{mn}$  modes. The quantity  $\beta_{mn}$  in Silver is the phase constant for propagating modes, given by Silver (1949:Eq. (7-15)), and is replaced by  $k = 2\pi/\lambda$  for the TEM mode in a TEM waveguide. Inspection of the bracketed terms Eqs. (10-11,10-13) in Silver, which correspond to those in Eqs. (17A,B) above, putting  $\beta_{mn}/k=1$ , and  $\Gamma = k_v$ , shows that both sets of terms are identical. The remaining terms in

the equations in Silver express the aperture array pattern factors appropriate to the circular waveguide geometry and the structure of the waveguide  $TE_{mn}$  and  $TM_{mn}$  modes, and therefore are not expected to be the same as the corresponding remaining terms in Eqs. (17A,B).

For a rectangular waveguide Silver (1949:Eqs. (10-20, 21,22,23)), the same comparative results as discussed in the preceding paragraph are obtained. Typical bracketed terms (i.e., Silver (1947:Eq. 10-20)) are

$$\left[ 1 + \frac{\beta_{mn}}{k} \cos \theta + \Gamma \left( 1 - \frac{\beta_{mn}}{k} \cos \theta \right) \right] \quad (18A)$$

and

$$\left[ \cos \theta + \frac{\beta_{mn}}{k} + \Gamma \left( \cos \theta - \frac{\beta_{mn}}{k} \right) \right] \quad (18B)$$

which are identical to the corresponding terms in Eqs. (16A) and (16B), respectively, when  $\beta_{mn} = k$  (TEM mode) and  $\Gamma = k_v$ . There is a typographical error in the bracketed term in Eq. (10-22) of Silver for  $E_\phi$ , in that  $\cos \phi$  should be  $\cos \theta$ , which can be verified reference to Eq. (10-20) for  $E_\phi$  in Silver.

In Eqs. (10-23) Silver gives the E- and H-plane patterns of the  $TE_{10}$  mode in rectangular waveguide of dimensions  $a \times b$ . The aperture  $\vec{E}$  field is polarized in the Y direction, so the YX plane is the E-plane, and the XZ-plane is the H-plane of the radiation pattern. See Fig. 3(b). The E-plane equation in Silver (Eq. 10-23a) is repeated below to facilitate comparison

2

with Eq. (17A):

$$E_{\theta} = \frac{2m_0 A b e^{-jk r}}{\pi \lambda^2 r} \left[ 1 + \frac{\beta_{10}}{k} \cos \theta + \Gamma \left( 1 - \frac{\beta_{10}}{k} \cos \theta \right) \right] \frac{\sin \left( \frac{\pi b}{\lambda} \sin \theta \right)}{\frac{\pi b}{\lambda} \sin \theta} \quad (19)$$

Upon replacing  $\beta_{10}/k$  by unity,  $\Gamma$  by  $k_v$ , and  $b$  by  $2b$ , it is seen that the angular-dependent portions of both equations are identical.

### 2.3.5 COMPARISON WITH MARTINS (1973)

Equations (17A,B,C) are now compared with their counterparts, Eqs. (28,27 and 29) respectively in Martins (1973), which are repeated below for convenience.

XZ-plane (Eq.28):

$$E_{\theta}(j\omega, r, \theta', \frac{\pi}{2}) = \frac{V_0(1+R_2) \frac{a}{b} e^{-jk(l+r)}}{2\pi r(1-R_1 R_2 e^{-2jk_2 l}) \cos \theta'} \left[ e^{jk b \cos \theta'} - e^{-jk b \cos \theta'} \right] \quad (20A)$$

YZ-plane (Eq.27):

$$E_{\theta}(j\omega, r, \frac{\pi}{2}, \phi') = \frac{V_0(1+R_2) e^{-jk(l+r)} \tan \phi'}{2\pi r(1-R_1 R_2 e^{-2jk_2 l})} \left[ e^{jk a \cos \phi'} - e^{-jk a \cos \phi'} \right] \quad (20B)$$

Boresight (Eq.29):

$$E_{\theta}(j\omega, r, \frac{\pi}{2}, \frac{\pi}{2}) = \frac{jk V_0(1+R_2) a e^{-jk(l+r)}}{\pi r(1-R_1 R_2 e^{-2jk_2 l})} \quad (20C)$$



In the above equations,  $R_2 = k_v$  = the aperture reflection coefficient, and  $R_1$  = the reflection coefficient at the input, as seen from the horn. The voltage at the aperture  $Z = l$  of the horn is Martins 1973:Eq. (26))

$$V(l) = \frac{V_0 (1+R_2) e^{-j\kappa l}}{1-R_1 R_2 e^{-j2\kappa l}} \quad (21A)$$

where  $V_0$  is the initial traveling voltage wave on the TEM horn line, given by (Martins 1973:Eq. (25))

$$V_0 = \frac{V_g Z_0}{Z_0 + Z_1} \quad (21B)$$

where

$V_g$  = generator voltage

$Z_1$  = feed line impedance

$Z_0$  = TEM horn impedance

The incident TEM wave fields at the aperture are

$$E_{xi} = V_0 / 2b ; H_{yi} = E_{xi} / \eta_0 \quad (21C)$$

The aperture fields are then

$$E_{xa} = \frac{V(l)}{2b} = \frac{E_{xi} (1+R_2) e^{-j\kappa l}}{1-R_1 R_2 e^{-j2\kappa l}} \quad (21D)$$

$$H_{ya} = \frac{E_{xi} (1-R_2) e^{-j\kappa l}}{\eta_0 (1-R_1 R_2 e^{-j2\kappa l})} \quad (21E)$$

These aperture fields do not correspond to a Huygens' source, unless  $R_2=0$ . It is incorrect to compute the radiation from  $E_{xa}$  alone, which is apparently the case in Martins (1973:Eqs. (27-29)).

To simplify the comparison, first put  $R_1=0$  (matched input). This detracts little from generality; in addition, the actual TEM horn was matched (Martins 1973:108). Second, the end bracketed exponential terms in Martins (1973:Eqs. (27,28) are replaced by their  $\frac{\sin x}{x}$  equivalents, as follows:

$$e^{jka\cos\phi'} - e^{-jka\cos\phi'} = j2ka\cos\phi' \frac{\sin(ka\cos\phi')}{ka\cos\phi'} \quad (21F)$$

$$e^{jkb\cos\theta'} - e^{-jkb\cos\theta'} = j2kb\cos\theta' \frac{\sin(kb\cos\theta')}{kb\cos\theta'} \quad (21G)$$

Third, the coordinate system in Martins (1973), designated herein as  $(r, \theta', \phi')$  and shown in Fig. 3(c), are transformed to the spherical  $(r, \theta, \phi)$  coordinates used in this report by the following equations:

$$\cos\theta = \sin\theta' \sin\phi' ; \sin\theta = \sqrt{1 - \sin^2\theta' \sin^2\phi'} \quad (21H)$$

$$\cos\phi = \frac{\cos\theta'}{\sqrt{1 - \sin^2\theta' \sin^2\phi'}} ; \sin\phi = \frac{-\sin\theta' \cos\phi'}{\sqrt{1 - \sin^2\theta' \sin^2\phi'}} \quad (21I)$$

Using the above three steps, omitting the common  $e^{-jkz}$  term, and using  $V_0 = 2b(E_{xi})$  from Eq. (21c), Eqs. (20A,B,C) become the following:

XZ-plane ( $\phi = 0, \pi; \phi' = \pi/2, 3\pi/2$ ) or E-plane: Eq. (20A):

$$E_\theta(j\omega, r, \theta, \frac{\pi}{2}) = \frac{jE_{xi}(1+R_2)e^{-jkr}A}{2\lambda r} \left[ 2 \frac{\sin(kb\sin\theta)}{kb\sin\theta} \right] \quad (22A)$$

YZ-plane ( $\phi = \pi/2, 3\pi/2; \theta' = \pi/2, 3\pi/2$ ) or H-plane; Eq. (20B):

$$E_\theta(j\omega, r, \frac{\pi}{2}, \phi') = \frac{jE_{xi}(1+R_2)e^{-jkr}A}{2\lambda r} \left[ 2\cos\theta \frac{\sin(ka\sin\theta)}{ka\sin\theta} \right] \quad (22B)$$

Boresight ( $\theta = 0, \theta' = \phi' = \pi/2$ ) Eq. (20C):

$$E_\theta(j\omega, r, \frac{\pi}{2}, \frac{\pi}{2}) = \frac{jE_{xi}(1+R_2)e^{-jkr}A}{\lambda r} \quad (22C)$$

Comparison between the corresponding pairs of equations among Eqs. (17A,B,C) and Eqs. (22A,B,C) shows the following differences:

(1) XZ or E-plane:

Eq. (17A) has the factor  $[1 + \cos\theta + R_2(1 - \cos\theta)]$  vs.  $2(1+R_2)$  in Eq. (22A). These are equal only if both  $R_2=0$  and  $\theta = 0$ .

(2) YZ or H-plane:

Eq. (17B) has the factor  $\left[1 + \cos \theta - R_2(1 - \cos \theta)\right]$  vs.  
 $2(1+R_2)\cos \theta$  in Eq. (22B). These are equal only if  
both  $R_2=0$  and  $\theta = 0$ .

(3) Boresight:

There is no  $(1+R_2)$  factor in Eq. (17C).

2.4 RADIATION IN THE BORESIGHT DIRECTION; COMPARISON WITH  
MARTINS (1973)

The radiation in the boresight direction warrants a separate and more detailed discussion, for a number of reasons, such as:

- (a) The general boresight direction is the most important direction for horns used to feed parabolic reflectors.
- (b) The equation for boresight radiation tends to be the simplest one, lending itself to useful closed-form approximations, valuable for insight and for absolute or relative comparisons with results derived by different methods.
- (c) Passage from the  $e^{j\omega t}$  excitation result to a general time domain result is relatively simple.

Comparison between Eqs. (17C) and (22C) shows that the Martins (1973:Eq. (29)) result, for the front aperture alone of the TEM horn, is higher by a factor  $(1+R_2)$ . For the TDR measured value  $R_2=0.7$  (Martins 1973:171), this factor  $=1+0.7=1.7$ . When the radiation in the boresight direction due to the two side

apertures is taken into account, which is not done quantitatively in Martins (1973), then for smaller horns, it has been shown by Maddocks (1974) that the approximate result is to introduce an additional factor of two into the denominator of Eq. (17C). Then the amplitude ratio between the two sets of results is, approximately,

$$\frac{1+0.7}{1/2} = 3.4 \quad (22D)$$

Equations such as (17C, 22C) may be used to infer the response to arbitrary time-waveform excitation by noting that for  $e^{j\omega t}$  excitation  $d/dt = j\omega$ , so

$$\frac{jE_{xi}}{1} = \frac{j\omega E_{xi}}{2\pi c} = \frac{1}{2\pi c} \frac{dE_{xi}}{dt} \quad (23A)$$

Then Eq. (22C) becomes

$$E_{\theta}(t) = \frac{(1+R_2)A}{2\pi rc} \frac{dE_{xi}}{dt} \quad (23B)$$

In the notation of Martins (1973),  $V_0 = V_i(t)$ , so that from Eq. (21C)

$$E_{xi} = \frac{V_i(t)}{2b} \quad (23C)$$

where  $V_i(t)$  is the standard impulse test wave form of amplitude = 384 volts (Martins 1973:173, 212). Then Eq. (23B) becomes, remembering that  $A = 4ab$ ,

$$E_{\theta}(t) = \frac{(1+R_2)4ab}{2\pi rc} \frac{1}{2b} \frac{dV_i(t)}{dt}$$

$$E_{\theta}(t) = \frac{(1+R_2)a}{\pi rc} \frac{dV_i(t)}{dt} \quad (23D)$$

Eq. (23D) is Eq. (95) in Martins (1973). For smaller horns, such as the TEM horn under discussion, it is believed, as stated above, that this result is in error, and should be, approximately,

$$E_{\theta}(t) = \frac{a}{2\pi rc} \frac{dV_i(t)}{dt} \quad (23E)$$

$$\approx \left( \frac{1}{3.4} \right) \text{ value in Eq. (23D)}$$

## 2.5 DERIVATION OF THE BORESIGHT RADIATED FIELDS IN THE TIME DOMAIN, USING THREE DIFFERENT APPROACHES, SMALL TEM HORNS

### 2.5.1 INTRODUCTION

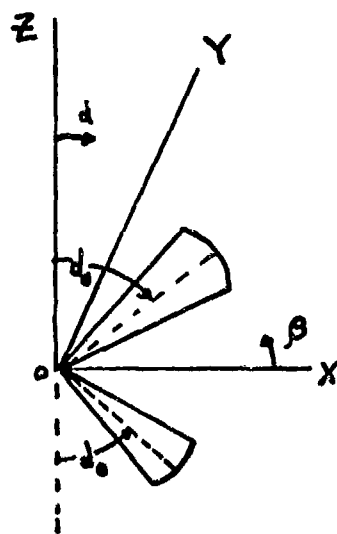
The radiation in the boresight direction (normal to the front aperture of the horn) is important for the reasons discussed in Section 2.4 above. Maddocks (1974) has derived equations for the general radiation fields of general TEM horns, using (1) the Chernousov formulation based upon aperture fields (Maddocks 1974:chap. 2) and (2) a vector potential  $\bar{A}$  formulation based upon the sheet-current flow in the conducting wedges (Maddocks (1974:chap. 3). For smaller horns Maddocks (1974) has developed approximate closed-form equations for the radiation in

the equatorial plane, which include the boresight and backfire directions as special cases. In addition, using a third approach, an equation for the boresight radiation of a small TEM horn is developed in this section based upon a V-dipole model of the horn. To within the accuracy of the small-horn approximations, as described below, all three approaches produce identical results in the boresight and backfire directions. These three approaches and their results are discussed in the following three sections.

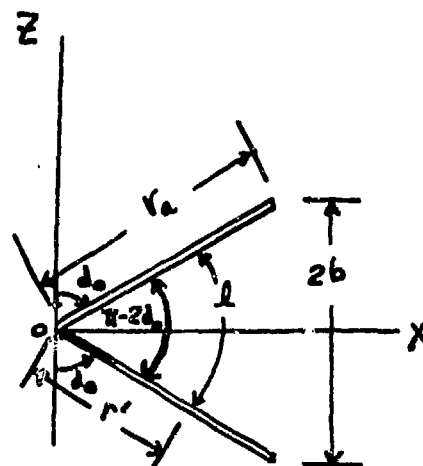
#### 2.5.2 APERTURE APPROACH

Using the Chernousov aperture field approach Maddocks (1974:chap. 2) has derived, strictly in the time domain, the radiation equations for arbitrary time excitation, in any angular direction, for constant-impedance TEM horns. The assumptions involved in this aperture-model of the TEM horn are discussed in Section 2.2. The horn geometry is shown in Fig. 4. The actual front aperture is shown in Fig. 3(a), which is assumed to be approximately equivalent to the planar rectangular front aperture shown in Fig. 4(d), exemplified by the BD and M 8" TEM horn. Field points  $(r, \theta, \phi)$  and horn points  $(r', \alpha, \beta)$  are in standard spherical coordinates as shown.

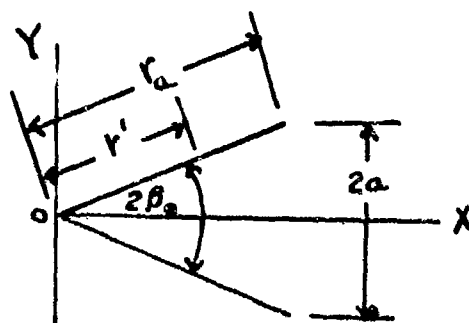
For sufficiently small TEM horns, Maddocks (1974:chap. 2) has derived relatively simple approximate closed-form expressions from the general equations for the radiation in the



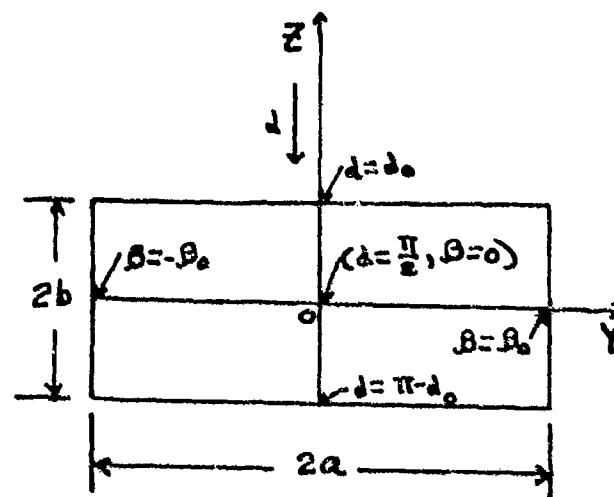
(a) 3-D view



(b) Side view



(c) Top view



(d) Front aperture approximated by planar rectangle

FIG. 4 TEM horn.



equatorial plane (XY or H-plane or horizontal plane, or  $\theta = \pi/2$  plane, for "vertical" E polarization). These are reviewed briefly and discussed below for the boresight direction (+X axis, or  $\theta = \pi/2$ ,  $\phi = 0$ , or "forward-fire" direction).

By a "small horn" is meant a horn with front aperture dimensions such that the aperture travel times are less than or comparable with the characteristic time dimensions of the excitation waveform. The travel time = distance/c, where c = propagation velocity =  $3 \times 10^8$  m/s; one inch = 84.7 psec., one foot = 1,016 psec.  $\approx 1$  nsec. For example the 8" BD and M TEM horn (Martins 1973) has the following aperture dimensions: height  $2b = 1 \frac{5}{16}$ " (travel time = 111 psec.), and width  $2a = 8$ " (travel time = 678 psec.). The IKOR model IMP 100 output voltage waveshape has a pulse width (null-to-null) of approximately 500 psec. (Martins 1973:212). Hence the E-plane dimension ( $2b$ ) of the front aperture is "small". The H-plane dimension ( $2a$ ) is only approximately or quasi-small; this results in "smearing-out" of the details of the radiated time-wave forms.

The traveling-wave exciting TEM fields in the matched-input TEM horn are taken as (Maddocks 1974:Eqs. (2-1,2-2))

$$\bar{E}(r',t) = \frac{f(\alpha,\beta)}{r'} \left[ V_i(t - \frac{r'}{c}) + k_v V_i(t + \frac{r'}{c} - \frac{2r_a}{c}) \right] \hat{a}_0 \quad (24A)$$

$$\bar{H}(r',t) = \frac{f(\alpha,\beta)}{\eta_0 r'} \left[ V_i(t - \frac{r'}{c}) - K_v V_i(t + \frac{r'}{c} - \frac{2r_a}{c}) \right] \hat{a}_\phi \quad (24B)$$

where:

$V_i(t)$  = incident voltage from pulse generator that approaches the input terminals of the feed (e.g., Martins (1973:107)).

$f(\alpha,\beta)$  = illumination amplitude taper factor, discussed below.

$K_v$  = E- field or voltage reflection coefficient at the aperture, determined by TDR measurements (=  $R_2$  in Martins (1973:143)).

The first terms in Eqs. (24) are the incident waves, traveling in the  $+r'$  direction, originating at the horn input, where no further reflections occur, since the horn is assumed to be matched at its input. The second terms in Eqs. (24) are the traveling waves, due to reflection at the front aperture.

For small-aperture horns, especially for small E-plane flare, which is the case for the B" BD and M horn, the  $f(\alpha,\beta)$  factor, which is not the usual illumination taper function, may be evaluated as follows: For the  $+r'$  traveling wave, the  $\bar{E}$  field is given by the usual equation

$$\bar{E}^+(r',t) = \frac{V_i(t - \frac{r'}{c})}{\eta(r')} \hat{a}_\theta \quad (25A)$$

On the other hand, from Eq. (24a),

$$\bar{E}^+(r', t, \alpha, \beta) = \frac{f(\alpha, \beta) V_i(t - r'/c) \hat{a}_\theta}{r'} \approx \frac{f(\frac{\pi}{2}, 0) V_i(t - r'/c) \hat{a}_\theta}{r'} \quad (25B)$$

where  $l(r')$  is shown in Fig. 4(6), and is given by

$$l(r') = (\pi - 2\alpha_0) r' \quad (25C)$$

In equation (25B),  $f(\alpha, \beta)$  has been approximated by its value at the aperture center  $(\frac{\pi}{2}, 0)$ . Then from Eqs. (25A, B, C), it follows that

$$f(\frac{\pi}{2}, 0)(\pi - 2\alpha_0) \approx 1 \quad (25D)$$

The result in Eq. (25D) is needed in the analysis which follows.

In the boresight direction ( $\theta = 90^\circ, \phi = 0^\circ$ ) it can be shown that (Maddocks:1974, chap. 2, Eqs. (2-9, 2-23))

$$\begin{aligned} \frac{4\pi r \bar{E}_\theta(r, \frac{\pi}{2}, 0)}{(\pi - 2\alpha_0) f(\frac{\pi}{2}, 0)} &\approx \frac{4r_a \beta_0}{c} V_i'(T) - \frac{2\sin\beta_0}{1 - \cos\beta_0} \left\{ V_i(T) \right. \\ &\quad \left. - V_i\left(T - \frac{r_a}{c}(1 - \cos\beta_0)\right) \right\} - \frac{2kv\sin\beta_0}{1 + \cos\beta_0} \left\{ \right. \\ &\quad \left. V_i\left(T - \frac{r_a}{c}(1 - \cos\beta_0)\right) - V_i\left(T - \frac{2r_a}{c}\right) \right\} \quad (26) \end{aligned}$$

where  $\tau = t - r/c$  = retarded time, and  $V_i'$  = time derivative of  $V_i(t)$ . The first term in Eq. (26) is the boresight radiation due to the front aperture only, which involves the time-derivative of the excitation waveform. This is typical of boresight aperture radiation in the time domain, when the aperture is excited such that all points have the same value simultaneously (Martins 1973: Eq. 95, Handelsman 1972:96). The second term in Eq. (26) is an approximately derivative-like radiation due to the two side apertures (the approximation involved is discussed below) in the boresight direction. The third and last term is the "backward" radiation (in the boresight direction of the reflected  $-r'$  traveling waves in the two side apertures).

To show the approximation to a time-derivative of the second term in Eq. (26), put

$$\Delta t_B \equiv \frac{r_a}{c} (1 - \cos \beta_0) \quad (27A)$$

then

$$\frac{V_i(\tau) - V_i(\tau - \frac{r_a}{c} (1 - \cos \beta_0))}{1 - \cos \beta_0} = \frac{r_a}{c} \frac{V_i(\tau) - V_i(\tau - \Delta t_B)}{\Delta t_B} \quad (27B)$$

For sufficiently small values of the aperture angular width  $2\beta_0$ , the quantity  $\Delta t_B$  may be treated as differentially small. For example, for the 8" TEM horn (Martins 1973:127),

$$\beta_0 \approx \arcsin\left(\frac{a}{r_a}\right) = \arcsin\left(\frac{4''}{7\frac{3}{8}''}\right) = 33^\circ$$

$$\therefore \Delta t_\beta = \frac{r_a}{c} (1 - \cos \beta_0) = \frac{0.186 \text{ m}}{3 \times 10^8} (1 - 0.84) = 99 \text{ psec.}$$

Comparing this value to the 500 psec. pulse width, it is seen that  $\Delta t_\beta$  is not quite small enough to be treated as a differential. Thus for the 8" horn, the second term in Eq. (26) is more accurately treated as the difference between two functions displaced in time. However, for smaller aperture horns, the differential approximation would become increasingly accurate. It is useful here to retain the derivative approximation, with the understanding that this is a very rough approximation, so as to be able to compare the first and second terms in Eq. (5) on the same basis. Then Eq. (27B) becomes

$$\frac{V(T) - V(T - \frac{r_a}{c} (1 - \cos \beta_0))}{1 - \cos \beta_0} \approx \frac{r_a}{c} V'_i(T) \quad (27C)$$

and the second term in Eq. (26) becomes

$$\frac{2a}{r_a} \frac{r_a}{c} V'_i(T) = \frac{2a}{c} V'_i(T) \quad (27D)$$

Finally, in the third term in Eq. (26) let

$$\frac{2 \sin \beta_0}{1 + \cos \beta_0} = 2 \tan\left(\frac{\beta_0}{2}\right) \approx \frac{a}{r_a} \quad (27E)$$

Substituting Eqs. (25D, 27D, 27E) into Eq. (26), there is obtained

$$\begin{aligned} E_\theta(\text{boresight}) \approx & \frac{a}{\pi r c} V_i'(T) - \frac{a}{2\pi r c} V_i'(T) \\ & - \frac{k_v}{4\pi r} \frac{a}{r_a} \left\{ V_i\left(T - \frac{r_a}{c}(1 - \cos \beta_0)\right) \right. \\ & \left. - V_i\left(T - \frac{2r_a}{c}\right) \right\} \end{aligned} \quad (28A)$$

It is seen that the second term (side aperture radiation) acts to reduce the first term (front aperture radiation) by (approximately) a factor of two. Combining these terms results in

$$E_\theta(\text{boresight}) \approx \frac{a V_i'(T)}{2\pi r c} - \frac{k_v a}{4\pi r c} \left\{ V_i\left(T - \frac{r_a}{c}(1 - \cos \beta_0)\right) - V_i\left(T - \frac{2r_a}{c}\right) \right\} \quad (28B)$$

In Maddocks (1974:Eq. (2-26),  $r_a \beta_0$  appears in place of  $a$  in the first term, and  $\beta_0$  in place of  $(a/r_a)$  in the second term.

In the aperture approach, it is possible to identify the separate contribution of the various apertures, as done above. The front-aperture contribution (first term of Eq. (28A)) differs from the result in Martino (1973:108), which is

$$E_\theta = \frac{(1+R_2)}{\pi c r} a V_i' \quad (29)$$

by the factor  $(1+R_2) = 1+0.7 = 1.7$ . The side-aperture contribution (second term in Eq. (28A)), which is not treated quantitatively in Martins (1973:43,74), turns out to be approximately one-half that of the front aperture, but of opposite sign. When this is taken into account, as in Eq. (28B), the derivative-like field (first term in Eq. (28B)) is less than the result in Martins (1973:108 or Eq. (29) above) by the factor  $2(1+R_2)=3.4$ .

It is worthwhile to note at this point some differences and similarities between aperture and dipole radiation (Appendix A, Eqs. (A-6, A-15)). The front aperture is excited essentially simultaneously, with the result that its boresight radiation is a derivative of the excitation. Both the side apertures and dipoles radiate in similar fashion as they are both excited by traveling waves. They both radiate replicas of the excitation in directions broadside (normal) to their length, and derivatives of the excitation in directions parallel to their length.

### 2.5.3 CURRENT-SHEET APPROACH

This approach is based upon the standard vector potential  $\bar{A}$  formulation (Jordan and Balmain 1968:315), using the current sheets  $\bar{J}$  amps/m which flow on the metal-conductor wedges of the TEM horn. This current model is consistent with the traveling-wave TEM field model discussed in Section 2.2. If  $\bar{H}$  is the TEM magnetic field at any point at the surface of the wedges in the horn, then the linear current density at that

point is given by (Jordan and Balmain 1968:108)

$$\bar{J} = \hat{M} \times \bar{H} \quad (30)$$

Thus  $\bar{J}$  is a TEM-mode current distribution consisting of an incident and a reflected wave. The  $\bar{H}$  field, and therefore the currents  $\bar{J}$  on the outer surfaces of the wedges and any higher non-TEM modes are neglected, consistent with the assumptions discussed for the TEM-fields aperture model in Section 2.2.

The geometrical model of the TEM horn in this current sheet approach is a section of a biconical antenna (Maddocks 1974: chap. 3 and Fig. 3.1). This was found to be strongly necessary to render practicable the analytic integration over the current-sheet surfaces required to calculate the radiation fields. Such integrations are enormously simplified when the surfaces to be integrated over are constant-coordinate surfaces. Thus in the aperture-fields model, these constant-coordinate surfaces are the front aperture (a spherical sector at  $r=r_a$ ) and the two side apertures (at constant angles  $\pm \beta_0$ , respectively). In the current-sheet model, the constant surfaces are the two metal conductors, which in the biconical TEM horn, are surfaces of constant angle  $\alpha = \theta_0$  and  $\alpha = \pi - \theta_0$  respectively (Maddocks 1974: Fig. 3.1).

For small E-plane flare, the biconical-section TEM horn differs only slightly in geometry from the Sperry Rand horn or the 8-inch BD and M horn, which facilitates comparison.



For small-aperture, small E-plane flare biconical-section TEM horns, it has been shown by Maddocks (1974:Eq. (2-26)) that the approximate equation for the equatorial (azimuth) plane radiation reduces, for the boresight direction, to a result which is identical to Eq. (28B) above, obtained using the aperture model. Hence there is no need to repeat this equation here or to discuss it further. The same has been shown for the backfire radiation field. In other directions in the equatorial plane, a comparison between the calculated radiated fields obtained from the two models (aperture-field model and current-sheet model) of the TEM horn is given by Maddocks (1974: Sections 2.4,3.3).

It is, of course, possible to compare the radiated fields due to the two models in any direction by digital computer calculation. This has not been done for the following reason: The aperture-fields model was solved first and programmed for numerical calculation. The current-sheet model was solved later, and in view of the agreement of the approximate analytical expressions between the two models in the boresight and backfire directions, it was not considered worthwhile to expend the considerable time required to program the current-sheet model equations solely for further numerical comparison.

#### 2.5.4 V-DIPOLE APPROACH

It is intuitively obvious that a sufficiently small TEM horn can be approximated as a V-dipole. The smaller the E-

and H-plane flares, and consequently the smaller (narrower) the width of the conductor wedges compared to the excitation waveform's characteristic times, the better this approximation should be. It is shown below, using the results for dipole radiation given in Appendix A, that this approach does indeed lead, with comparative simplicity, directly to the same results for the boresight radiation as given by Eq. (28B), obtained by both the aperture-field and the current-sheet models.

From Appendix A, Eq. (A-6), for a dipole whose geometry is shown in Fig. 5, matched at its input ( $k_0=0$ ) as is the case for the TEM horn, the radiation from one wire, say the upper wire (u.w.), is given by the following equation:

$$\begin{aligned}
 \text{u.w. } E_\theta = & \frac{\mu_0}{4\pi r} \frac{1+\cos\theta}{\sin\theta} \left[ I_i(T) - I_i\left(T - \frac{r_0}{c}(1-\cos\theta)\right) \right] \\
 & + \frac{k_e \mu_0}{4\pi r} \frac{1-\cos\theta}{\sin\theta} \left[ I_i\left(T - \frac{r_0}{c}(1-\cos\theta)\right) - I_i\left(T - \frac{2r_0}{c}\right) \right]
 \end{aligned}
 \tag{31}$$

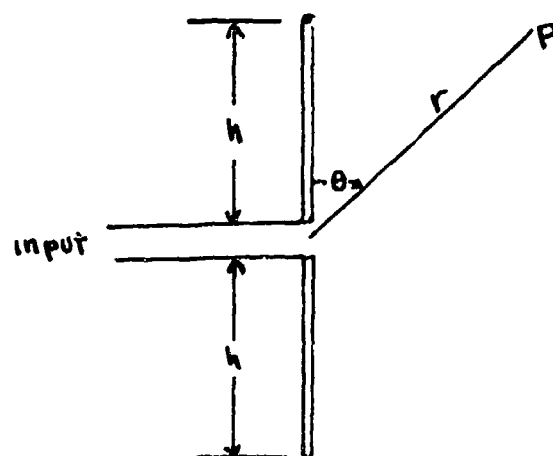
where:

$I_i$  = incident current wave on the dipole

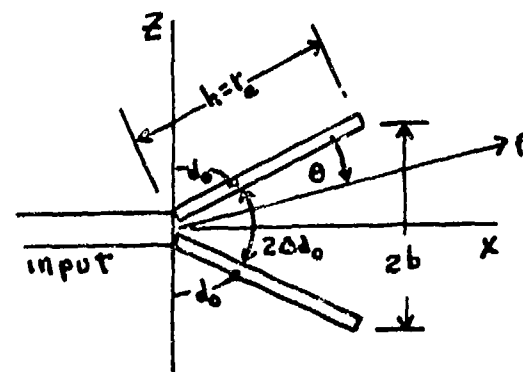
$a = h$  = dipole wire length

$\theta$  = angle measured from dipole wire direction

$k_e$  = current reflection coefficient at ends =  $-k_v$



(a) Straight symmetrical dipole



(b) V-dipole side view

FIG. 5 Dipoles.

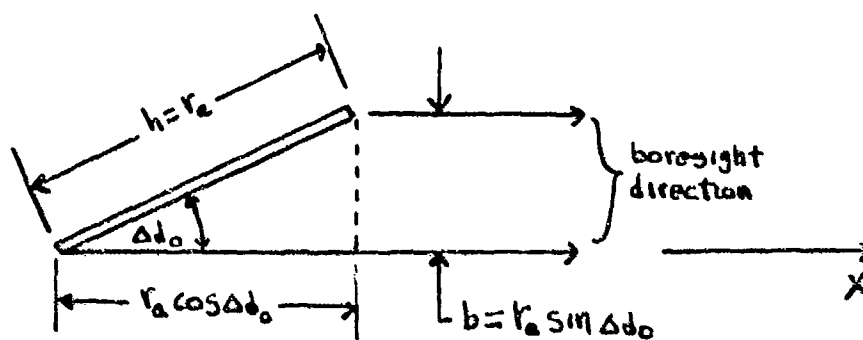


FIG. 6 Boresight radiation, V-dipole upper arm.

The first bracketed term in Eq. (31), designated as  $E_o^+$ , is the radiation due to the forward-traveling wave on the dipole's upper wire. The second bracketed term, designated  $E_o^-$ , is the radiation due to the reflected wave. There are no further reflected waves as the dipole (TEM Horn) is assumed matched at the input.

The boresight direction of the V-dipole is the +X-axis, which corresponds to a value of  $\theta$  given by (see Fig. 5(b))

$$\theta|_{\text{boresight}} = \frac{\pi}{2} - \Delta\phi \equiv \Delta\phi_0 \quad (32)$$

For horns with small E-plane flare, which is the case here,  $\Delta\phi_0$  is sufficiently small so that the quantity

$$\Delta t_d \equiv \frac{r_a}{c} (1 - \cos \theta) = \frac{r_a}{c} (1 - \cos \Delta\phi_0) \quad (33)$$

may be treated as a differential. Thus for the BD and M 8-inch horn (Martins 1973:127) using  $r_a = 7 \frac{3}{8}$  inches = 0.186 m., it follows that

$$\Delta\phi_0 \approx \arcsin\left(\frac{\frac{1 \frac{5}{16}''}{2}}{7 \frac{3}{8}''}\right) \approx 5^\circ$$

$$\Delta t_d \approx \frac{0.186}{3 \times 10^8} (1 - 0.9960) \approx 2.5 \text{ psec.}$$

Hence  $\Delta t_d$  is differentially small compared to a 500 psec. pulse width. From a physical viewpoint,  $\Delta t_d$  = the travel-time difference in the +X-axis direction between radiation leaving the dipole wire at the V-apex (input) and that leaving its end, as illustrated in Fig. 6.

Using the identity

$$\frac{1 + \cos \theta}{\sin \theta} = \frac{\sin \theta}{1 - \cos \theta}$$

and Eqs. (32,33), the u.w.  $E_{\theta}^+$  becomes

$$\begin{aligned} \text{u.w. } E_{\theta}^+ &= \frac{\eta_0}{4\pi r} \frac{r_a}{c} \sin \Delta \theta_0 \left[ \frac{I_i(\tau) - I_i(\tau - \Delta t_d)}{\Delta t_d} \right] \\ \therefore \text{u.w. } E_{\theta}^+ &= \frac{\eta_0 b}{4\pi r c} I_i'(\tau) \end{aligned} \quad (34)$$

Since the dipole is matched at its input, the incident-wave voltage and current are related by

$$I_i(t) = \frac{V_i(t)}{Z_0}; \quad I_i' = \frac{V_i'}{Z_0} \quad (35)$$

where  $Z_0$  is the dipole (TEM horn) and also the input transmission line characteristic impedance = 50 ohms. Hence Eq. (34) becomes

$$\text{u.w. } E_0^+ = \frac{\eta_0 b}{4\pi r c} \frac{V_i'}{Z_0} \quad (36)$$

A simplified equation for the  $Z_0$  of the horn will now be developed. The 50-ohm 8-inch TEM horn has a constant height-to-width ratio  $2b/2a = 1.5/16"/8" = 0.164$ , which is considerably less than unity. For such low ratios, the E field fringing is relatively small. As a result, the horn behaves, to a rough first approximation, as a diverging, constant  $(b/a)$  ratio parallel-plate transmission line (Ramo and Whinnery 1953:320) for which

$$Z_0 = \frac{V}{I} = f \frac{2b}{2a} \frac{E}{H} = f \frac{b}{a} \eta_0 \quad (37A)$$

where  $f$  is a correction factor less than unity which depends upon the  $(b/a)$  ratio. As a specific example, for the 8-inch BD and M horn,  $b/a = 0.164$ ,  $Z_0 = 50$  ohms, and  $f = 50/(0.164 \times 377) = 0.81$ . For smaller  $b/a$  ratios, the  $f$  factor approaches unity, as can be seen from the wave of  $Z_0$  vs.  $b/a$  in Martins (1973:41). Examination of this curve shows that the slope at the origin as the ratio  $(b/a)$  approaches zero, where  $f=1$ , is

$$\left. \frac{dZ_0}{d(b/a)} \right|_{b/a \rightarrow 0} = \eta_0 = 377 \Omega \quad (37B)$$

Hence it is a reasonable and useful approximation for sufficiently small TEM horns to put

$$Z_0 \approx \frac{b}{a} \eta_0 \quad (37C)$$

Alternatively Eq. (37C) is another way of saying that the horn dimensions are sufficiently small so that their corresponding travel-times are significantly less than the exciting waveform's characteristic times. In particular, the width of the 8-inch horn varies from about 1 to 8 inches, with a mean value 4 inches  $\approx$  340 psec. which is not small compared to the 500 psec. null-to-null pulse width. In the dipole approximation to the horn, the actual varying width is modeled as a thin, constant-width wire. The effect of the actual width is to "blur" or "smear" out the details of the radiation waveform based upon a dipole model. From the impedance viewpoint, use of the approximation of Eq. (37C) for the 8-inch TEM horn is not so bad ( $f=0.81$  instead of 1.0); the resultant simplification in the analytic results is worthwhile.

From Eqs. (36, 37C),

$$\text{u.w. } E_{\theta}^{+} = \frac{a V_i'}{4\pi r c} \quad (37D)$$

The lower wire of the V-dipole contributes an equal amount, so that for the entire dipole

$$\text{boresight } E_{\theta}^{+} = \frac{a V_i'}{2\pi r c} \quad (37E)$$

It is seen that Eq. (37E) is exactly the same as the first term in Eq. (28B) above due to the forward-traveling wave, obtained during the aperture-field approach. It now will be shown that the  $\vec{E}_\theta^-$  radiation term (second bracketed term in Eq. (31)) for the entire V-dipole is identical to the second and remaining term in Eq. (28B).

The u.w.  $\vec{E}_\theta^-$  term in Eq. (31), using Eqs. (32,33,35), becomes

$$\text{u.w. } \vec{E}_\theta^- = \frac{-k_v m_0}{4\pi r} \frac{1 - \cos \Delta \theta_0}{\sin \Delta \theta_0} \left[ \frac{V_i}{Z_0} (T - \Delta t_d) - \frac{V_i}{Z_0} \left( T - \frac{2r_a}{c} \right) \right] \quad (38A)$$

Using

$$\frac{1 - \cos \Delta \theta_0}{\sin \Delta \theta_0} \approx \frac{\Delta \theta_0}{2} \quad (38B)$$

and Eq. (37C),

$$\frac{m_0}{Z_0} \frac{(1 - \cos \Delta \theta_0)}{\sin \Delta \theta_0} = \frac{a}{b} \frac{\Delta \theta_0}{2} = \frac{\beta_0}{2} = \frac{a}{2r_a} \quad (38C)$$

Hence Eq. (38A) becomes

$$\text{u.w. } \vec{E}_\theta^- = \frac{-k_v \beta_0 / 2}{4\pi r} \left[ V_i (T - \Delta t_d) - V_i \left( T - \frac{2r_a}{c} \right) \right] \quad (38D)$$



The lower wire of the V-dipole contributes an equal amount, leading to the following total  $E_{\theta}^{-}$  field:

$$\text{boresight } E_{\theta}^{-} = \frac{-k_V \beta_0}{4\pi r} \left[ V_i(\tau - \Delta t_d) - V_i\left(\tau - \frac{2r_a}{c}\right) \right] \quad (38E)$$

The complete boresight field for the V-dipole is the sum of Eqs. (37E, 38E), given by

$$\text{boresight } E_{\theta} = \frac{a V_i'}{2\pi r c} - \frac{k_V a}{4\pi r r_a} \left[ V_i(\tau - \Delta t_d) - V_i\left(\tau - \frac{2r_a}{c}\right) \right] \quad (39)$$

In the dipole approximation to the TEM horn, the horn size must be sufficiently small so that the aperture width  $2a$  and azimuth angle  $2\beta_0$  are small, at least to first order. It then follows that the quantity  $\frac{r_a}{c}(1 - \cos \beta_0)$  in Eq. (28B) is small to second order, i.e., it is differentially small compared to the excitation waveform's characteristic times. Then both this quantity and  $\Delta t_d = \frac{r_a}{c}(1 - \cos \Delta \beta_0)$  in Eq. (39) are differentially small, and both may be neglected in the arguments of the second terms of Eqs. (28B) and (39), respectively. Then the V-dipole radiation equation of Eq. (39) becomes identical to the aperture-fields radiation equation given by Eq. (28B), in the small TEM horn case.

Equation (39) will now be interpreted. The first term is the derivative of the excitation, and is due to the forward-traveling wave on the dipole (horn). The second term, due to the reflected wave, (first term in the brackets) is a negative replica of the excitation waveform, slightly displaced in time by  $\Delta t_1$ , which is very small compared to the pulse length, and with an amplitude approximately 1/8 that of the first term, in the case of the BD and M 8" horn, as shown below. Thus the second term acts to decrease the positive swing and to increase the negative swing of the derivative term by a factor of about 1/8. The radiation then goes to zero until time  $T = 2 r_a/c$ , which occurs when the traveling wave returns to the apex. At this time the third term (second term in brackets) produces a positive replica of the excitation, reduced in amplitude by 1/8. Examination of the theoretical computer-calculated curve for the boresight radiation of the 8" horn obtained by Maddocks (1974: Fig. 2.7) shows precisely this behavior. It is considered remarkable that the simple V-dipole model can obtain results so similar to the more complicated aperture-field model.

The ratio of amplitudes of the two types of terms in Eq. (39) is

$$\text{ratio} = \frac{aV_i'}{2\pi r c} \cdot \frac{4\pi r r_a}{k_v a V_i} = \frac{2 r_a V_i'}{k_v c V_i} \quad (40)$$

For the 8" TEM horn, this ratio is 7.8, using  $r_a = 7 \frac{3}{8}" = 0.178 \text{ m}$ ;  $k_v = R_2 = 0.7$ ,  $V_i = 384 \text{ volts}$ , and maximum  $V_i' = 1.67 \times 10^{12} \text{ volt/sec}$  (Martins 1973:139). In terms of absolute values, the quantity  $(rE_\theta)$  corresponding to the first term in Eq. (39) is

$$rE_\theta = \frac{aV_i'}{2\pi c} = \frac{0.1016 \times 1.67 \times 10^{12}}{2\pi \times 3 \times 10^8} = 90 \text{ volts}$$

This agrees well with the amplitude of the first peak of the computer-calculated theoretical curve for the 8" TEM horn in Fig. 2.7 of Maddocks (1974), whose value  $4.1 \times 10^{-2}$  corresponds to

$$rE_\theta = 4.1 \times 10^{-2} \times (5.62) \times (384) = 88.5 \text{ volts}$$

The first multiplier (5.62) is the  $f(d, \theta)$  factor discussed in Maddocks (1974, chap. 2), and the second multiplier (384) is necessary to convert from the unity-amplitude pulse of Maddocks (1974) to the 384 volt-amplitude pulse of Martins (1973). The value 7.8 of the ratio as given by Eq. (40) above also agrees well with that read off from Fig. 2.7 of Maddocks (1974) which is, approximately,  $4.1/0.5 = 8.2$ .

## 2.6 COMPARISON OF THEORY WITH EXPERIMENT

### 2.6.1 COMPARISONS USING NORMALIZED CURVES

Comparison between theory and experiment for TEM horns is given by Maddocks (1974). He compares curves of  $(rE_\theta)$  vs. time for three different Sperry-Rand horns, for various azimuthal

(H-plane) angles, against experimental data obtained by Susman and Lamensdorf (1970:42-44). These comparison curves appear in Maddocks (1974, Figs. 2.3,2.4,2.5). In general, the agreement can be seen to be reasonably good. For further discussion see Maddocks (1974, Section 2.4). The curves necessarily are presented normalized to equal peak values as the experimental data is given in relative, not absolute values.

Maddocks also compares curves of ( $rE_\theta$ ) vs. time for the 8" BD and M TEM horn, for three azimuthal angles, against experimental data obtained by Martins (1973, Figs. 55a,b,c,114c). These comparison curves appear in Maddocks (1974, Figs. 2.7,2.8, 2.9). The theoretical vs. experimental curves for the boresight direction,  $\phi = 0^\circ$ , (Maddocks 1974, Fig. 2.7) are normalized to the same peak value. The next two sets of curves for azimuth directions  $\phi = 50^\circ, 100^\circ$  (Maddocks 1974, Figs. 2.8,2.9) are each drawn with the same relative scale factor as established for the two curves in the  $\phi = 0^\circ$  case. The agreement can be seen to be reasonably good. For further discussion of these curves, see Maddocks (1974, Section 2.6).

The theoretical curves were not compared on an absolute basis against the available absolute experimental data (Martins 1973) because, as of the time of this report, there exist a number of unresolved questions concerning the calibration and/or self-consistency of this experimental data. This is discussed in Section 2.6.2 below.

## 2.6.2 DISCUSSION OF PREDICTED VS. MEASURED RESULTS OBTAINED BY MARTINS (1973)

The experimental program reported in Martins (1973) measured the radiation fields of a number of primary feed antennas, with and without reflectors, in both transmit and receive modes, using various sensor antennas (Martins 1973:144). The sensors were calibrated essentially by the measured radiation from the base of a long monopole/dipole antenna (Martins 1973:125), of which one part consists of the extended center conductor of a coaxial cable, tapered out over a 0.075" transition to a 3/8" diameter rod 50" long, and the other part consists of the 3/8" diameter solid aluminum sheath, approximately 10' long. The absolute scale of this set of measurements was established by an equation for the radiation from the base of this monopole/dipole feed, given by Martins (1973, Eq. (94)). As shown in Appendix A, Section 7, this equation is derived for a center-fed balanced dipole. This poses an obvious question concerning the equivalence between the actual monopole/dipole used in the experimental program, and a balanced dipole.

A second question (or rather a set of inter-related questions) is pointed out by Martins (1973) in his Tables 10, 11, and 12. Table 10 compares predicted and measured transmit and receive crest amplitudes for six different feeds on boresight at a range of 25 feet. The six feeds include the long monopole/dipole, constant-impedance 3" and 8" TEM horns, a variable-impedance horn, a bicone, and a bow tie antenna. Agreement between

measured and predicted values for all six feeds in the transmit mode is very good. The predicted values are based upon the theoretical development in Martins (1973). For example, for the 8" TEM horn, the Martins (1973, Eq. (95)) result given in Eq. (23D) is used. However, for three of the feeds in the receive mode, differences between predicted and measured values are noted by Martins (1973:181,182,205) being as large as 3:1 for the 3" TEM horn and 4:1 for the 8" TEM horn and for the bicone. The predicted values in the receive mode for each feed are based upon use of the reciprocity theorem together with the transmit mode transfer functions derived for that feed (Martins 1973: 176,181). In addition to the above discrepancies as reported by Martins, another problem is posed because, as discussed in Section 2.4, Martins' transmit Eq. (23D) for the 8" TEM horn is thought to be too large by a factor of 3.4. This implies that problems also exist in the transmit mode comparisons, for which the reported agreement is good. Finally, Tables 11 and 12 in Martins (1973) concern various feed and reflector combinations. Since the same types of problems carry over into these antenna combinations, there appears to be no point in repeating the above discussion.

Because of the lack of self-consistency between predicted and measured results in the Martins (1973) report, it was not deemed advisable to use the Martins experimental data on an absolute basis in this report.

## CHAPTER 3

### TRANSIENT RADIATION FROM A PARABOLOID

#### 3.1 INTRODUCTION

This chapter is intended to serve principally as an introduction to the characteristics of the transient radiation of a paraboloidal antenna. A much more complete and detailed time-domain analysis, using the Chernousov formulation, is given by Maddocks (1974) for the radiation fields in any direction.

Maddocks (1974) also presents digital-computer calculation and graphs for the radiation time-waveforms in a number of specific directions, including the boresight direction. The paraboloidal reflector-feed coordinate systems are shown in Maddocks (1974, Figs. 4.1, 4.2). The analysis by Maddocks (1974) includes two types of feeds. The first is a hypothetical point source feed, with an isotropic radiation pattern, at least over the solid angle subtended by the paraboloid. The second feed is the BD and M 8-inch TEM horn. For this second feed, Maddocks (1974, Fig. 5.7) compares the theoretical graph of  $E$  vs. time with an available experimental curve presented by Martins (1973: 235) for the 48-inch diameter paraboloidal reflector. The agreement between the shapes of the two curves is quite good, both curves being normalized to the same maximum value.

The first type of feed described above is important as it produces an almost-uniform TEM field excitation (illumination) over the exit aperture of the 48-inch reflector. The

closeness of the approximation to uniformity is discussed later in this chapter. The uniform illumination case is important, as it permits derivation of a simple equation for the boresight radiation, which is useful for the reasons given in Section 2.4. As shown below, an equation for the boresight radiation in this case can be calculated in a simple, closed form, with relative ease using only time-domain techniques (almost a "back-of-the-envelope" type of calculation). This result agrees with an equation given by Martins (1973:109) without proof, but presumably using the method embodied in Eq. (23A) above. This, also, is discussed in more detail below.

By contrast, for non-uniform illumination, the equations for the radiation fields are of a complexity such that, even for the restricted case of the boresight direction, it has not been possible to date (Maddocks 1974, chap. 5) to obtain a simple, closed-form expression. Thus the fields, of necessity, must be calculated by digital-computer evaluation of equations involving various integrals which depend upon the feed pattern and the reflector-feed geometry.

### 3.2 ASSUMPTIONS

The radiation fields of the paraboloid reflector are calculated using the Chernousov formulation assuming that only the fields over the exit aperture of the reflector are non-zero. All other fields and edge effects are neglected. The reflector



is assumed to be perfectly conducting, and in the far field of the feed. The feed is assumed to be effectively a point source at the focus. The commonly-used geometrical-optics approximation is assumed, which results in a one-to-one correspondence between the fields at the reflector surface at which plane-wave boundary conditions are invoked, and the fields over the exit aperture. The theory underlying this approach is given in Silver (1949, Sections 4.4-4.6, 12.2, 12.3). The reflector/feed geometry as given in Maddocks (1974, Fig. 4.1) follows closely, but not exactly, the geometry used by Silver (1949:416), and is repeated here for convenience in Fig. 7.

### 3.3 EXIT-APERTURE EXCITATION PRODUCED BY AN ISOTROPIC PRIMARY FEED

The field intensity due to an isotropic primary feed at origin  $O$ , which is the focal point of the paraboloid, varies inversely as the distance  $\rho$  from  $O$  to the point  $P'$  on the paraboloid surface. The point  $P$  on the exit aperture which corresponds to point  $P'$ , is the projection of  $P'$  on the exit aperture, as shown in Fig. 7. To find the aperture field, following Silver (1949:419), it is noted that all the reflected rays  $P'P$  are parallel. Hence the fields remain constant in magnitude along the reflected rays. The field  $\bar{E}$  at point  $P(r, \xi)$  in the aperture is then the same as the field  $\bar{E}$  at point  $P'(\rho, \xi, \psi)$  on the reflector, except for the time retardation  $\overline{P'P}/c$  due to the path-length distance from  $P'$  to  $P$ .



The  $\bar{E}$  field at any point  $P'(\rho, \xi, \psi)$  on the reflector varies as  $1/\rho$  for an isotropic source feed. There is no variation with angle  $(\xi, \psi)$ . There is a spatial variation with distance as  $1/\rho$ . This may be seen from Silver (1949:418, Eqs. (6,7)), in which  $G_f(\xi, \psi)$  is a constant. Then the  $\bar{E}$  field at the corresponding point  $P(r, \xi)$  also varies as  $1/\rho$ . Thus an isotropic primary feed produces a field over the exit aperture of the paraboloid whose amplitude has a taper governed by the  $1/\rho$  variation. The maximum value of this taper is the ratio of the maximum value of  $\rho (= \bar{\rho} = f)$  to the value of  $\rho (= \rho_0)$  at the reflector edge. For the 48-inch BD and M paraboloidal reflector (Martins 1973:135),  $D = 48"$  and  $f = 20.16"$ . From Silver (1949:415,416):

$$\Psi = \arcsin \left[ \frac{D/2f}{1 + (D/4f)^2} \right] = 61^\circ 33' \quad (41A)$$

$$\rho_0 = f \sec^2(\Psi/2) = 27.3" \quad (41B)$$

Hence the amplitude taper is  $27.3/20.16 = 1.35$ , or the power taper is 2.6 db; the field at the edges of the paraboloid being 2.6 db down from that at the center. This taper is not far from uniform, being much less than the usual tapers of 10 db or more, common in many systems.

It will be convenient, for the reasons previously explained, to assume that a constant amplitude field exists across the exit aperture (defined as uniform amplitude excitation or illumination), as generated by a TEM wave. For the same excitation E field at the center of the aperture, the actual tapered illumination produces a smaller radiated boresight field than the uniform illumination. The radiated boresight field depends directly upon the product of the aperture area and the time derivative of the exciting waveform as shown below. By dividing the area of the circular exit aperture into a number of equal subareas, it is then simple to show, using numerical integration, that the boresight field due to the hypothetical uniform excitation is larger than that due to the actual tapered excitation by a factor of approximately 1.12 for the 48 inch reflector discussed above. This result is used later.

In a paraboloid/primary feed system, all path lengths from the focus O to the exit aperture are equal, i.e.,

$$OP' + P'P = \rho_0 \quad (42)$$

It is assumed that such a point as O exists, corresponding to equal retardation times in the time domain due to a "point" source, or the phase center in the frequency domain. Hence all points in the exit aperture are excited simultaneously relative to the primary source at O. Therefore, in the time domain, the fields in the exit aperture follow, in time, the source excitation waveform, retarded by  $\rho_0/c$  seconds. Hence the temporal behavior

of the aperture excitation is the same that produced by a planar TEM wave. The paraboloid transforms the spherical wave from the feed into this planar wave over the exit aperture.

The spatial and temporal characteristics of the excitation fields over the exit aperture have now been shown to be closely correspondent to those produced by a planar TEM wave. It now remains to discuss the polarization characteristics of the aperture fields, and the correspondence to a linearly polarized planar TEM wave. For a linearly polarized primary feed, or equivalently, the  $\theta$ -polarized source field of Maddocks (1974, chap. 4), the resultant aperture field has both principal and cross-polarized polarization components as shown in Silver (1949, Fig. 12.2). The principal component (shown vertical or in the E-plane direction in Silver), which is parallel to the principal E-plane of the feed, is all in the same direction over the aperture, and significantly larger in magnitude than the cross-polarized component (shown horizontal or in the H-plane direction in Silver), especially over the central sections of the aperture. In addition, the cross-polarized components are not in the same direction at various points in the aperture, being anti-symmetrical with respect to the principal planes or the boresight direction. As a result, in the principal planes (and therefore also in the boresight direction), it is pointed out by Silver (1949:422) that the field is linearly polarized in the direction determined essentially by the principal polarization component of the aperture field. Hence, for practical

purposes, in calculating the radiated boresight field, it is a good assumption to use an aperture field that is linearly polarized, exactly the same as that produced by a linearly polarized planar, TEM wave.

In summary, it has been shown that the exit-aperture excitation produced by a primary feed which is isotropic in all directions, or at least isotropic over the solid angle subtended by the reflector, may be approximated by a planar TEM wave with regard to amplitude, temporal and polarization characteristics. The actual excitation amplitude is tapered, which results in a boresight field less than that produced by uniform illumination by a factor of approximately 1.12 for the BD and M 48 inch reflector. The temporal characteristics of the excitation are exactly the same as for a planar TEM wave. The polarization characteristics of the excitation, as far as the radiation in the principal planes and in the boresight direction is concerned, is essentially linear and therefore the same as that for a planar, linearly polarized TEM wave. The approximate TEM wave nature of the exit aperture fields is used in the following section to obtain a simple equation for the boresight radiation.

For the radiation in any direction, the more general and precise formulation and computer-calculated results by Maddecka (1979) must be consulted.

### 3.4 PRINCIPAL-PLANE RADIATION FROM A RECTANGULAR APERTURE WITH TEM-WAVE EXCITATION

Chernousov (1965, Eq. (16)) derives an equation for the transient radiation from a planar rectangular aperture of dimensions  $a \times b$ , in the XY plane, radiating in the Z direction. The aperture is excited so that the field at any point in the aperture at any given time has the same value. The aperture field  $\bar{E}_i$  is polarized in the Y direction, and  $\bar{H}_i$  is in the -X direction.

For the case where  $\bar{E}_i, \bar{H}_i$  form the front of an advancing, free-space TEM wave (a Huygens-type source), Chernousov derives the following equation for the radiation pattern in a principal plane such as the XY plane:

$$E(\bar{r}, t) = \frac{A(1 + \cos\theta)}{4\pi cr} \left[ \frac{E_i(T + \tau_a) - E_i(T - \tau_a)}{2\tau_a} \right] \quad (43A)$$

where:

$A$  = area =  $ab$

$\theta$  = polar angle with respect to the Z axis

$T$  =  $t - r/c$  = retarded time

$$\tau_a = \frac{a \sin\theta}{2c} \quad (43B)$$

For the radiation in the other principal plane YZ, replace

$\tau_a$  by  $\tau_b = b \sin\theta / (2c)$  in Eq. (43). Thus the radiation in both principal planes can be calculated.

From Eq. (43B) it is seen that  $\tau_a$  is the travel-time difference between the path lengths from the aperture edges  $x = \pm a/2$  and the origin  $O$ . Thus the radiation in the XZ plane is the difference between two waves which appear to originate at the aperture ends  $x = \pm a/2$ . Each wave has the same time waveform as the exciting TEM wave, but has different delay times dependent upon the angle  $\theta$ . For a one-dimensional antenna (linear aperture), an equation similar to Eq. (43) has been derived by Cheng (1964).

For sinusoidal time excitation  $e^{j\omega t}$ , the general time-domain result Eq. (43) reduces to the previously-derived Eq. (17B) as will now be shown. Since Eq. (43) is based upon a reflectionless TEM wave excitation, then  $k_v = 0$ . Equation (17B) is based upon an aperture dimension  $2a$ , so  $a$  must be replaced by  $2a$  in Eq. (43). Use

$$E_i(t \pm \tau_a) = E_i e^{j\omega(t - r/c \pm \tau_a)} = E_i e^{j\omega t} e^{-jkr} e^{\pm j\omega \tau_a} \quad (44A)$$

Drop  $e^{j\omega t}$ , and use

$$\omega \tau_a = 2\pi f \left( \frac{2a \sin \theta}{2c} \right) = ka \sin \theta \quad (44B)$$

Equation (43A) becomes



$$E = \frac{A(1+\cos\theta)e^{-jkr}}{4\pi cr} \cdot \frac{(e^{jka\sin\theta} - e^{-jka\sin\theta})}{(2) \frac{2a\sin\theta}{2c}}$$

which reduces to

$$E = \frac{jE_i A e^{-jkr}}{2\lambda r} (1+\cos\theta) \cdot \frac{\sin(ka\sin\theta)}{ka\sin\theta} \quad (44C)$$

Equation (44C) is identical to Eq. (17B) with  $k_y = 0$ . The minus sign in Eq. (17B), which does not appear in Eq. (44C) is due to an  $E_{xi}$  polarization for Eq. (17B) and  $E_{yi}$  for  $E_i$ . (43A). This confirms that the radiation produced by  $e^{j\omega t}$  excitation is a special case of the general Chernousov time-domain Eq. (43).

### 3.5 BORESIGHT RADIATION FROM ANY PLANAR APERTURE WITH TEM-WAVE EXCITATION

In the boresight direction  $\theta = 0$ , the bracketed quantity in Eq. (43A) becomes the time derivative  $E'_i$  of the aperture field, and  $(1+\cos\theta)$  is replaced by two. Thus the boresight radiation field magnitude is

$$E_{\text{boresight}} = \frac{AE'_i}{2\pi rc} \quad (45)$$

The boresight field due to uniform aperture excitation (or flat-plate scattering) therefore depends upon the area  $A$  of the aperture (or plate) and the time derivative of the exciting waveform.

Equation (45) is valid for any planar area A, independent of its shape or contour, excited by a uniform, planar, linearly-polarized, reflectionless TEM wave. This point is made by Martin (1973:94).

For a circular aperture of diameter D, such as the exit aperture of a paraboloid of revolution, Eq. (45) becomes

$$E_{\text{boresight}} = \frac{D^2 E_i'}{8rc} \quad (46)$$

Equation (46) is given by Martins (1973:109). Alternatively, Eq. (46) follows from the equation for the radiation field of a circular aperture, with  $e^{j\omega t}$  excitation, which is (Silver 1949: 194)

$$E = \frac{2jAE_i e^{-jkr}}{\lambda r} \cdot \frac{J_1(ka \sin \theta)}{ka \sin \theta} \quad (47A)$$

For boresight  $\theta = 0$ ; then using Eq. (23A) and

$$\lim_{x \rightarrow 0} \frac{J_1(x)}{x} = \frac{1}{2} \quad (47B)$$

and dropping the  $e^{-jkr}$  factor, Eq. (47A) reduces to Eq. (46).

### 3.6 RATIO OF PARABOLOID TO PRIMARY FEED BORESIGHT FIELDS

#### 3.6.1 ISOTROPIC FEED APPROXIMATION TO TEM HORN

When a primary feed is used to excite a secondary reflector, a natural measure of the gain obtained through use of the reflector is the ratio of the boresight field of the

combination (or system) to that of the feed alone, at the same range. This ratio is calculated below for the system consisting of the BD and M 48" paraboloid and the 8" TEM horn (Martins 1973, Figs. 32b, 33b). The intent is to obtain this ratio using simple approximations, and to check it against the more exact computer-calculated results of Maddocks (1974).

By an isotropic feed in this instance is meant a feed with zero angular variation in gain at least over the solid angle subtended by the reflector. As a rough first approximation, it will be assumed that the 8" TEM horn can be modeled as such a feed. The tapered illumination actually produced in the paraboloid's exit aperture by the horn is treated in detail by Maddocks (1974, Section 5.4).

The peak amplitude boresight field  $E_h$  produced by the horn is given by Eq. (28B):

$$E_h = \frac{aV_i'}{2\pi rc} \quad (48A)$$

The excitation time waveform will be the BD and M "standard impulse" shape (Martins 1973:139,140), for which

$$V_i(t) = V_i e^{-dt^2} \quad (48B)$$

where  $V_i = 384$  volts and  $d = 2.4 \times 10^{19} \text{ sec}^{-2}$ . It then follows that (Martins 1973:140)

$$V_i'_{\max.} = \sqrt{\frac{2d}{e}} V_i = 0.86 \sqrt{d} V_i = 1.62 \times 10^{12} \text{ volts/sec} \quad (48C)$$

$$V_i''_{\max.} = 2d V_i' = 1.84 \times 10^{22} \text{ volts/sec}^2 \quad (48D)$$

when the horn is the primary feed, the field at the center of the paraboloid aperture  $E_{ap}$  is given by Eq. (48A), with  $r$  replaced by focal length  $f$ :

$$E_{ap} = -\frac{aV_i'}{2\pi fc} \quad (49A)$$

The field elsewhere in the aperture then varies as  $1/\rho$  as described in Section 3.3, under the approximation of an isotropic feed. The paraboloid boresight field  $E_p$  is then given by Eq. (46), modified by the 1.12 factor derived in Section 3.3. Hence

$$E_p = \frac{1}{1.12} \cdot \frac{D^2 E_{ap}'}{8rc} = \frac{1}{1.12} \cdot \frac{D^2}{8rc} \cdot \frac{aV_i''}{2\pi fc} \quad (49B)$$

Note the second time-derivative nature of this field. The first differentiation occurs at the aperture of the horn, and the second at the aperture of the reflector.

The ratio of paraboloid to horn boresight fields is, from Eqs. (48A, 49B),

$$\frac{E_p}{E_h} = \frac{1}{1.12} \frac{D^2}{8fc} \frac{V_i''}{V_i'} \quad (50A)$$

Substituting numerical values,  $f = 20.16''$ ,  $D = 48''$ , and  $V_i'$ ,  $V_i''$  as given by Eqs. (48C, 48D), then

$$\frac{E_p}{E_h} = 12.3 \quad (50B)$$

The above value is now compared with that obtained from the computer-calculated curves in Maddocks (1974). Reading from his curves in Figs. 2.7 and 5.5, respectively,  $rE_h = 4.1 \times 10^{-2}$  volts and  $rE_p = 4.8 \times 10^{-1}$  volts, so that

$$\left. \frac{E_p}{E_h} \right|_{\text{computer}} = \frac{4.8 \times 10^{-1}}{4.1 \times 10^{-2}} = 11.7 \quad (50C)$$

Equations (50B) and (50C) agree to within 5 percent.

Thus, the relatively simple, closed-form expression Eq. (50A) yields a very good approximation to the computer-calculated value. This is made possible by the approximation of the horn feed as an isotropic source. This is not the case for the actual horn, as discussed in section 3.6.2 below.

A cross-check is afforded by comparing  $E_h$  and  $E_p$  calculated separately from approximate equations (48A, 49B) with the values calculated by digital computer from the complete equation (Maddocks 1974, Figs. 2.7, 5.5). The curves in these figures are for unit amplitude pulse and unity horn illumination function. For the BDM pulse ( $V_i = 384$ ) and 8" horn ( $f(a, \beta) = 5.62$ ), multiply the curve values by  $384 \times 5.62 = 2158.1$ . Substituting numerical values  $a = 4'' = 0.1016$  m.,  $V_i' = 1.62 \times 10^{12}$ ,  $D = 48'' = 1.219$  m.,

$f = 20.16'' = 0.512 \text{ m.}$ , and  $V_i'' = 1.84 \times 10^{22}$  into Eqs. (48A,49B) results in  $rE_h = 87.3 \text{ volts}$ , and  $rE_p = 1072.6 \text{ volts}$ . These compare very well with the values read from Figs. 2.7 and 5.5 in Maddocks (1974):  $rE_h = 4.1 \times 10^{-2} \times 2158.1 = 88.5$  and  $rE_p = 0.48 \times 2158.1 = 1035.9$ , respectively. The ratio  $E_p/E_h = 1072.6/87.3 = 12.3$ , as before (Eq. 50B).

### 3.6.2 ACTUAL 8-INCH TEM HORN FEED

For the actual 8" TEM horn feed, no "simple" approximate model of its fields over the paraboloid's exit aperture has been found. Maddocks (1974, Section 5.2) has solved the problem of modeling the horn's field by expressing this field in terms of an empirical equation, containing five constants adjusted to fit the horn's radiation patterns. The resultant boresight radiation waveform of the paraboloid/feed system, which requires computer calculation of many integral expressions, is shown in Maddocks (1974, Fig. 5.7). The wave is clearly the negative of the second time-derivative of the exciting waveform. The negative sign occurs due to the reversal of the E field upon reflection from the surface of the paraboloid.

Note that the peak value of  $rE_\theta$  in Fig. 5.7 of Maddocks (1974) using the actual horn feed is approximately  $2.75 \times 10^{-1}$  volts as compared to  $4.8 \times 10^{-1}$  volts in Fig. 5.5, using the simplified isotropic model of the horn. This decrease is most reasonable, as the illumination due to the actual horn is more heavily tapered. In addition to the boresight radiation waveform using the actual horn, Maddocks (1974, Figs. 5.8,5.9) presents curves for  $rE_\theta$  at  $\phi = 0^\circ$  and  $rE_\phi$  at  $\phi = 90^\circ$ , with  $\theta$  as a parameter.

### 3.7 COMPARISON OF THEORY WITH EXPERIMENT

Comparison between theory and experiment for the 48" paraboloidal reflector with the 8" TEM horn feed is given by Maddocks (1974, Fig. 5.7). He compares the theoretically computed curve of  $rE_{\theta}$  vs. time for the boresight direction, with the experimental curve given in Martins (1973:235), over a time slot which spans the principal, second-derivative, part of the waveform. The curves are presented normalized to the same peak value; absolute values are not used for the experimental curves for the reasons discussed in Section 2.6.2. The normalized curves are in reasonably good agreement. Comparisons for directions other than boresight are not possible due to a lack of available experimental data. Experimental data for the paraboloid system in directions other than boresight would be highly useful.

## CHAPTER 4

### CONCLUSIONS AND RECOMMENDATIONS

#### 4.1 CONCLUSIONS

##### 4.1.1 APERTURE-FIELD AND CURRENT-SHEET APPROACHES TO THE TEM HORN

Two principal approaches to time-domain radiation from the TEM horn have been developed, both based upon a transmission-line, traveling TEM-mode wave model of the horn with TDR-measured reflection coefficients at the front aperture. These are the Chernousov aperture-field formulation using assumed fields in the front and side apertures, and the classical vector potential formulation using a current sheet distribution on the wedge conductors consistent with the TEM traveling-wave model. A detailed analysis and equations for the TEM horn radiation at all angles, using the above two approaches, are given by Maddocks (1974, Eqs. B-89, B-90, 3-26, 3-27). It is concluded that these two approaches, applied to the TEM-mode transmission-line model of the TEM horn, are self-consistent, since they produce identical approximate closed-form equations for the radiation in the bore-sight (and also the backfire) directions, developed for small-aperture horns by Maddocks (1974, Eqs. 2-26, 6-2, 3-36, 3-38). Digital computer calculations and graphs of the theoretical results based upon the Chernousov formulation compare sufficiently well, on a relative basis, with experimental data for 3 Sperry Rand horns (Maddocks 1974, Figs. 2.3, 2.4, 2.5) and the 8" BDM horn (Maddocks 1974, Figs. 2.7, 2.8, 2.9) to justify the tentative conclusion that the TEM horn model and the theory of its radiation are sufficiently rigorous for first-order engineering applications. Comparison on an absolute basis is essential to finalize this conclusion, but this was found not to be



possible as the Sperry-Rand data is on a relative basis, and it was evident (Section 2.6.2)\* that there were unresolved questions concerning the absolute levels of the BDM data.

#### 4.1.2 V-DIPOLE MODEL OF SMALL-APERTURE HORN

It is concluded that the small-aperture TEM horn can also be modeled as a V-dipole. It is shown (Section 2.5.4), using the small-horn approximations, that the equation for the boresight radiated field of the V-dipole is identical to the closed-form expressions obtained by Maddocks (1974) described in the paragraph above.

#### 4.1.3 ASSUMPTIONS UNDERLYING TEM HORN MODEL

The use of the field equivalence theorem and the assumptions underlying the TEM-mode model of the TEM horn are discussed in Section 2.2. It is concluded that it might be theoretically possible, although probably most difficult, to obtain an improved understanding of the time-domain model of the TEM horn by appropriate use of an available exact time-harmonic solution for the radiation from the open end of an infinitely-wide, semi-infinitely-long parallel plate guide, with an incident dominant TEM mode, based upon the Wiener-Hopf technique. This would lead to a better understanding of the aperture fields and the aperture reflection coefficient, whose value is presently determinable only through TDR-measurement.

---

\* Unless otherwise indicated, such references refer to Vol. 1 of this report.

#### 4.1.4 TEM HORN RADIATION FORMULA BY BDM

In their report BDM acknowledge that they did not include the radiation from the two side apertures; only the radiation from the front aperture is calculated. However, an analysis (Sections 2.3.5, 2.4) of the derivation of the TEM horn radiation by BDM leads to the conclusion that their front aperture radiation equation itself is not correct. As a result of these two factors, their theoretical magnitudes and angular variations are incorrect. For example, their calculated boresight field for the 8" TEM horn is too large by a factor of approximately 3.4.

#### 4.1.5 PARABOLOID ANTENNA RADIATION

The time-domain radiation from a paraboloid is calculated from the fields in the exit aperture using the Chernousov formulation. The exit aperture fields are obtained by appropriate transformations from an assumed spherical-wave, point-type source feed located at the focus of the paraboloid. The angular variation of the radiation field of the feed, over the aspect angle subtended by the paraboloid, is expressed initially in general non-isotropic form (Maddocks 1974, Eqs. 4-1 and 4.2). The resultant equations for the time-domain radiation fields of a paraboloid are derived by Maddocks (1974, Eqs. C-92 and C-93).

For the instructive case (because an almost-uniform TEM-wave excitation is produced over the paraboloid exit aperture as shown in Section 3.3) where the angular pattern of the feed is isotropic (gain = 1) or at least constant over the solid angle subtended by the paraboloid, equations are derived for the radiated boresight fields (Maddocks 1974, Eqs. 4-42 and 4-43). The time history waveform of the boresight field is computed and

plotted by Maddocks (1974, Fig. 5.5) for the BDM 48" paraboloid and a gaussian exciting time waveform at the apex of the horn. It is concluded that these digital-computer results appear to be correct insofar as the radiated waveform is concerned, as the waveform is the negative second derivative of the exciting waveform, as expected from approximate, closed-form equations (Martins 1973, Eq. 83, or Section 3.6.1, Eq. 49B). The first differentiation is at the exit aperture of the horn, the second is at the exit aperture of the paraboloid, and the negative sign arises at the reflection from the paraboloid surface. Maddocks (1974, Fig. 5.6) also computes and plots the radiated field waveform in several directions away from boresight, along with the boresight field for comparison. Examination of these numerically-computed waveforms leads to the conclusion that as the angle away from boresight increases, the waveforms change from the negative second time derivative to delayed replicas of the fields exciting the exit aperture. It is concluded that this computed result is also correct, as it is predicted by Chernousov's equation for TEM-wave excitation of an aperture (Section 3.4, Eq. 43A).

Consider now the actual case of the BDM 48" paraboloid with the 8" TEM horn. The fields produced by the horn over the paraboloid exit aperture were numerically computed starting with the horn radiation equations (Maddocks, 1974, Eqs. B-89, B-90). The resulting field waveforms, for unit gaussian excitation at the horn apex, in the azimuth and polar planes of the horn, are shown in Figs. 5.1-5.4 incl. in Maddocks (1974). Next, an approximate closed-form equation which represents the horn fields over the exit aperture was determined (Maddocks 1974, Eq. 5-4). This equation has five

available parameters determinable from curves such as Figs. 5.1 and 5.2. Using this characterizing equation for the fields over the exit aperture, the paraboloid radiation time waveforms can then be computed (Maddocks 1974, Eqs. C-92 and C-93). The results are plotted in Figs. 5.7-5.9 incl. in Maddocks (1974). Figure 5.7 in Maddocks (1974) shows both the theoretically computed and the experimentally observed (Martins 1973:235) boresight curves, normalized to the same peak amplitude. It is concluded that the agreement is reasonably good. Comparison on an absolute basis is not feasible, for the reasons given in Section 4.1.1 above. It is seen that the computed peak paraboloid boresight field using the 8" TEM horn (Maddocks 1974, Fig. 5.7) is smaller in magnitude than that computed using an isotropic point feed (Maddocks 1974, Fig. 5.5). It is concluded that this is quite reasonable, as the illumination produced by the actual horn over the paraboloid aperture is more heavily tapered than that produced by an isotropic feed.

#### 4.1.6 RADIATION FROM TRANSIENTS ON LINEAR DIPOLE ANTENNAS

Based upon the theory and agreement with experiment reported in Appendix A, it is concluded that the radiation of transients from a linear dipole can now be calculated from the time-domain equations in all angular directions, including the end-fire direction. It is also shown in Appendix A that the time domain equation results agree with a frequency-domain approach by Martins (1973) for a number of special cases in angular direction and exciting waveform. In Appendix B an additional discussion is given on the state of the art concerning the time-domain, traveling-wave, transmission-line model, and its terminal reflection coefficients, for the circuit response and transient radiation of a dipole antenna. It is concluded that further study would be valuable in this area.

#### 4.2 RECOMMENDATIONS

(a) An obvious recommendation is that it would be of great benefit to study the means whereby the considerable body of experimental data in Martins (1973) could be put on a self-consistent basis with the theory.

(b) More experimental data on the transient radiation of paraboloids in directions other than boresight is recommended, especially in directions for which theoretical results have been established.

(c) More theoretical work on a model for the TEM horn, possibly along the approach outlined in Sections 2.2 and 4.1.3 above, is recommended.

(d) Study of the transmission-line model of the dipole antenna in the time domain, to establish its applicability and limitations, as discussed in some detail in Appendix B, is strongly recommended.

## REFERENCES

- Cheng, D. K., and Tseng, F. I., Transient and Steady-State Antenna Pattern Characteristics for Arbitrary Time Signals, IEEE Trans. on Antennas and Propagation, Vol. AP-12, No. 4, pp. 492-493, 1964.
- Chernousov, V. S., Nonstationary Radiation of Antenna Systems, Radio Engineering and Electronic Systems (Russian-English translation), Vol. 10, No. 8, pp. 1246-1252, 1965.
- Colin, Robert E., and Zucker, Francis J., Antenna Theory Part 1, McGraw-Hill Book Co., 1969.
- Handelsman, Morris (1972), Time Domain Impulse Antenna Study, Rome Air Development Center Final Technical Report RADC-TR-72-105, May, 1972. (AD 744 837)
- Harrison, C. W., Jr., and Williams, C. S., Jr., Transients in Wide-Angle Conical Antennas, IEEE Trans. on Antennas and Propagation, Vol. AP-13, Sec. IIIM, pp. 238-246, March, 1965.
- Jordan, Edward C., and Balmain, Keith G., Electromagnetic Waves and Radiating Systems, 2nd Ed., Prentice-Hall, Inc., 1968.
- King, R. W. P., and Schmitt, H. J., The Transient Response of Linear Antennas and Loops, IRE Trans. on Ant. and Prop., pp. 222-228, May, 1962.
- Liu, Yu-Ping, and Sengupta, P. L., Transient Radiation from a Linear Antenna with Nonreflecting Resistive Loading, IEEE Trans. on Antennas and Propagation, Vol. AP-22, No. 2, pp. 217-220, March, 1974.
- Maddocks, Hugh C., The Transient Electromagnetic Far Fields of a Paraboloid Reflector/TM Horn Antenna Using Time Domain Techniques, Ph.D. Dissertation, University of Vermont, Elect. Engr. Dept., June, 1974 (also Vol. 2 of this report).
- Magnusson, P.C., Transmission Lines and Wave Propagation, Allyn and Bacon, 2nd Ed., 1970.
- Mennebach, Charles (1923), Radiation from Transmission Lines, Trans. A.I.E.E., Vol. 42, pp. 289-301, Feb. 1923.
- Martins, Vasco C., Van Meter, Joseph L., Proud, Joseph M., Fitzgerald, Derek J. (1973), Picosecond Pulse Reflector Antenna Investigation, Braddock, Dunn & McDonald, Inc., and TROR, Inc., Rome Air Development Center Final Technical Report RADC-TR-73-215, July, 1973. (AD 774 132)

- Palciauskas, J. R., and Beam, R. E., Transient Fields of Thin Cylindrical Antennas, IEEE Trans. on Antennas and Propagation, Vol. AP-18, pp. 276-277, March, 1970.
- Ramo, Simon, and Whinnery, John R., Fields and Waves in Modern Radio, 2nd Ed., John Wiley and Sons, 1953.
- Ramo, Simon, Whinnery, John R., and Van Duzer, Theodore, Fields and Waves in Communication Electronics, John Wiley and Sons, 1965.
- Ross, G. F., A New Wideband Antenna Receiving Element, NEREM Record, pp. 78-79, November, 1967.
- Ross, G. F., Bates, R. H., Susman, L., Robbins, K., Hanley, G., and Smith, R. (1966), Transient Behavior of Radiating Elements, Sperry Rand Research Center, Rome Air Development Center Interim Report RADC-TR-86-441, Sept., 1966. (AD 802 634)
- Schellkunoff, Sergei A. (1952), Advanced Antenna Theory, John Wiley and Sons, pp. 102-109, 1952.
- Schellkunoff, Sergei A. (1972), On Teaching the Undergraduate Electromagnetic Theory, IEEE Trans. on Education, Vol. E-15, No. 1, pp. 15-25, Feb., 1972.
- Schellkunoff, Sergei A., and Friis, Harold T., Antennas, Theory and Practice, John Wiley and Sons, Inc., 1952.
- Schmitt, H. J., Harrison, C. W., Jr., and Williams, C. S., Jr., Calculated and Experimental Response of Thin Cylindrical Antennas to Pulse Excitation, IEEE Trans. on Antennas and Propagation, Vol. AP-14, No. 2, pp. 120-127, March, 1966.
- Shen, Liang-Chi, Wu, Tai Tsun, and King, Ronald, W. P., A Simple Formula of Current in Dipole Antennas, IEEE Trans. on Antennas and Propagation, Vol. AP-16, No. 5, pp. 542-547, September, 1968.
- Silver, Samuel (Editor), Microwave Antenna Theory and Design, McGraw-Hill Book Co., Inc., 1949 (same as Silver (1965), published by Dover).
- Stekert, J. J., and Fitzgerald, D. J. (1973), Transient Response of an Asymmetric Cylindrical Antenna, IKOR Inc., internal publication, Jan. 8, 1973.
- Susman, Leon, and Lamensdorf, David, Picosecond Pulse Antenna Techniques, Rome Air Development Center Interim Report RADC-TR-70-205, Contract No. F30602-70-C-0088, Sperry-Rand SRRC-CR-70-21, August, 1970. (AD 877 569)
- Susman, Leon, and Lamensdorf, David, Picosecond Pulse Antenna Techniques, Rome Air Development Center Final Technical Report RADC-TR-71-65, Contract No. F30602-70-C-0088, Sperry-Rand SRRC-CR-71-4, February, 1971. (AD 884 646)

Wu, Tai Tsun, Theory of the Dipole Antenna and the Two-Wire Transmission Line, Jour. Math. Phys., Vol. 2, No. 4, pp. 550-574, July-August, 1961-1.

Wu, Tai Tsun, Transient Response of a Dipole Antenna, Jour. Math. Phys., Vol. 2, No. 6, pp. 892-894, November-December, 1961-2.

Wu, Tai Tsun, Transient Response of a Dipole Antenna, Section 8.12 in Antenna Theory, by Colin and Zucker, Part 1, McGraw-Hill Book Co., 1969.



## APPENDIX A

### RADIATION FROM TRANSIENTS ON LINEAR DIPOLE ANTENNAS

#### 1. INTRODUCTION

There are a number of reasons for Appendix A, as follows:

(a) To present a more complete time-domain equation for the radiation due to transient pulse excitation of a symmetrical center-fed linear dipole antenna (or a monopole over a ground plane) than given previously (Handelsman, 1972). In particular, a previously discussed (Handelsman, 1972:70) apparently anomalous behaviour of the fields in the end-fire directions is shown to no longer exist.

(b) To show that the predicted results of the above equation agree quite well with published theoretical data, including angles close to the end-fire direction.

(c) Special cases of interest such as broadside and end-fire radiation, and response due to impulse, step-function and ramp time waveforms are treated and compared with a frequency-domain approach (Martins 1973).

(d) The radiation of a small TEM horn can be calculated approximately by treating it as a V-dipole, as shown in this report. Hence the equation for the radiation from a dipole is required.

#### 2. DERIVATION OF RADIATION EQUATION

For a current wave  $I(t-Z/c)$  traveling in the  $+Z$  direction on a linear antenna, the radiation fields are given by

$$H_{\phi}(r,t) = \frac{\sin \theta}{1 - \cos \theta} \frac{1}{4\pi r} I(t - \frac{r}{c}) \quad (A-1)$$

$$E_{\theta} = \eta_0 H_{\phi} \quad (A-2)$$

where:

$$\eta_0 = \sqrt{\mu_0/\epsilon_0} = 120 \pi \text{ ohms}$$

$$c = 1/\sqrt{\mu_0 \epsilon_0} = \text{velocity along wires}$$

See Fig. 8 . Equation (A-1) is based upon an infinitely thin, perfectly conducting wire, extending to infinity, or before the leading edge of the current waveform has reached an antenna end at  $Z=h$ , or other discontinuity. This result was stated by Manneback (1923). Schelkunoff (1952:102; also 1972) showed that this equation satisfied Maxwell's equations exactly. Ross (1966:142) derived the equation using the magnetic vector potential  $\bar{A}$ . Handelsman (1972:47) using an approach based upon radiation from accelerating charges, derived the following equation:

$$H_{\phi}(r,t) = \frac{\sin \theta}{1 - \cos \theta} \frac{1}{4\pi r} \left[ I(t - \frac{r}{c}) - I(t - \frac{r}{c} - \frac{1}{c}(1 - \cos \theta)) \right] \quad (A-3)$$

For physically-real non-infinite slopes for  $I$ , the second term in Eq. (A-3) which is the current at the leading edge of  $I$ , at  $Z=L$ , is zero, as long as  $I$  has not reached the antenna ends  $Z=\pm h$ . Thus Eq. (A-3) reduced to Eq. (A-1) for  $|Z| < L$ . However, when the traveling current wave reaches  $Z=\pm h$ , it is necessary to account for terminal conditions by retaining the second term and introducing a reflection coefficient, as explained below.

If there is no reflected wave at the end, due to a perfectly absorbing termination, this is equivalent to starting

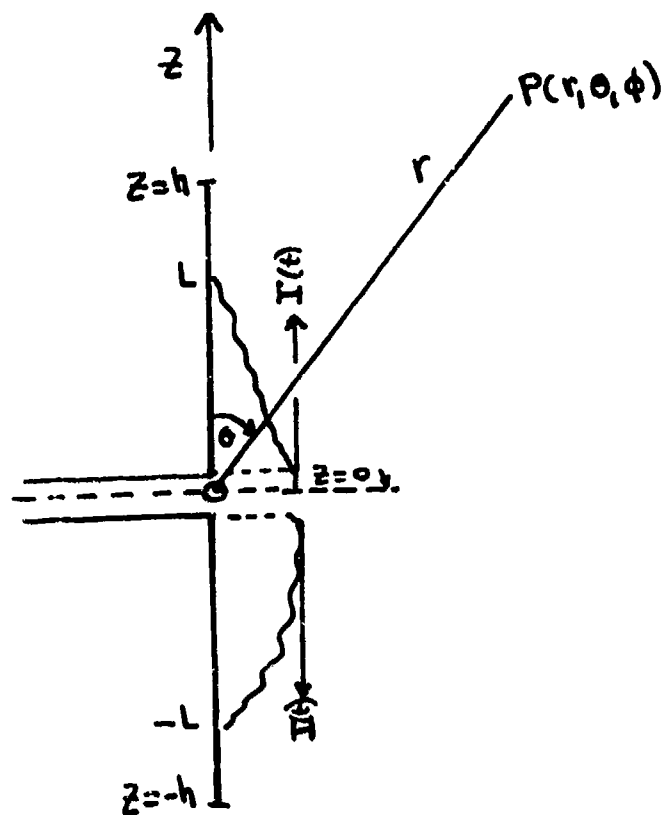


FIG. 8 Dipole geometry.

a current  $-I$  at  $Z=h$ , flowing in the same  $+Z$  direction, producing cancellation of current along the wire imagined to be extended beyond  $Z=h$ . This terminal condition is treated in this manner in Manneback (1923:294) and Schelkunoff (1952:104). Equation (A-3) becomes, for this case,

$$H_{\phi}(r,t) = \frac{\sin\theta}{1-\cos\theta} \frac{1}{4\pi r} \left[ I\left(t-\frac{r}{c}\right) - I\left(t-\frac{r}{c} - \frac{h}{c}(1-\cos\theta)\right) \right] \quad (A-4)$$

To account for reflection at the end, it is necessary to add an additional current wave of amplitude  $k_e I$  traveling back from the end in the  $-Z$  direction (Manneback 1923:294) where  $k_e$  is a current reflection coefficient, which to date has been obtained only through measurements (Ross 1966:31; Martins 1973). Introducing a reflection coefficient  $k_o$  at  $Z=0$ , the radiation equation becomes the following:

$$\begin{aligned} (4\pi r \sin\theta) H_{\phi} = & (1+\cos\theta) \left[ I(\tau) - I(\tau-t_u) \right] \quad (+Z \text{ u.w.}) \\ & + k_e(1-\cos\theta) \left[ I(\tau-t_u) - I(\tau-2h/c) \right] \quad (-Z \text{ u.w.}) \\ & + k_e k_o(1+\cos\theta) \left[ I(\tau-2h/c) - I(\tau-2h/c-t_u) \right] \quad (+Z \text{ u.w.}) \\ & + k_e^2 k_o(1-\cos\theta) \left[ I(\tau-2h/c-t_u) - I(\tau-4h/c) \right] \quad (-Z \text{ u.w.}) \\ & + \dots \text{etc. for upper wire} \dots \quad (A-5) \\ & + (1-\cos\theta) \left[ I(\tau) - I(\tau-t_p) \right] \quad (-Z \text{ l.w.}) \\ & + k_e(1+\cos\theta) \left[ I(\tau-t_p) - I(\tau-2h/c) \right] \quad (+Z \text{ l.w.}) \\ & + \dots \text{etc. for lower wire} \dots \end{aligned}$$

$$E_{\theta} = \eta_0 H_{\phi} \quad (A-6)$$

where:

$k_e$  = current reflection coefficient at ends  $Z=\pm h$

$k_o$  = current reflection coefficient at input  $Z=0$ , viewed  
from the antenna

$T=t-r/c$  = retarded time at P

$$t_N = \frac{h}{c} (1 - \cos \theta)$$

$$t_P = \frac{h}{c} (1 + \cos \theta) = \frac{2h}{c} - t_N$$

$\pm Z$  = waves traveling in  $\pm Z$  directions

u.w. = upper wire

l.w. = lower wire

The various terms in Eq. (A-5) are identified as  
follows:

1<sup>st</sup> term = radiation from initial +Z traveling wave, u.w.

2<sup>nd</sup> term = radiation from 1<sup>st</sup> reflected -Z traveling wave, u.w.

3<sup>rd</sup> term = radiation from 2<sup>nd</sup> reflected +Z traveling wave, u.w.

etc. term = radiation from subsequent  $\pm Z$  traveling wave, u.w.

5<sup>th</sup> term = radiation from initial -Z traveling wave, l.w.

6<sup>th</sup> term = radiation from 1<sup>st</sup> reflected +Z traveling wave, l.w.

etc. term = radiation from subsequent  $\pm Z$  traveling wave, l.w.

All the lower wire equations are obtainable from the upper  
wire equations by replacing  $\cos \theta$  by  $-\cos \theta$  and  $t_N$  by  $t_P$ .

The derivation of Eq. (A-5) assumes negligible atten-  
uation of the traveling waves during each passage along the  
wires due to radiation and conductor losses. In effect the  
reflection coefficients  $k_e$  and  $k_o$  not only account for the  
actual terminal reflections but also serve to substitute for

the actual continuous attenuation a series of discrete attenuation factors, introduced at the reflection points  $Z=th$  and  $Z=0$ .<sup>\*</sup>

The time-domain approach used to derive Eq. (A-5) may also be applied to non-symmetrical linear antennas (e.g., Stekert (1973), but this is not pursued further in this report.

### 3. SIMPLE ILLUSTRATIVE EXAMPLE - A DIPOLE WITH MATCHED ENDS

As a simple example, consider a dipole with matched ends, as shown in Fig. 9. Equation (A-5), for  $k_e=0$  becomes

$$4\pi r H_p = \frac{1+\cos\theta}{\sin\theta} \left[ I(\tau) - I\left(\tau - \frac{h}{c}(1-\cos\theta)\right) \right] + \frac{1-\cos\theta}{\sin\theta} \left[ I(\tau) - I\left(\tau - \frac{h}{c}(1+\cos\theta)\right) \right] \quad (A-7)$$

Let the exciting waveform be a rectangular pulse of duration  $\tau < h/c$  seconds, given by

$$I(t) = A \left[ u(t) - u(t-\tau) \right] \quad (A-8)$$

where  $u(t)$  is the unit step function. For simplicity, consider the radiation at  $\theta = 90^\circ$  (broadside direction). Then  $t_N = t_p = h/c$  and Eq. (A-8) becomes

$$H_p = \frac{A}{2\pi r} \left[ u(\tau) - u(\tau-\tau) - u\left(\tau - \frac{h}{c}\right) + u\left(\tau - \tau - \frac{h}{c}\right) \right] \quad (A-9)$$

Equation (A-9) is shown in Fig. 10. The radiation waveform is a pair of pulses, each the replica of the exciting waveform.

---

<sup>\*</sup> Additional discussion on reflection coefficients is given in Appendix B.

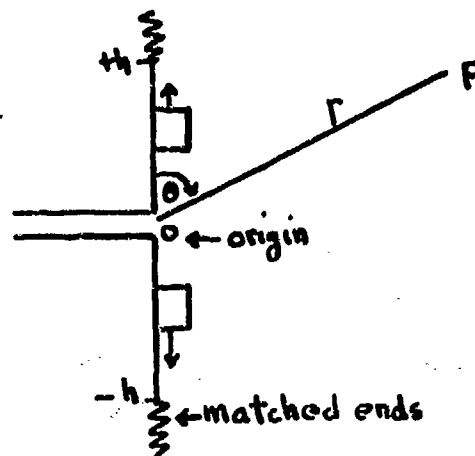


FIG. 9 DIPOLE WITH MATCHED ENDS.

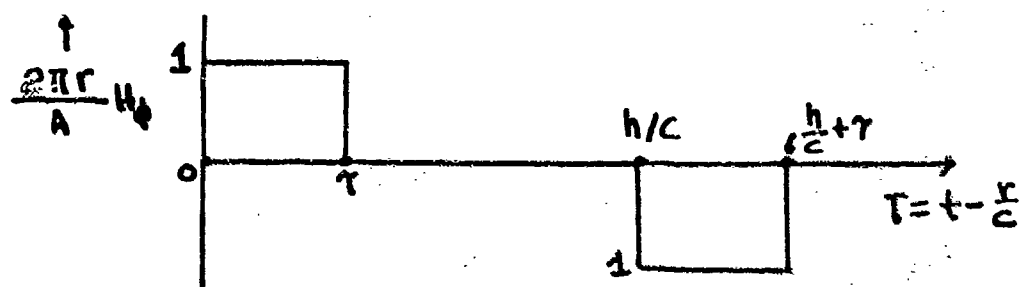


FIG. 10 DIPOLE RADIATION, PULSE EXCITATION,  $k_0 = 0$ .

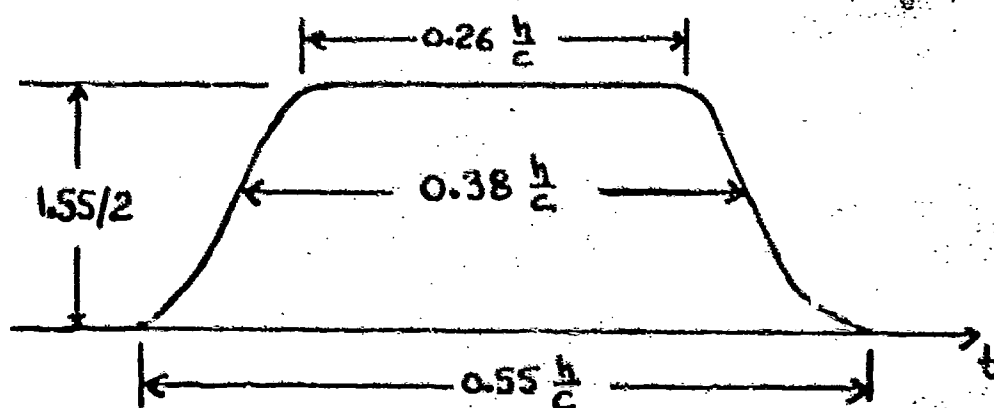


FIG. 11 TRAPEZOIDAL PULSE SHAPE  $I(t)$ .

#### 4. RADIATION IN END-FIRE DIRECTIONS $\theta = 0^\circ, 180^\circ$

##### 4.1 THEORY

For simplicity, with no significant loss in exposition of the fundamental results concerning radiation in the end-fire directions, assume that the dipole antenna is matched at its input ( $k_0=0$ ). Then Eq. (A-6) becomes

$$\begin{aligned} \left(\frac{4\pi r}{\eta_0}\right)E_\theta = & \frac{1+\cos\theta}{\sin\theta} \left[ I(\tau) - I(\tau - t_H) \right] \\ & + \frac{k_e(1-\cos\theta)}{\sin\theta} \left[ I(\tau - t_H) - I(\tau - \frac{2h}{c}) \right] \\ & + \frac{1-\cos\theta}{\sin\theta} \left[ I(\tau) - I(\tau - t_p) \right] \\ & + \frac{k_e(1+\cos\theta)}{\sin\theta} \left[ I(\tau - t_p) - I(\tau - \frac{2h}{c}) \right] \quad (A-10) \end{aligned}$$

In the end-fire direction  $\theta=0$ , as  $\theta$  approaches zero and  $\cos\theta$  approaches unity,  $t_H$  becomes differentially small, and we can write

$$t_H = \frac{h}{c}(1-\cos\theta) \equiv \Delta\tau; \quad t_p = \frac{2h}{c} - \Delta\tau \quad (A-11)$$

Using

$$\lim_{\theta \rightarrow 0} \frac{1-\cos\theta}{\sin\theta} = 0 \quad (A-12)$$



Eq. (A-10) becomes

(A-13)

$$E_{\theta} = \frac{\eta_0}{2\pi r \sin\theta} \left\{ \left[ I(\tau) - I(\tau - \Delta\tau) \right] + k_e \left[ I\left(\tau - \frac{2h}{c}\right) + I\left(\tau - \frac{2h}{c} + \Delta\tau\right) \right] \right\}$$

The two bracketed terms [ ] in Eq. (A-13) are each the difference between the waveform and a delayed replica of the waveform, where the delay  $\Delta\tau$  approaches zero as  $\theta$  approaches zero. It is now obvious that Eq. (A-13) can be written in the derivative form

$$E_{\theta} = \frac{\eta_0}{2\pi r} \frac{\Delta\tau}{\sin\theta} \left\{ \frac{I(\tau) - I(\tau - \Delta\tau)}{\Delta\tau} + k_e \frac{I\left(\tau - \frac{2h}{c} + \Delta\tau\right) - I\left(\tau - \frac{2h}{c}\right)}{\Delta\tau} \right\} \quad (A-14)$$

then as  $\Delta\tau$  approaches zero,

$$E_{\theta} = \frac{\eta_0}{2\pi r} \frac{h}{c} \tan\left(\frac{\theta}{2}\right) \left[ I'(\tau) + k_e I'\left(\tau - \frac{2h}{c}\right) \right] \quad (A-15)$$

where

$$I'(\tau) \equiv \frac{d}{d\tau} I(\tau) = \text{time derivative of excitation waveform}$$

$$\frac{\Delta\tau}{\sin\theta} = \frac{h}{c} \frac{(1 - \cos\theta)}{\sin\theta} = \frac{h}{c} \tan\left(\frac{\theta}{2}\right) \quad (A-16)$$

Thus as  $\theta$  varies from the broadside ( $\theta = 90^\circ$ ) to the end-fire direction ( $\theta = 0^\circ$ ), the radiation waveform changes from replicas of the excitation to the time-derivative of the excitation. Further, with the complete radiation equation as given by Eq. (A-5), there is no end-fire "infinity catastrophe" as  $\theta \rightarrow 0^\circ$  (or  $180^\circ$ , as shown below). Instead, as shown by Eq. (A-15),

the field approaches the product of  $\tan(\theta/2)$ , which approaches zero, and the time derivatives  $I'$ , which in the actual physical case cannot be infinite. Hence the end-fire radiation approaches zero, as expected. Thus the infinity paradox discussed in Handelsman (1972:70) has been resolved. The apparent paradox originally arose because of an incomplete mathematical description of the role played by the time-derivatives of the traveling waveform in determining the end-fire radiation.

For the other end-fire direction  $\theta \rightarrow 180^\circ$ , then  $\cos\theta$  approaches -1,  $t_p$  becomes differentially small, and we can write

$$t_p = \frac{h}{c}(1+\cos\theta) \equiv \Delta T'; \quad t_N = \frac{2h}{c} - \Delta T' \quad (\text{A-17})$$

Using

$$\lim_{\theta \rightarrow \pi} \frac{1+\cos\theta}{\sin\theta} = 0 \quad (\text{A-18})$$

Eq. (A-10) becomes identical to Eq. (A-14), with  $\Delta T$  replaced by  $\Delta T'$ . Using

$$\frac{\Delta T'}{\sin\theta} = \frac{h}{c} \frac{(1+\cos\theta)}{\sin\theta} = \frac{h}{c} \cot\left(\frac{\theta}{2}\right) \quad (\text{A-19})$$

the final result is

$$E_\theta = \frac{\eta_0}{2\pi r} \frac{h}{c} \cot\left(\frac{\theta}{2}\right) \left[ I'(\tau) + k_0 I'\left(\tau - \frac{2h}{c}\right) \right] \quad (\text{A-20})$$

Thus, as  $\theta \rightarrow 180^\circ$ ,  $E_\theta$  also approaches zero.

#### 4.2 COMPARISON WITH PUBLISHED RESULTS

In Handelsman (1972:63-69) the time-domain equations were compared with published theoretical results for a center-driven cylindrical antenna. This was driven by a source excitation pulse with approximately a trapezoidal shape, of base width of about  $0.55 h/c$ , a flat top of about  $0.26 h/c$  and a width of about  $0.38 h/c$  at the 50 percent of peak amplitude point (Palciauskas 1970) shown in Fig. 11. The radiation waveforms in Palciauskas (1970) are calculated using an inverse Fourier transform of the response to sinusoidal excitation  $e^{j\omega t}$ . For the non-end-fire directions  $\theta = 90^\circ, 70^\circ, 60^\circ$ , and  $45^\circ$  the agreement between the radiation waveforms as predicted by the relatively simple time-domain equations and the more exact inverse Fourier transform method has been shown (Handelsman 1972:66-67) to be fairly good as measured by the number of pulses, their amplitudes, widths and positions. For this purpose the trapezoidal pulse shape was approximated by a simple rectangular pulse of width  $0.4 h/c$ . The amplitude was normalized to  $1.55/2$  so that at  $\theta = 90^\circ$  the leading peaks of both sets of curves have equal amplitudes  $4\pi r H_0(90) = 2I(r) = 2 \times \frac{1.55}{2} = 1.55$  = peak amplitude of first pulse, Palciauskas (1970:Fig 2).

For smaller  $\theta$ , it is necessary to use the actual pulse shape, as the time-derivative of  $I(r)$  now determines the end-fire radiation waveform. This derivative is obtained from Fig. 11 as follows:

$$\text{derivative} \approx \frac{\text{rise}}{\text{rise} - \text{Time}} \approx \frac{1.55/2}{(0.275-0.13)\frac{h}{c}} = \frac{5.35}{h/c} \quad (\text{A-21})$$

For  $\theta = 20^\circ$ ,  $t_H = \frac{h}{c}(1 - \cos 20^\circ) = 0.06 \frac{h}{c}$  compared to a rise time  $\approx 0.145 \frac{h}{c}$ , so the use of derivatives is justified only to a rough first approximation. Within the spirit of this approximation, from Eqs. (A-5, A-15), the leading terms for the radiation  $H_\phi(20^\circ)$ , in " $4\pi r$ " units, are as follows:

$$\begin{aligned} 4\pi r H_\phi(20^\circ) = & 2 \frac{h}{c} \tan\left(\frac{20^\circ}{2}\right) \left\{ \left[ I'(\tau) - I'(\tau - \tau) \right] \right. \\ & + \left[ k_0 I'(\tau - \frac{2h}{c}) - k_0 I'(\tau - \frac{2h}{c} - \tau) \right] \\ & + \dots \text{other terms, u.w.} \left. \right\} \\ & + \frac{1 - \cos 20^\circ}{\sin 20^\circ} \left\{ \left[ I(\tau) - I(\tau - \tau) \right] - \left[ I(\tau - \frac{h}{c}(1 + \cos 20^\circ)) \right. \right. \\ & \left. \left. + I(\tau - \frac{h}{c}(1 + \cos 20^\circ)) \right] \right. \\ & + \dots \text{other terms, l.w.} \end{aligned} \quad (\text{A-22})$$

Hence the amplitude of the first peak, in " $4\pi r$ " units is

$$\begin{aligned} 4\pi r H_\phi(20^\circ) &= 2 \frac{h}{c} \tan(10^\circ) I'(\tau) + \frac{1 - \cos 20^\circ}{\sin 20^\circ} I(\tau) \\ &= 2 \frac{h}{c} (0.176) \left( \frac{5.35}{h/c} \right) + \frac{1 - 0.94}{0.342} \left( \frac{1.55}{2} \right) \end{aligned}$$

$$\therefore 4\pi r H_\phi(20^\circ) = 1.87 + 0.136 = 2.01 \quad (\text{A-23})$$

as compared to the published value of 1.7. From Eq. (A-22), using  $k_0 \approx 1.5$  (Handelsman 1972:64), the subsequent major peak amplitudes are -2.01, -1.69 and 1.69, as compared to published values of -1.8, -2.0 and 2.0 (as well as can be read off curves). Thus it may be concluded that the time-domain equations (A-5) give a reasonably accurate description of the radiation at all angles, including the end-fire directions.

##### 5. SUMMATION FORMULA FOR EQUATION (A-6)

Equation (A-6) may be written in compact summation form as follows:

$$\begin{aligned} \left( \frac{2\pi r \sin \theta}{\eta_0} \right) E_\theta = & I(\tau) - (1-k_0) \sum_1^\infty k_0^m k_0^{m-1} I\left(\tau - \frac{2mh}{c}\right) \\ & - \frac{1}{2} \left[ 1 + \cos \theta - k_0 (1 - \cos \theta) \right] \sum_0^\infty k_0^m k_0^m I\left(\tau - \frac{2mh}{c} - t_N\right) \\ & - \frac{1}{2} \left[ 1 - \cos \theta - k_0 (1 + \cos \theta) \right] \sum_0^\infty k_0^m k_0^m I\left(\tau - \frac{2mh}{c} - t_P\right) \end{aligned} \quad (A-24)$$

##### 6. ADDITIONAL CASES OF INTEREST

###### 6.1 INTRODUCTION

It is considered worthwhile to include a discussion of a number of special cases because of their intrinsic interest, and also to show agreement with results obtained by Martins (1973) using a frequency-domain approach.

To convert from current reflection coefficients  $k_o$  and  $k_e$  as used in this report to voltage reflection coefficients  $R_1$  and  $R_2$  as used in Martins (1973:19,20), the following equations are given:

$$R_1 = \frac{Z_{line} - Z_o}{Z_{line} + Z_o} = -k_o \quad (A-25)$$

$$R_2 = \frac{Z_{end} - Z_o}{Z_{end} + Z_o} = -k_e \quad (A-26)$$

where:

$Z_{line}$  = input transmission line characteristic  
impedance = surge impedance

$Z_o$  = dipole characteristic (surge) impedance

$Z_{end}$  = dipole effective terminal impedance at  
ends  $Z=\pm h$ .

## 6.2 SPECIAL CASE, IMPULSE EXCITATION, $R_1 = -1$ , $R_2 = 1$

Here the following conditions are assumed:

$I(t) = \delta(t)$  = impulse current excitation

$$k_o = -R_1 = 1 \quad (A-27)$$

$$k_e = -R_2 = -1$$

The assumption  $R_2 = 1$  implies complete reflection at the ends of the dipole, while  $R_1 = -1$  implies that  $Z_o > Z_{line}$ , which is true for 50 ohm line.

Equation (A-24) becomes

$$\begin{aligned} \left( \frac{2\pi r \sin \theta}{\eta_0} \right) E_\theta &= \delta(T) - (1-|R_1|) \sum_1^{\infty} (-1)^m |R_1|^{m-1} \delta\left(T - \frac{2mh}{c}\right) \\ &\quad - \sum_0^{\infty} (-1)^m |R_1|^m \delta\left(T - \frac{2mh}{c} - t_N\right) \quad (A-28) \\ &\quad - \sum (-1)^m |R_1|^m \delta\left(T - \frac{2mh}{c} - t_P\right) \end{aligned}$$

The first ten terms of Eq. (A-28), in time-sequence are as follows:

$$\begin{aligned} \left( \frac{2\pi r \sin \theta}{\eta_0} \right) E_\theta &= \delta(T) - \delta\left(T - \frac{h}{c}(1-\cos \theta)\right) - \delta\left(T - \frac{h}{c}(1+\cos \theta)\right) \\ &\quad + (1-|R_1|) \delta\left(T - \frac{2h}{c}\right) + |R_1| \delta\left(T - \frac{h}{c}(3-\cos \theta)\right) \\ &\quad + |R_1| \delta\left(T - \frac{h}{c}(3+\cos \theta)\right) - |R_1|(1-|R_1|) \delta\left(T - \frac{4h}{c}\right) \\ &\quad - |R_1|^2 \delta\left(T - \frac{h}{c}(5-\cos \theta)\right) - |R_1|^2 \delta\left(T - \frac{h}{c}(5+\cos \theta)\right) \\ &\quad + |R_1|^2(1-|R_1|) \delta\left(T - \frac{6h}{c}\right) + \dots \quad (A-29) \end{aligned}$$

Equation (A-29) is plotted in Fig. 12. This is identical to that given in Martins (1973:p.24, Fig. 2), taking into account the following apparently typographical errors in Fig. 2 in

Martins:  $R_1$  should =  $-|R_1|$ , the 10<sup>th</sup> pulse should be at  $ct/h$   
 = 6 and of magnitude  $|R_1|^2(1-|R_1|)$ .

### 6.3 SPECIAL CASE, IMPULSE EXCITATION, $R_1=0$ , $R_2=1$

Here the following conditions are assumed:

$I(t) = \delta(t)$  = impulse current excitation

$k_o = -R_1 = 0$

$k_e = -R_2 = -1$

The assumption  $R_1=0$  implies a matched input (a match between the transmission line and the dipole input terminals), while  $R_2=1$  implies complete reflection at the ends of the dipole.

Eq. (A-24) reduces to

$$\left( \frac{2\pi r_0 \sin \theta}{\eta_0} \right) E_0 = \delta(T) - \delta\left(T - \frac{h}{2}(1-\cos \theta)\right) - \delta\left(T - \frac{h}{2}(1+\cos \theta)\right) + \delta\left(T - \frac{2h}{2}\right) \quad (A-30)$$

Equation (A-30) is plotted in Fig. 13, which is identical to Martins (1973:p. 26, Fig. 3).

### 6.4 GENERAL EXCITATION, BROADSIDE DIRECTION ( $\theta = 90^\circ$ ), $R_1=0$ (MATCHED INPUT), $R_2=1$

#### 6.4.1 INTRODUCTION

It greatly simplifies discussion of the results without too much loss in generality to assume

$k_o = -R_1 = 0$  (matched input)

$k_e = -R_2 = -1$  (complete end reflections)

(A-31)



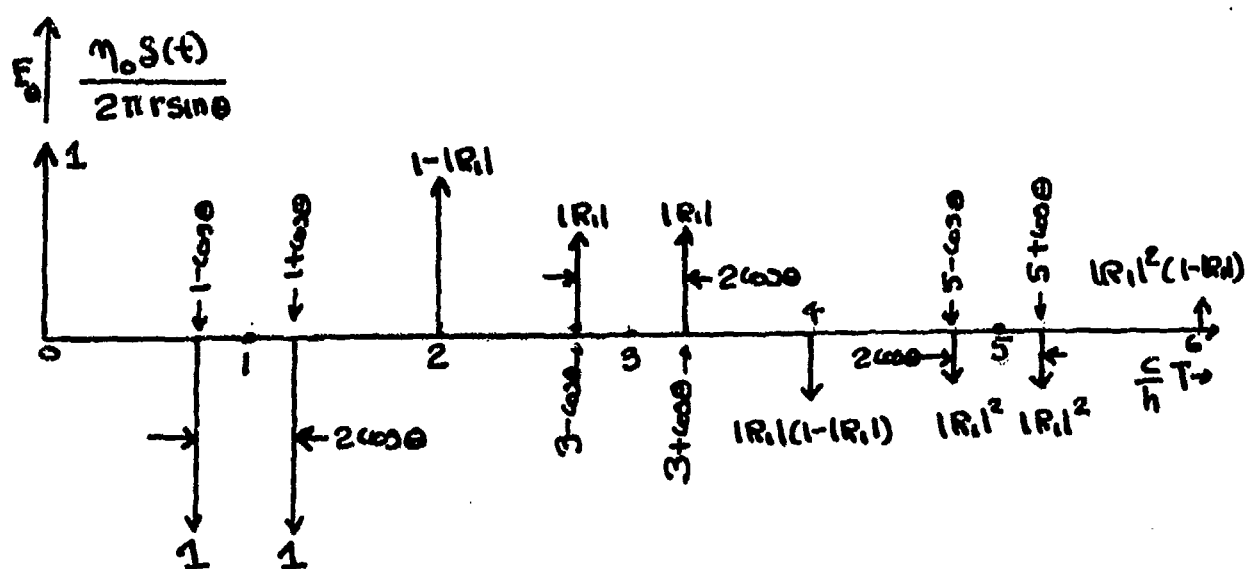


FIG. 12 Radiation of impulse excitation,  $R_1 = -|R_1|$ ,  $R_2 = 1$ .

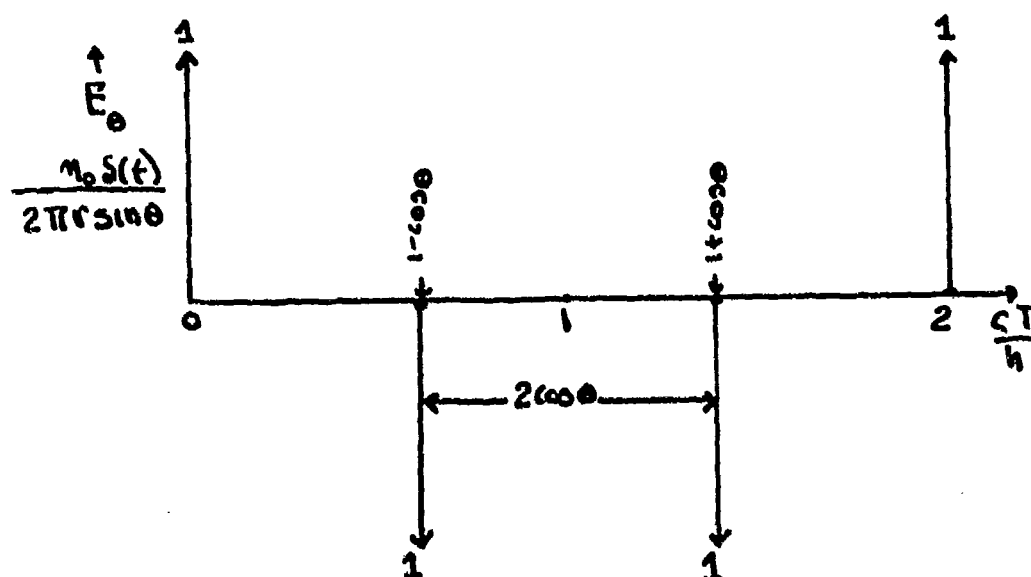


FIG. 13 Radiation of impulse excitation,  $R_1 = 0$ ,  $R_2 = 1$ .

#### 6.4.2 GENERAL RESULT

In the direction broadside to the dipole,  $\theta = 90^\circ$ , and using Eq. (A-31), Eq. (A-24) reduces to

$$E_\theta = \frac{\eta_0}{2\pi r} \left[ I(\tau) - 2I\left(\tau - \frac{h}{c}\right) + I\left(\tau - \frac{2h}{c}\right) \right] \quad (\text{A-32})$$

Thus at broadside, the time-waveform pattern consists of a delayed replica of the waveform originating at origin 0, followed by an inverted (negative) replica of double amplitude due to reflection at the two ends (assumed complete), and finally a third replica as the traveling wave returns to 0, at time  $2h/c$  later. Because  $R_1=0$  there are no further reflected traveling waves from 0. If  $R_1 \neq 0$ , then additional delayed replicas of the exciting waveform  $I(t)$ , with diminishing amplitude, are radiated.

#### 6.4.3 SHORT DIPOLE

When  $h/c \ll$  waveform characteristic risetime, then Eq. (A-32) can be written as follows:

$$E_\theta = \frac{\eta_0}{2\pi r} \left( \frac{h}{c} \right)^2 \left[ \frac{I(\tau) - 2I(\tau - \Delta\tau) + I(\tau - 2\Delta\tau)}{(\Delta\tau)^2} \right] \quad (\text{A-33})$$

where:

$$\Delta\tau \equiv \frac{h}{c}$$



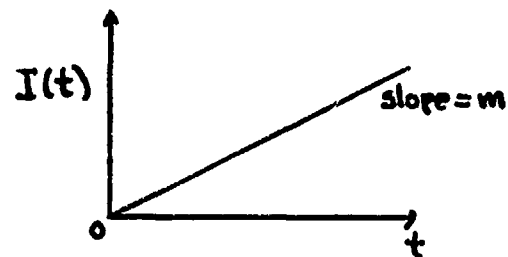
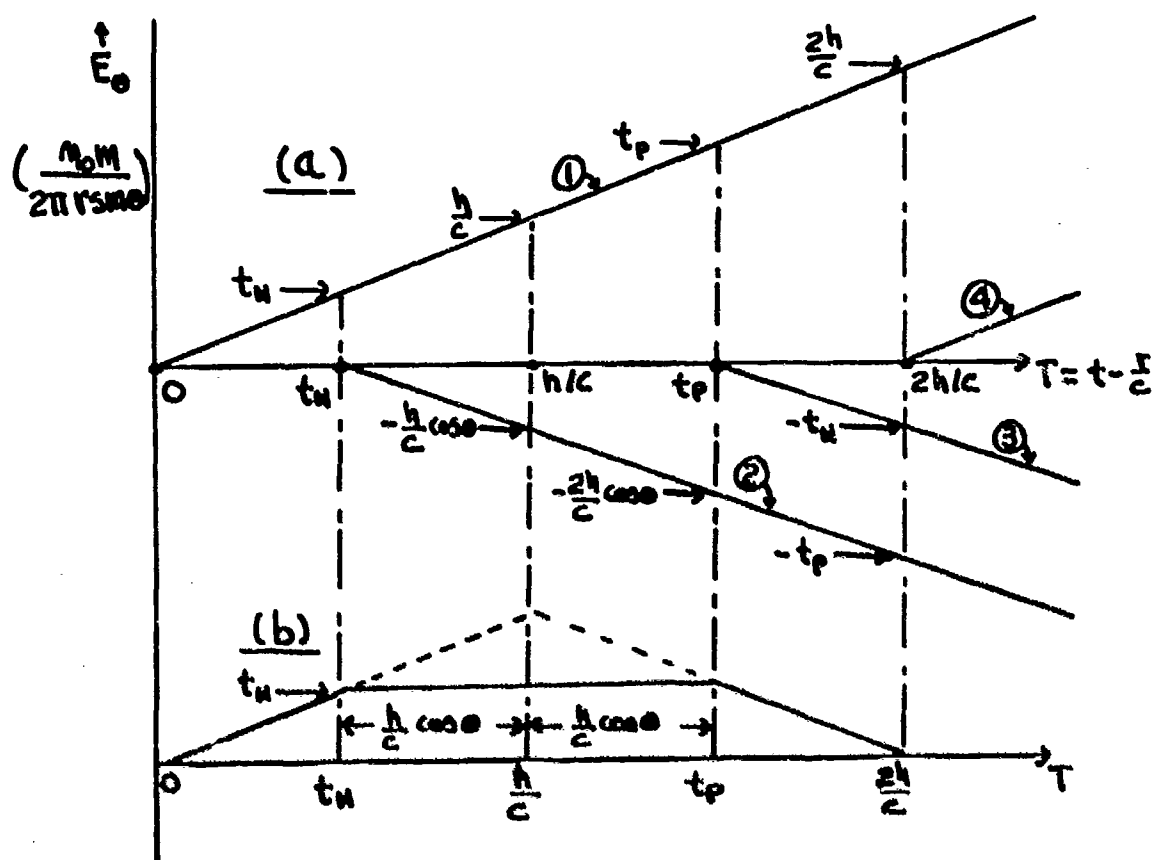


FIG. 14 Ramp excitation waveform.



(a) Component waveforms

(b) Sum =  $E_\theta$

FIG. 15 Radiation of ramp waveform,  $R_1=0$ ,  $R_2=1$ .

The resultant radiated waveform is a trapezoid, which for the special case of the broadside direction ( $\theta = 90^\circ$ ) becomes a triangle. The trapezoid peak amplitude is given by

$$\text{peak } E_\theta = \frac{\eta_0 m t_N}{2\pi r \sin\theta} = \frac{\eta_0 m h (1 - \cos\theta)}{2\pi r c \sin\theta}$$

$$\therefore \text{peak } E_\theta = \frac{\eta_0 m}{2\pi r} \frac{h}{c} \tan\left(\frac{\theta}{2}\right) \quad (\text{A-37})$$

Fig. 15 and Eq. (A-37) are identical to Fig. 4 and Eq. (13), respectively, in Martins (1973). In Eq. (13) in Martins (1973),  $I_0(l/v) = I_0(h/c) = mh/c$ .

#### 6.6 PULSE EXCITATION, $R_1=0$ (MATCHED INPUT), $R_2=1$

The excitation waveform is given by Eq. (A-8), and is shown in Fig. 16. It is a rectangular pulse of amplitude  $A$  and duration  $\tau$ . There are two cases of special interest:

- (a) duration  $\tau \ll h/c$
- (b) duration  $\tau \gg h/c$

These two cases are discussed below.

##### 6.6.1 PULSE DURATION $\tau \ll$ ANTENNA TRIP TIME $h/c$

This is the case of a long dipole. In the broadside direction,  $\theta = 90^\circ$ , and using Eq. (A-32), there is obtained

$$E_{\theta} = \frac{\mu_0 A}{2\pi r} \left[ u(\tau) - u(\tau - \tau) - 2u(\tau - \frac{h}{c}) \right. \quad (A-38) \\ \left. + 2u(\tau - \frac{h}{c} - \tau) + u(\tau - \frac{2h}{c}) - u(\tau - \frac{2h}{c} - \tau) \right]$$

Equation (A-38) is shown plotted in Fig. 17, which agrees with Stekert (1973:Fig. 2c).

#### 6.6.2 PULSE DURATION $\tau \gg$ ANTENNA TRIP TIME $h/c$

This is the case of a short dipole. In the broadside direction,  $\theta = 90^\circ$ , Eq. (A-38) still holds, of course, but now  $h/c \ll \tau$ . The resultant radiation is plotted in Fig. 18 along with the component waveforms. Fig. 18 agrees with Stekert (1973: Fig. 2b). The double differentiation, characteristic of short dipole radiation is evident (see Section 6.4.3 above). The first differentiation of the pulse produces a pair of impulses separated in time by  $\tau$ . The second differentiation produces a pair of doublets, also separated in time by  $\tau$ , as shown (approximately) by the waveform in Fig. 18.

### 7. BROADSIDE RADIATION FIELD IN TERMS OF INCIDENT IMPULSE

#### VOLTAGE

A useful equation for  $E_{\theta}$  in the broadside direction, non-matched input, for  $0 < t < h/c$ , appears in Martins (1973: p. 108, Eq. (94)). This is the radiation produced by the traveling waveform on the dipole before it has reached the ends  $z = \pm h$

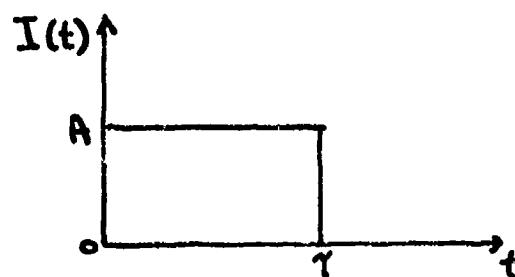


FIG. 16 Rectangular pulse excitation waveform.

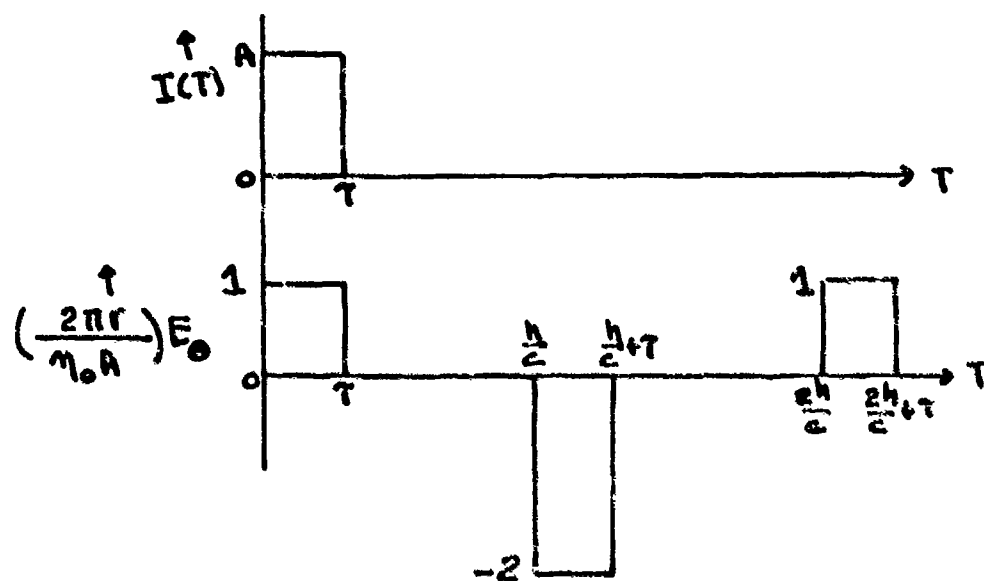


FIG. 17 Radiation for  $\tau \ll \frac{h}{c}$ , broadside direction,  $R_1=0$ ,  $R_2=1$ .

(long dipole). This equation is

$$E_{\theta}(\theta) = \frac{\eta_0}{\pi r} \cdot \frac{V_i(t)}{Z_c + Z_a} \quad (0 < t < \frac{h}{c}) \quad (A-39)$$

In Eq. (A-39),  $Z_c$  = input cable characteristic impedance (50 ohms),  $Z_a$  = antenna input terminal impedance, and  $V_i$  = amplitude of the incident voltage produced by an impulse generator, matched to the cable line, which travels toward the input terminals of the antenna.

As shown below, this equation can be derived in a relatively simple fashion from the time-domain results presented in this appendix.

The transmission line circuit is shown in Fig. 19. The impedances are assumed to be real, as determined in tests, according to Martins (1973:108). The voltage at the antenna is given by

$$V_{ant.} = (1 + \Gamma) V_i \quad (A-40)$$

where:

$$\Gamma = \text{voltage reflection coefficient} = \frac{Z_a - Z_c}{Z_a + Z_c}$$

$V_i$  = incident voltage wave amplitude

The antenna current is

$$I(t) = \frac{V_{ant.}}{Z_a} = \frac{(1 + \Gamma) V_i}{Z_a} = \frac{2 V_i}{Z_c + Z_a} \quad (A-41)$$

From Eq. (A-6), for  $\theta = 90^\circ$ , and using the two terms involving



I(T) only (prior to the first reflections from the ends), there is obtained

$$E_{\theta} = \frac{\eta_0}{4\pi r} 2I(t) = \frac{\eta_0}{\pi r} \frac{V_i(t)}{Z_c + Z_a} \quad (A-42)$$

which is the same as Eq. (A-39).

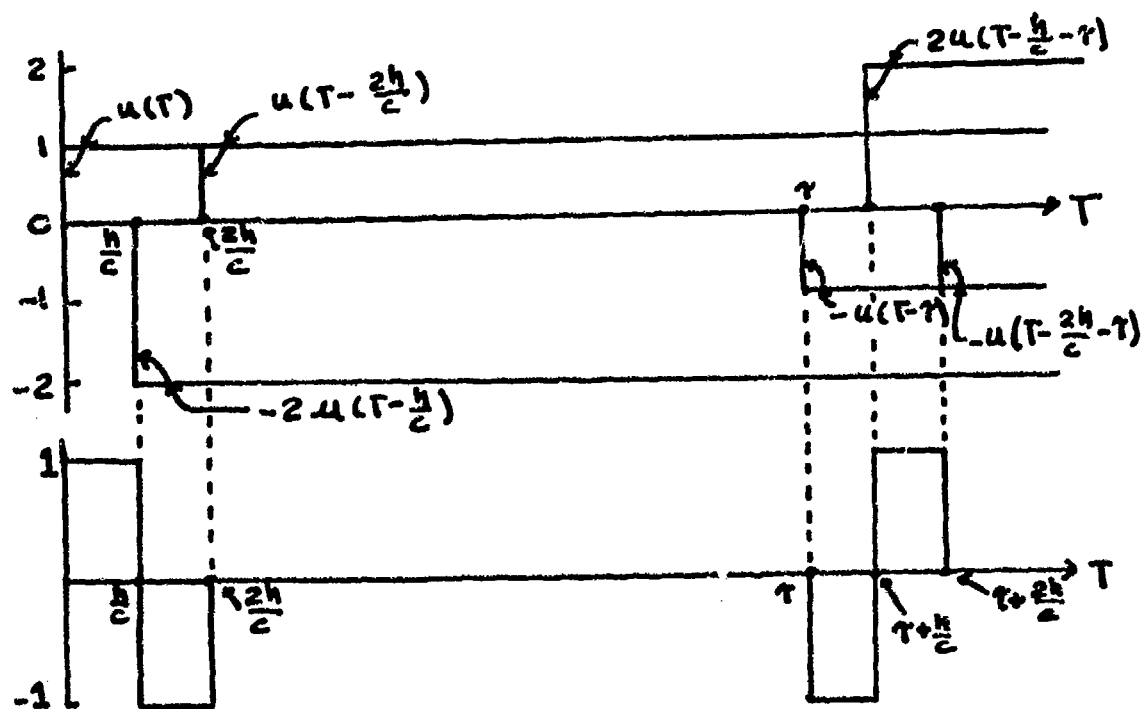


FIG. 18 Radiation for  $\tau \gg \frac{h}{c}$ , broadside direction,  $R_1=0$ ,  $R_2=1$ .

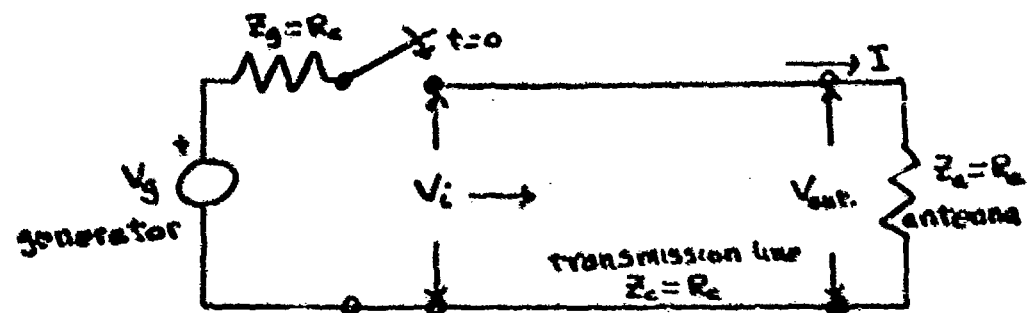


FIG. 19 Transmission line circuit.

APPENDIX B  
ADDITIONAL DISCUSSION ON TERMINAL REFLECTION  
COEFFICIENTS FOR LINEAR DIPOLE ANTENNA

1. INTRODUCTION

1.1 PURPOSE

The use of terminal current reflection coefficients  $k_o$  (at the input) and  $k_e$  (at the dipole ends or tips) is introduced in Appendix A, Section 2. The purpose of this Appendix B is to review briefly some of the known characteristics of these reflection coefficients, theoretically and experimentally, and to point out some areas where further work is recommended. It will be seen that a considerable amount is known about  $k_o$  but comparatively little about  $k_e$ .

1.2 GENERAL "PHYSICAL" DISCUSSION

Consider a short pulse, of duration  $\tau$  less than antenna travel time  $h/c$ , incident at the input of a linear dipole antenna from a transmission line. The antenna conductor resistance is assumed to be negligible. There results, in the time domain, a reflected pulse back into the line, and a transmitted pulse which travels along the antenna at essentially the speed of light. Thus far this is similar to a simple transmission line problem involving the junction of two lines. However, in the antenna case, during the period  $\tau$  of pulse incidence at the input, radiation is also produced (King and Schmitt (1962), Schmitt et al (1966)). Therefore the concept of a reflection coefficient  $k_o$ , unlike the simpler case of the transmission line discontinuity, must in some manner take this radiation into account.

The energy in the input pulse must equal the sum of the energies in the reflected and the transmitted pulses plus the energy radiated and stored.

It is stated by King and Schmitt (1962:224), that only the impedance of an infinitely long antenna can be involved in the antenna response during the interval before the first reflection from the end arrives at the input. This impedance is known for sinusoidal steady-state excitation, and is used by King and Schmitt (1962) to formulate an average reflection coefficient, as explained in Section 2 below, which is effective in the time domain.

During the interval in which the lagging end of the transmitted pulse has cleared the input terminals, but the leading edge has not yet reached the antenna end, there is essentially no far-field radiation from this pulse traveling on the antenna, independent of the waveform shape. Experimentally this appears to be borne out by measurements (Schmitt et al (1966, Fig. 5). Discussion-wise or theoretically this is predicted or implied by many sources, for example: King and Schmitt (1962:227), Schelkunoff (1952,1972), Manneback (1923:299; see discussion by Slepian concerning a dispute between Steinmetz and Carson on the existence of radiation from a freely-traveling wave), Schmitt et al (1966, Fig. 4), Martins (1973, Fig. 2), and Handelsman (1972). The assumption that the antenna conductor resistance is negligible or has an insignificant effect upon the amplitude, shape, or velocity of the pulse, makes this a "freely-traveling" pulse in Slepian's terminology. For resistance-loaded antennas see Liu and Sengupta (1974) and the various references cited therein.

When the leading edge of the traveling pulse reaches the antenna end, radiation is again produced during the period  $\tau$  of pulse incidence at this end (King and Schmitt (1962), Schmitt et al (1966)). The reflection coefficient  $k_e$  must therefore account for both the reflected wave and the radiation. Thus the end cannot act completely in the sense of an open end of a transmission line with  $k_e = -1$  (zero terminal current). The radiation must decrease the incident pulse energy through decrease of pulse amplitude, waveform shape, or both. Thus a reflection coefficient  $k_e = -1$  is impossible if radiation is to occur, as this implies a reflected pulse identical in all respects to the incident pulse, except for a change in sign. Effective experimental values for  $k_e$  can be deduced from pulsed TDR or radiation measurements, as demonstrated in Section 4 below.

## 2. INPUT REFLECTION COEFFICIENT

As pointed out by King and Schmitt (1962:223), the initial reflection from their antenna corresponds to a "predominantly" resistive termination, with resistance  $R > R_c$ , where  $R$  is the apparent antenna resistance and  $R_c$  is the characteristic resistance (50 ohms) of the transmission line. Their antenna was a monopole over a ground plane. As a specific case, for a particular diameter ( $=2a$ ) antenna of length  $l = 9$  feet, a pulse with  $\tau = 3 \times 10^{-9}$  sec. and a rise time about  $1 \times 10^{-9}$  sec., the input voltage reflection coefficient  $r = 0.72$ , as measured by comparison of the amplitude of the first reflected pulse, with the line terminated by the antenna, with the amplitude of the pulse reflected from the line terminated in an open circuit.

In the words of King and Schmitt, this corresponds "in some manner" to an input impedance

$$Z = R_c \frac{1+r}{1-r} = 50 \frac{1+0.72}{1-0.72} = 307.1 \text{ ohms} \quad (\text{B-1})$$

King and Schmitt (1962) show that this value is reasonable by integrating the input impedance  $Z(\omega)$  of an infinitely long antenna, for which a formula is available (due to Wu(1961-1)), as follows:

$$\bar{Z} \equiv \overline{Z(\omega)} = \frac{1}{\omega_c} \int_0^{\omega_c} S(\omega) Z(\omega) d\omega \quad (\text{B-2})$$

Here  $\overline{Z(\omega)}$  is the average impedance over the range of frequencies in the pulse,  $\omega_c$  is the upper angular frequency limit of the pulse, and  $S(\omega)$  is the frequency spectrum of the pulse. The magnitude of the reflection coefficient is then defined as

$$|r| = \left| \frac{\overline{Z(\omega)} - R_c}{\overline{Z(\omega)} + R_c} \right| \quad (\text{B-3})$$

In the evaluation of the integral in Eq. (B-2), King and Schmitt approximate  $S(\omega) = 1$  over the frequency range  $0 \leq \omega \leq \omega_c$ . An alternative formulation defines the average reflection coefficient as the integrated value of  $r(\omega)$  as follows:

$$\bar{r} \equiv \frac{1}{2\omega_c} \int_{-\omega_c}^{\omega_c} \frac{Z(\omega) - R_c}{Z(\omega) + R_c} d\omega \quad (\text{B-4})$$

The above two formulations are shown by King and Schmitt (1962) to agree very closely when plotted against the variable ( $C/\omega_c a$ ), and in addition to agree with experimental values of  $r$ . It is pointed out by this writer that the alternative formulation of Eq. (B-4) depends only upon the upper frequency limit of the pulse, and not at all upon the detailed structure within the pulse spectrum function  $S(\omega)$  as does Eq. (B-2). In practice however, the approximation  $S(\omega) = 1$  as used in Eq. (B-2) also ignores the spectrum detailed structure, so the two formulations in effect ignore the same thing. It would seem to this writer that the shape of the pulse waveform (in time) and therefore that of its frequency spectrum should enter in some manner into the reflection coefficient; hence the formulation of Eq. (B-2) is preferable from this viewpoint.

In any case it can be concluded that in a formal mathematical sense, the above frequency-domain approach to the input reflection coefficient does lead to results that were experimentally verified in the time domain for the waveforms as described. However, it would be desirable and probably valuable from the viewpoint of additional engineering insight, if a time-domain approach or solution could be developed, similar to the standard traveling-wave solutions for transients on transmission lines (e.g., Magnusson (1970, chaps. 2,3,4,7)). This type of approach, even if it led to only approximate results, would fit in more naturally with the time-domain traveling-wave solutions already developed for the propagation and radiation of transients on antennas (e.g., Appendix A).

An exact solution is available for the transient response of a linear circular tubular dipole antenna to a step-function driving voltage,

valid up to the time  $t < h/c$ , which is the time that the discontinuity traveling from the input reaches the ends at  $Z = \pm h$ . This solution was given by Wu (1961-2) and also later by Morgan (1962). Both solutions were corrected by Wu (1969, 347-351). Wu (1969:350) points out that his final expression for  $I(Z,t)$ , which is the current on the antenna as a function of position along the antenna and time, is already quite complicated, and holds only for  $t \leq h/c$ . He states that in principle the solution for  $I(Z,t)$  for later times  $h/c < t \leq 3h/c$ ,  $3h/c < t \leq 5h/c$ , etc., should be attainable using the Wiener-Hopf method, but this has not been done. He comments further that for  $t > h/c$  the results are most probably too complicated to be instructive.

Concerning the above solution by Wu (1969), approximations and simplifications are needed to make this into a more widely-used tool for engineering applications. Wu himself points out that his solution, even for the restricted case  $t \leq h/c$ , is quite complicated. Since Wu's solution is already in the time domain, it is not unreasonable to hope that this may lend itself to interpretations and tractable approximations in the form of traveling waves along the antenna suitable for engineering uses. Further, if the solutions described by Wu for  $t > h/c$  could be developed, and in turn, interpreted in terms of traveling waves, this should clarify the role of the antenna end which is reached by the transient at  $t=h/c$ .

Ross et al (1966, Section 4.2) derive an equation for the driving point (dp) impulse response  $h_{11}(t)$  of a dipole of infinite length by an approximate evaluation of the inverse Fourier transform of the equation for the driving point admittance  $Y(\omega)$  derived by Wu (1961-1). From this, the



dp response to arbitrary excitation can be found in the time domain by the convolution integral. Ross et al (1966:34) show that the approximation to  $Y(\omega)$  by King and Schmitt (1962) invalidates their results for sufficiently narrow pulses on antennas with reasonable radii.

### 3. END (OR TIP) REFLECTION COEFFICIENT

King and Schmitt (1962:224) remark that the tip of the antenna acts in the sense of an open end since the pulse reflected at this point is in phase with the incident pulse. This is from the voltage viewpoint; from the current viewpoint the reflected current would be opposite in direction to that of the incident pulse.

Ross et al (1966) model the finite length dipole as a TEM line with characteristic impedance determined experimentally and the end replaced by a simple open circuit. Ross (1967) introduces a radiating cylindrical rod element which is tapered to a needle point at its end. The tapering, according to Ross, assures that the current at the end is zero (i.e., it is a perfect open circuit). Ross states that driving-point measurements indicate that this radiator can be closely approximated by an open-circuited transmission line.

For time-harmonic excitation, Shen et al (1968) derive an expression for the reflection coefficient at the end of a finite length dipole and state this is being studied for possible application to the calculation of the transient response to a short pulse. Their analysis shows the antenna acts in analogous fashion to a transmission line.

The biconical antenna has received considerable attention.

Martins (1973:25) uses narrow-angle cones to model a dipole. He selects  $R_2$  (end voltage reflection coefficient) = 1 in a number of examples, reasoning that much of the high frequency radiation takes place at the input, hence, by the time the wave reaches the end, the radiation impedance is large and approaching an open circuit condition. For a wide-angle bicone feed ( $67^\circ$  half-angle) with flat ends, Martins (1973:172) reports a TDR-measured value of  $R_2 = 0.378$ . Harrison and Williams (1965:244) in a paper on transients in wide-angle conical antennas with spherical-capped ends, support a suggestion by Prof. T. T. Wu that pulse radiation occurs from the antenna as the pulse of charge passes from the transmission line onto the antenna, and again as the charge turns the corner from the cone onto the spherical cap and back again, by approximate calculations and theoretical curves of the time history of the radiated field, the latter derived by Fourier transform from the known response to time-harmonic excitation. This is similar to the accelerating charge concept of radiation (Handelsman, 1972). From the time-history curves it might be possible to deduce effective values for  $R_2$ , but this has not been pursued further by this writer. For time-harmonic excitation, Jordan and Balmain (1968, chap. 14) summarize Schelkunoff's model of the bicone antenna as a uniform transmission line with an appropriate terminal end impedance, and its extension to the dipole as a non-uniform line with an average characteristic impedance.

#### 4. APPROXIMATE MODEL OF DIPOLE ANTENNA WITH TDR-MEASURED REFLECTION COEFFICIENTS

The circuit response, antenna traveling waves amplitudes, and the radiation from a pulsed dipole can be calculated very approximately from a

highly simplified "back-of-the-envelope" transmission-line model using TDR-measured reflection coefficients at the input and the ends (Handelsman 1972, Section 4.3) and Appendix A of this report. This model is intended for first-order, approximate engineering applications with simple rectangular pulse excitation. This model is described briefly below, and illustrated by comparison with data from three references. For simplicity, only the radiation in the boresight direction ( $\theta=90^\circ$ ) is considered. A more sophisticated model involving a dispersive filter at the input and a TEM mode line representation of the antenna, with an open circuit at the end, has been developed by Ross et al (1966, Section 4.2.2.3).

Each half of the dipole is considered to be a lossless, TEM-mode transmission line of length  $h$ . The voltage reflection coefficients are  $R_1$  at the input and  $R_2$  at the ends. Radiation occurs only during the periods of pulse incidence at the input and at the ends. Radiation losses are assumed to be accounted for through the measured reflection coefficients.

The antenna is driven by a transmission line with real characteristic impedance  $Z_0$  ohms. Let the amplitude of the initial wave or pulse incident upon the antenna input be  $V_0$  volts. A train of reflected pulses is observed in the line, separated by  $2h/c$  sec., with successive amplitudes  $V_1, V_2, V_3, \dots$ . Then

$$R_1 = \frac{V_1}{V_0} = \frac{Z_a - Z_0}{Z_a + Z_0} \quad (B-5)$$

where  $Z_a$  = effective antenna input or line characteristic impedance, taken as real. Since  $V_1$  and  $V_0$  are measured by TDR, then  $R_1$  and  $Z_a$  can be

calculated. The amplitude of the first pulse traveling towards  $Z=h$  is

$$V_1^+ = (1+R_1)V_0 \quad (B-6)$$

The first pulse reflected from the end at  $Z=h$  and traveling back to the antenna input at  $Z=0$  is

$$V_1^- = R_2 V_1^+ = R_2 (1+R_1) V_0 \quad (B-7)$$

At  $Z=0$ , this pulse gives rise to two pulses as follows:

(1) A reflected pulse which travels back on the antenna towards  $Z=h$ , given by

$$V_2^+ = -R_1 V_1^- = -R_1 R_2 (1+R_1) V_0 \quad (B-8)$$

(2) A pulse transmitted into the line, which is observed as  $V_2$ , given by

$$V_2 = (1-R_1) V_1^- = R_2 (1-R_1^2) V_0 \quad (B-9)$$

From Eqs. (B-5, B-9),  $R_2$  can be calculated. This allows calculation of an effective antenna end impedance  $Z_e$  taken as real, from

$$R_2 = \frac{Z_e - Z_a}{Z_e + Z_a} \quad (B-10)$$

Repeating the above process, there is obtained the following:

$$V_2^- = R_2 V_2^+ = -R_1 R_2^2 (1+R_1) V_0 = -R_1 R_2 V_1^- \quad (B-11)$$

$$V_3^+ = -R_1 V_2^- = R_1^2 R_2^2 (1+R_1) V_0 = -R_1 R_2 V_2^+ \quad (B-12)$$

$$V_3 = (1-R_1) V_2^- = -R_1 R_2^2 (1-R_1^2) V_0 = -R_1 R_2 V_2 \quad (B-13)$$

$$V_3^- = R_2 V_3^+ = R_1^2 R_2^3 (1+R_1) V_0 = -R_1 R_2 V_2^- \quad (B-14)$$

$$V_4^+ = -R_1 V_3^- = -R_1^3 R_2^3 (1+R_1) V_0 = -R_1 R_2 V_3^+ \quad (B-15)$$

$$V_4 = (1-R_1) V_3^- = R_1^2 R_2^3 (1-R_1^2) V_0 = -R_1 R_2 V_3 \quad (B-16)$$

... etc. ...

To calculate the radiation, assume for simplicity, that the excitation can be approximated by a rectangular pulse of duration  $\tau < h/c$  sec. Radiation is emitted during the periods of incidence at  $Z=0$ , th by the traveling current waves. These current waves are taken as pulses of duration  $\tau$  sec., with amplitudes derived from the voltages  $V_i^+, V_i^-$  of the traveling waves, where  $i=1,2$  etc., given by Eqs. (B-6,B-7,B-11,B-12, etc.). Thus

$$I_i^+ = V_i^+ / Z_a ; I_i^- = -V_i^- / Z_a \quad (B-17)$$

The radiation ( $\theta=90^\circ$ ) then consists, approximately, of a train of pulses of duration  $\tau$  sec., spaced  $h/c$  sec. apart, with normalized successive amplitudes as follows (Handelsman 1972, Section 3):

$$\begin{aligned} E_1 &\equiv 1, E_2 = -(1+R_2), E_3 = R_2(1-R_1), \\ E_4 &= R_1 R_2(1+R_2), E_5 = -R_2^2 R_1(1-R_1), \end{aligned} \quad (B-18)$$

... etc. ...

Example 1. King and Schmitt (1962).

The antenna is a monopole over a ground plane. For unity incident voltage amplitude, a train of reflected pulses is observed in the line, with the following amplitudes (read from Fig. 3 in this reference):

$$V_1 = 0.72, V_2 = 0.35, V_3 = -0.19, V_4 = 0.1$$

Then

$$R_1 = \frac{V_1}{V_0} = V_1 = 0.72$$

$$R_2 = \frac{1}{1-R_1^2} \frac{V_2}{V_0} = \frac{1}{1-(0.72)^2} \frac{0.35}{1} = 0.727$$

From Eqs. (B-13,B-16) it follows that the calculated values for  $V_3$  and  $V_4$  are -0.183 and 0.096 respectively. These compare very well with the observed values -0.19 and 0.1, respectively.

It is informative to calculate the results of assuming that the end is a perfect open circuit, i.e.,  $R_2 = 1$ . Then from Eqs. (B-9,B-13,B-16), the calculated values are  $V_2 = 0.482$ ,  $V_3 = -0.347$ ,  $V_4 = 0.25$ , which compare unfavorably with the observed values. Thus the model with  $R_1 = 0.72$ ,  $R_2 = 0.727$  gives much better agreement with observed results than a model with  $R_1 = 0.72$  and  $R_2 = 1$  (arbitrarily).

Example 2. Ross et al (1966, pp. 80-81).

The antenna is a monopole over a ground plane. The measured reflected pulse train in the transmission line has amplitudes 0.58, 0.42, -0.12, 0.05, etc., relative to unit incident excitation. Following the method illustrated in Example 1, there is obtained

$$R_1 = 0.58, R_2 = 0.633$$

$$V_3 = -0.154, V_4 = 0.056$$

These calculated values for  $V_3$ ,  $V_4$  compare well with the measured values -0.12 and 0.05, respectively.

Example 3. Palciauskas and Beam (1970).

This reference derives the radiation field of a center-driven dipole, using an inverse Fourier transform of the response to sinusoidal excitation. The excitation is a pulse of trapezoidal shape. The radiation field in the boresight direction has a waveform with recognizable pulse peak amplitudes, spaced  $h/c$  sec. apart, with the following values, as read from a curve:

$$E_1 = 1.55, E_2 = -2.9, E_3 = 0.35, E_4 = 1.62, E_5 = -0.15$$

From Eq. (B-18), the reflection coefficients are calculated as follows:

$$R_2 = -\frac{E_2}{E_1} - 1 = -\frac{-2.9}{1.55} - 1 = 0.871$$

$$R_1 = 1 - \frac{E_3}{E_1 R_2} = 1 - \frac{0.35}{(1.55)(0.871)} = 0.741$$

The approximate model of the dipole then predicts, from Eq. (B-18) the following values for  $E_4$  and  $E_5$ :

$$E_4 = R_1 R_2 (1 + R_2) E_1 = 1.87$$

$$E_5 = -R_2^2 (1 - R_1) E_1 = -0.226$$

These approximate values are to be compared with the more precisely calculated values  $E_4 = 1.62$  and  $E_5 = -0.15$ . The agreement is not as good as in the previous examples, but is not too bad.

## 5. SUMMARY AND CONCLUSIONS

It seems reasonable to conclude that the concept of an input reflection coefficient, at least in the form of an average input impedance or average coefficient as formulated by King and Schmitt (1962) is a viable one, capable of further development and application. The average impedance formulation can take into account the particular waveform of the transient excitation through its frequency spectrum. These results are limited to times less than that required for the first reflection from the end to arrive back at the input, being based upon the admittance  $Y(\omega)$  of an infinitely long antenna at a single frequency, derived by Wu (1961-1).

Using Wu's (1961-1) equation for  $Y(\omega)$ , Ross et al (1966) derive the driving point (dp) impulse response of an infinitely long dipole by approximate evaluation of the inverse Fourier transform of  $Y(\omega)$ . The dp response to arbitrary excitation waveform can then be found from the convolution integral. Hence this approach should be productive in further development of the concept of an input (dp) reflection coefficient.

An exact time-domain solution for the current  $I(Z,t)$  as a function of location  $Z$  along the antenna and time  $t$ , for step-function excitation, has been derived by Wu (1969). This is applicable only for  $t > h/c$ , i.e., the antenna behaves as if it were infinitely long. The result is quite complicated, to use Wu's own words. However, from this solution, the current distribution for arbitrary excitation can be obtained by a superposition integral in the time domain. Hence it is obvious that this exact solution is a prime candidate for further development, approximation and diverse engineering applications, including that of the concept of the input reflection coefficient.



In contrast to the input problem of the dipole for which at least two approximate and one exact time-domain solutions have been outlined above, there apparently exists no comparable time-domain solution, exact or even approximate for the problem of the antenna end and its related reflection coefficient. Wu (1969) states that in principle, his analysis for  $t \leq h/c$  can be extended to later times such as  $h/c < t \leq 3h/c$ , etc. (so that the end enters into the problem, at least implicitly) but this has not been carried out. Wu remarks that the results would most probably be too complicated to be instructive.

For time-harmonic excitation, an equation derived by Shen et al (1968) for the reflection coefficient at the end of a finite length dipole, and Schelkunoff's approximate model of a dipole are available. Such solutions, through use of the Fourier transform and the digital computer, afford numerical time-domain results, which can be used to test theory and/or models. The difficulties of obtaining analytical time-domain results from these particular frequency-domain solutions are unknown.

For the wide-angle bicone antenna the time-domain radiation has been calculated (Harrison and Williams 1965). For conical antennas, much has been published for time-harmonic excitation embodying a transmission-line model (Jordan and Balmain (1968)).

One approximate empirical model of the dipole antenna is described in Section 4 above. It models the antenna as a length  $h$  of lossless TEM transmission line, with input and end reflection coefficients determined through TDR measurements. Based upon three examples selected from the literature, this model does yield reasonably good approximate results for

the circuit response and radiation from a dipole excited by rectangular pulse excitation.

The end reflection and its resultant waveform distortion can be eliminated by the use of resistively loaded antennas so that the traveling current waves on the antenna are reduced to negligible magnitudes by the time they reach the ends (Liu and Sengupta 1974). If such antennas are used, various numerical and approximate analytical results are available for study of the input and radiation characteristics (Liu and Sengupta 1974, and pertinent references cited therein), for application towards practical engineering models.



## MISSION of *Rome Air Development Center*

RADC is the principal AFSC organization charged with planning and executing the USAF exploratory and advanced development programs for electromagnetic intelligence techniques, reliability and compatibility techniques for electronic systems, electromagnetic transmission and reception, ground based surveillance, ground communications, information displays and information processing. This Center provides technical or management assistance in support of studies, analyses, development planning activities, acquisition, test, evaluation, modification, and operation of aerospace systems and related equipment.

Source AFSCR 23-50, 11 May 70